

**THE IDENTIFICATION OF NRAGE: A NOVEL
IAP-INTERACTING PROTEIN**

Dissertation

For completion of the Doctorate degree in Natural Sciences at the Bayerische
Julius-Maximilians-Universität Würzburg



Bruce Jordan

from London, England

Würzburg 2001

Declaration:

I hereby declare that the submitted dissertation was completed by myself and no other. I have not used any sources or materials other than those enclosed.

Moreover I declare that the following dissertation has not been submitted further in this form or any other form, and has not been used to obtain any other equivalent qualifications at any other organisation/institution.

Additionally, I have not applied for, nor will I attempt to apply for any other degree or qualification in relation to this work.

Würzburg, den

Bruce W. M. Jordan

The hereby submitted thesis was completed from Jan 1997 until July 2001 at the Institut für Medizinische Strahlenkunde und Zellforschung, Bayerische Julius-Maximilians Universität, Würzburg under the supervision of **Professor Dr. Ulf.R.Rapp** (Faculty of Medicine) and **Professor Dr. E.Buchner** (Faculty of Biology).

Submitted on: 10.08.2001

Members of the thesis committee:

Chairman:

Examiner: Professor Dr. Ulf.R.Rapp

Examiner: Professor Dr. E.Buchner

Date of oral exam: 28.11.2001

Certificate issued on:

ACKNOWLEDGEMENTS

First of all, I would like to thank Prof. Dr. Ulf Rapp for inviting me to the MSZ, and for his strong scientific guidance during my studies, as well as for providing an international atmosphere at the institute. I would also like to thank Prof. Erich Buchner for accepting me to the faculty of biology, and especially for his support at the beginning of my doctorate degree. Also thanks to Prof. Michael Sendtner for the fruitful collaboration.

My research work was undertaken in the group "AG Stress", under the direction of PD Dr. Stephan Ludwig. A very special thanks to Stephan for "adopting" me into his group, and for the excellent supervision I received. I am deeply grateful for the strong camaraderie built up in the group over the years, without which my stay in Würzburg would not have been the enriching experience that it was. The diversity of the group members, and those in the institute as a whole, combined with all the new cultural experiences gained from living in Würzburg, have furnished me with many fond memories, and have certainly broadened my horizons.

In particular, my long-standing lab. colleagues, Dragomir Dinev, Bernd Neufeld, Marc Schmidt, Angelika Hoffmeyer, Egbert Flory, Peifeng Chen, Stephan Ludwig, Bille Schmidt, Christina Ehrhardt, Georgeos Keramas, Anne Grosse-Wilde, Ollie Hauss and Heide Häfner, as well as the new arrivals Andris Avots and Walter Würzer, I would like to thank for the many social and scientific events we have shared. Thanks to Frau Wagenbrenner and Frau Kraemer for keeping us supplied with clean equipment. I would also like to express my thanks to the many other MSZ-students past and present: Jannic, Dima, Jörg, Uli, Dorthe, Guido, Kerstin, Gordon, Anke, Oleg, Dennis, Britta, Jan, Helmut, Carsten, Enrico, Nina, Ines, Jian, Jochen, Wilfried, Branislav, Andrea, Friedrich, Carolyn, for always being up for a party. The same to David, Veronique, Bernd B., Tina, Petra, Angela and Bettina.

For assistance over and beyond the call of duty, and always with a smile, I would especially like to thank Ludmilla Wixler for her unrivalled technical expertise and enthusiasm. Much thanks to Jakob Toppmair for pretty much the same. Special thanks to Ewald Lipp for "those little contract emergencies", and to Frau Pfränger for short-notice slide preparation. Also to Reinholt for excellent sequencing and football knowledge. To the secretaries, Heidi, Monika, Anette, Frau Blättler, and especially Rosemary Röder I would like to thank for the smooth running of things. Thanks to "Meister" Tietsch for keeping the MSZ equipment in good working order.

A very special thanks to Suzana for her support and kindness, and for reminding me of the important things.

The greatest acknowledgement I reserve for my family, for their support, and for giving me the best start in life I could ever have hoped for, to whom I dedicate this Dissertation.

TABLE OF CONTENTS

SUMMARY.....	1
ZUSAMMENFASSUNG.....	2
INTRODUCTION.....	3
I.1. Apoptosis.....	3
I.2. Receptor mediated apoptosis.....	3
I.3. Stress mediated cell death.....	5
I.4. Survival signaling via cell membrane receptors.....	6
I.4.1. The TNF receptor in cell protection.....	6
I.4.2. Receptor tyrosine kinase signalling.....	7
I.4.3. Interleukin-3 and its receptor.....	8
I.5. Anti-apoptotic molecules.....	9
I.6. The inhibitor of apoptosis proteins.....	9
I.6.1. Regulation of IAP expression.....	10
I.6.2. IAP involvement in signal transduction.....	11
I.6.3. IAPs and direct caspase inhibition.....	13
I.6.4. Regulation of IAP function.....	14
I.6.5. The IAP RING domain.	15
I.7. The Bcl-2 family in apoptosis regulation.....	16
I.8. NRAGE and the p75 neurotrophin receptor.....	18
I.9. Experimental design and aim of the project.....	21
RESULTS.....	22
II-1 The identification of a novel IAP interacting protein.....	23
II-1.1 The result of the two-hybrid screen.....	25
II-1.2 direct yeast two-hybrid tests.....	26
II-1.3 Mammalian two-hybrid test.....	26
II-2 The molecular cloning of the complete <i>nrage</i> cDNA.....	27
II-2.1 Expression and screening for <i>nrage</i> in S194 plasmacytoma.....	27
II-2.2 Analysis, modification and expression of the complete <i>nrage</i> cDNA.....	28
II-2.3 Protein expression of NRAGE confirms successful site directed mutagenesis.....	31

II-2.4 Distribution of expression pattern of nrage transcripts in adult mouse tissue.....	31
II-3 Investigation of the IAP-NRAGE binding in co-immunoprecipitation.....	33
II-3.1 ITA interacts with NRAGE via its RING zinc-finger domain.....	33
II-3.2 XIAP binds to NRAGE.....	34
II-4: The influence of NRAGE on apoptosis in 32D cells upon IL-3 withdrawal.....	35
II-4.1 NRAGE expression in the IL-3 dependent 32D cell line augments factor withdrawal induced apoptosis.....	36
II-4.2 NRAGE binds XIAP in vivo upon IL-3 withdrawal in 32D cells.....	37
II-4.3 NRAGE overcomes Bcl-2 mediated cell protection.....	37
II-5 The participation of NRAGE and XIAP in signalling pathways.....	38
II-5.1 NRAGE and XIAP cooperate in JNK signalling.....	38
II-6 Cellular localisation of NRAGE and Δ NRAGE mutants.....	40
DISCUSSION.....	42
III-1. The discovery of a novel IAP-binding protein.....	42
III-2 NRAGE is a novel MAGE-like member with unique characteristics.....	46
III-3 The influence of NRAGE and XIAP on signal transduction.....	50
MATERIALS AND METHODS.....	54
IV-1. Materials.....	54
IV-1.1. Instruments.....	54
IV-1.2. Chemical reagents and general materials.....	55
IV-1.3. Cell culture materials.....	57
IV-1.4. Antibodies.....	58
IV-1.5. Enzymes.....	58
IV-1.6. Kits.....	59
IV-1.7. cDNA libraries and plasmid DNA.....	59
IV-1.8. Oligonucleotides.....	60
IV-1.9. Cell lines, yeast and bacterial strains.....	61
IV-2. Solutions and buffers.....	61
IV-2.1. Bacterial medium and DNA isolation buffers.....	61
IV-2.2. RNA buffers.....	62

IV-2.3. DNA buffers.....	64
IV-2.4. Protein analysis buffers.....	64
IV-2.5. Yeast media and solutions.....	67
IV-3. Methods.....	69
IV-3.1. Bacterial manipulation.....	69
IV-3.1.1. Preparation of competent cells (CaCl ₂ method)	69
IV-3.1.2. Transformation of competent bacteria.....	70
IV-3.1.2. Transformation of competent bacteria.....	70
IV 3.2. DNA methods.....	70
IV-3.2.1. Electrophoresis of DNA on agarose gel.....	70
IV-3.2.2. Isolation of plasmid DNA from agarose (QIAEX II agarose gel extraction protocol).....	70
IV-3.2.3. Purification of plasmid DNA (QIAquick PCR purification kit).....	71
IV-3.2.4. Ligation of DNA fragments.....	71
IV-3.2.5. Cohesive-end ligation.....	71
IV-3.2.6. Mini-preparation of plasmid DNA.....	72
IV-3.2.7. Maxi-preparation of plasmid DNA.....	72
IV-3.2.8. Measurement of DNA concentration.....	72
IV-3.2.9. DNA Sequencing (Sanger Dideoxy Method).....	72
IV-3.3. Extracting and handling RNA.....	74
IV-3.3.1. Isolation of RNA from tissue.....	74
IV-3.3.2. Isolation of RNA from cells.....	75
IV-3.3.3. Running RNA samples on denaturing gels.....	75
IV-3.3.4. Northern blotting.....	75
IV-3.4. Yeast two-hybrid methods.....	76
IV-3.4.1. The two-hybrid screen.....	76
IV-3.4.2. Colony lift β-galactosidase filter assay.....	77
IV-3.4.3. Transforming <i>S. cerevisiae</i> with plasmids (small scale)	77
IV-3.4.4. Direct two-hybrid tests.....	78
IV-3.4.5. Plasmid isolation from yeast cells.....	78
IV-3.4.6. Protein extraction from yeast.....	78

Table of contents

IV-3.5. Protein methodologies.....	78
IV-3.5.1. Immunoprecipitation.....	79
IV-3.5.2. In vitro kinase assay.....	79
IV-3.5.3. Measurement of Protein concentration (Bio-Rad protein assay)	79
IV-3.5.4. Sodium dodecyl sulfate polyacrylamide gel electrophoresis (SDS PAGE) ...	79
IV-3.5.5. Immunoblotting.....	80
IV-3.5.6. Immunoblot stripping.....	81
IV-3.5.7. Luciferase reporter gene assay.....	81
IV-3.5.8. β -galactosidase assay.....	82
IV-3.6. Cell culture techniques.....	82
IV-3.6.1. Cell maintenance	82
IV-3.6.2. Transient transfection of 293 cells (Calcium phosphate method).....	82
IV-3.6.3. Establishment of stable cell lines.....	83
IV-3.6.4. Cell survival assays.....	83
IV-3.6.5. Immunofluorescence.....	83
REFERENCES.....	85
APPENDIX.....	96
CURRICULUM VITAE.....	99

SUMMARY

The inhibitor of apoptosis proteins (IAPs) have been shown to interact with a growing number of intracellular proteins and signalling pathways in order to fulfil their anti-apoptotic role. In order to investigate in detail how the avian homologue ITA interfered with both TNF induced apoptosis and the NGF mediated differentiation in PC12 cells, a two hybrid screen was performed with a PC12 library using ITA as a bait.

The screen resulted in the identification of several overlapping fragments of a previously unknown gene. The complete cDNA for this gene was isolated, the analysis of which revealed a high homology with a large family of tumour antigens known as MAGE (melanoma associated antigens). This newly identified member of the MAGE family, which was later named NRAGE, exhibited some unique characteristics that suggested for the first time a role in normal cellular physiology for this protein family. MAGE proteins are usually restricted in their expression to malignant or tumour cells, however NRAGE was also expressed in terminally differentiated adult tissue.

NRAGE also interacted with the human XIAP in direct *two-hybrid* tests. The interactions observed in yeast cells were confirmed in mammalian cell culture, employing both coimmunoprecipitation and mammalian *two-hybrid* methods. Moreover, the results of the coimmunoprecipitation experiments indicated that this interaction requires the RING domain. The widely studied 32D cell system was chosen to investigate the effect of NRAGE on apoptosis. NRAGE was stably transduced in 32D cells, and found to augment cell death induced by the withdrawal of Interleukin-3. One reason for this reduced cell viability in NRAGE expressing cells could be the binding of endogenous XIAP, which occurred inducibly after growth factor withdrawal. Interestingly, NRAGE was able to overcome the protection afforded to 32D cells by the exogenous expression of human Bcl-2. Thus NRAGE was identified during this research doctorate as a novel pro-apoptotic, IAP-interacting protein, able to accelerate apoptosis in a pathway independent of Bcl-2 cell protection.

ZUSAMMENFASSUNG

Die Familie der „inhibitor of apoptosis proteins“ (IAPs) interagieren mit einer wachsenden Zahl an intrazellulären Proteinen und Signaltransduktionswegen um ihre anti-apoptotische Aufgabe zu erfüllen. Es konnte gezeigt werden, dass das ITA-Homolog aus dem Huhn sowohl die durch TNF induzierte Apoptose als auch die durch NGF induzierte Differenzierung von PC12-Zellen verhindert bzw. verlangsamt.

Um diese Befunde genauer zu untersuchen, wurde in dieser Arbeit ein "yeast two-hybrid screen" mit ITA als "bait" (Köder) und einer cDNA-Bank aus PC12-Zellen durchgeführt. In diesem "screen" konnten verschiedene Fragmente eines bis dahin unbekanntes Gens identifiziert werden. Die Untersuchung der isolierten Gesamt-cDNA ergab eine hohe Homologie mit einer Familie von Tumor-Antigenen namens MAGE (melanoma associated antigens). Im Gegensatz zu den bisher identifizierten MAGE, zeigte dieses neue Familienmitglied, welches später NRAGE genannt wurde, einige Charakteristika die das erste mal eine Rolle in der normalen zellulären Physiologie nahe legten.

In einem direkten "yeast two hybrid test" konnte die Interaktion zwischen NRAGE und humanem XIAP gezeigt werden. Diese Interaktion konnte sowohl in Ko-Immunpräzipitationen als auch im sogenannten Säuger two-hybrid bestätigt werden. Desweiteren zeigten die Ko-Immunpräzipitationen, dass für die Interaktion dieser beiden Proteine die RING-Domäne von ITA benötigt wird. Um Effekte von NRAGE auf die Apoptose zu untersuchen, wurde das etablierte 32D Zellsystem verwendet. NRAGE wurde stabil in 32D-Zellen exprimiert, wodurch die Apoptoserate der Zellen, induziert durch die Kultivierung in IL-3 freiem Medium, gesteigert wurde. Ein Grund für diese erhöhte Apoptoserate, könnte in der Bindung von XIAP, welches nach dem Entzug von Wachstumsfaktoren induziert wird, an NRAGE liegen. Interessanterweise war NRAGE auch fähig die protektive Wirkung von exogen exprimiertem Bcl-2 aufzuheben. Somit konnte in dieser Arbeit NRAGE als pro-apoptotisches und mit IAP interagierendes Protein beschrieben werden. Desweiteren konnte gezeigt werden, dass die Verstärkung der Apoptose unabhängig von dem bekannten durch Bcl-2 bedingten anti-apoptotischen Signalweg erfolgt.

INTRODUCTION

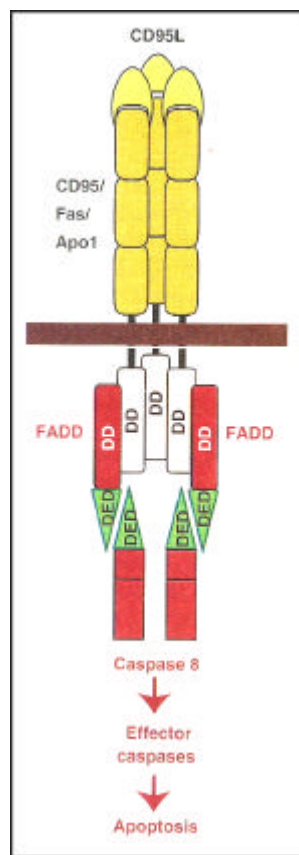
I.1. Apoptosis

Over the past 150 years the process of cell death has been recognised as an important part of homeostasis in multicellular organisms both during embryonic development and in adult life [1, 2]. A great deal of interest was generated in this field with the observation in the nematode *C.elegans* that this process was under genetic control [3]. The discovery that many diseases such as cancer [4], autoimmunity [5], and degenerative diseases [6] are concomitant with dysfunction of programmed cell death (PCD) led to an explosion of research in this field. This resulted in the identification of many of the key players involved in apoptosis, and a better understanding of the ways in which these play their parts in the processes that hold the balance between the intended cellular fate and the unwanted disease state. The pathways leading to cell death can be broadly classified into extrinsic (receptor mediated) or intrinsic (cellular/mitochondrial stress) pathways, and triggering of one or both of these results in cleavage and thereby activation of a family of cysteine proteases known as caspases. The death signal is transmitted through the cell in the form of a proteolytic caspase cascade, whereby the executioner caspases inactivate or activate their specific cellular targets by proteolysis. Once these caspases are engaged, many of the cell's homeostasis and repair mechanisms are disabled, apoptosis inhibitors are inactivated, and the cell is summarily disassembled. This then gives rise to the characteristic morphological changes seen in dying apoptotic cells such as chromatin condensation, cytoplasmic shrinkage and membrane blebbing. An alternative pathway leading to cell death also exists, distinct from apoptosis, and has been termed necrosis. Principal elements of necrosis include mitochondrial oxidative phosphorylation, reactive oxygen production, and non-caspase proteolytic cascades depending on serine proteases, calpains, or cathepsins [7].

I.2. Receptor mediated apoptosis

The tumour necrosis factor receptor (TNFR) superfamily regulates a large number of biological functions, such as growth and differentiation, in addition to apoptosis. The extracellular ligand-binding regions are characterised by variable numbers of cysteine rich repeats. Death receptors belonging to this family include the TNF-RI (p55), CD95 (Fas/Apo-1) and p75 neurotrophin

receptor (p75NTR) [7] [8]. What distinguishes these from the other TNFR members e.g TNF-R2 and CD40, is that they contain an intracellular death domain (DD), or in the case of p75NTR a region resembling the DD but with some crucial structural differences [9]. The important domains in death signalling, i.e. DD, death effector domain (DED) and caspase recruitment domain (CARD) display very similar 3D structures. Each consists of six antiparallel, amphipathic α helices, with a conserved set of hydrophobic amino acids in all domains, which form the hydrophobic core of the proteins [10] [11]. The differences between the domains lie in the surface residues that stabilise complex formation [12].



The DDs tend to be present in the intracellular parts of death receptors, whereas the DEDs and CARDS are found in the adapter molecules which mediate receptor or mitochondrial death signals [13] [11].

These domains are important in mediating protein-protein interactions, and thus transducing the signal from membrane surfaces to the cytosol, whereby the adapter proteins provide the link to the upstream regulators of cell death. The TNF-R1-associated death domain protein (TRADD) is recruited to the TNF-R1, which trimerises upon TNF ligand binding, in turn allows binding of the fas-associated protein with death domain (FADD). TRADD can further recruit the adapter protein RAIDD and the RIP kinase, as described in Fig.I-2. As depicted opposite, FADD is able to bind directly with CD95 (Fig.I-1).

Fig.I-1: Apoptosis signalling by CD95. DD, death domain; DED, death effector domain. (Mod.[14])

It is through these interactions that ligation of TNF-R1 or CD95 can result in the formation of a death inducing signalling complex (DISC), a complex constituting the activated receptors, adapter proteins, and initiator caspases. This results in the activation of the initiator protease Caspase 8 [14] [8] [7].

I.3. Stress mediated cell death

In addition to the signals transduced by death receptors, an intrinsic pathway leading to cell death also exists. Irreparable DNA damage by mutagens and ionising radiation, or the deprivation of essential growth factors can trigger a series of events leading to the release of a number of molecules from the intermembrane space of the mitochondria [15] [16], including apoptosis-inducing factor (AIF) [17] and smac/DIABLO [18] [19]. Release of one of these proteins, cytochrome c, into the cytosol enables it to come into contact with the adapter molecule Apaf-1, initiating a series of events resulting in the activation of effector caspases [20]. Analogous with the receptor signalling molecule FADD, Apaf-1 recruits and promotes trans-activation of an initiator caspase [21]. The initiator caspases possess long prodomains that enable them to interact with the DEDs or CARDs present in these adapter molecules [13]. Apaf-1 contains at least three functional domains including a CARD, a CED-4 domain required for self-oligomerisation, and a series of WD40 repeats which possibly mediate protein-protein interactions [22]. Upon cytochrome c binding, Apaf-1 is able to hydrolyse dATP or ATP and undergoes oligomerisation, whilst at the same time recruiting and processing caspase 9 [23]. This complex has been termed the 'apoptosome', and once formed transmits the death signal further by processing the effector caspases 3 and 7 [24]. Indeed, the fully processed caspases 3 and 7 have been found within this complex, indicating that not only caspase 9 mediated cleavage but also autocatalytic processing of these effector caspases takes place within the apoptosome [24].

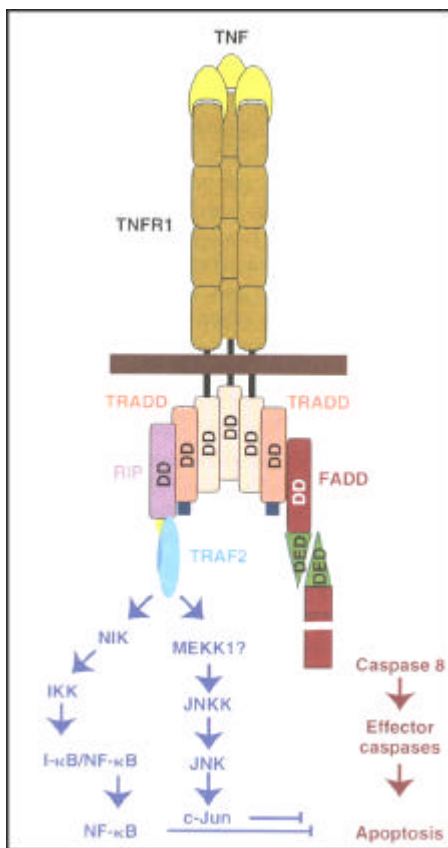
Engagement of the mitochondria was not thought to be universally required in the early stages of apoptosis, when the stimulus is directed via extracellular death receptors. Very recently however, a direct link has been discovered between receptor signalling and mitochondrial apoptosis. This novel direct link between both types of signalling involves the cleavage and subsequent activation of Bid, a newly cloned member of the Bcl-2 family (see below). Bid is cleaved by activated caspase 8 [25], and subsequently binding tightly to the mitochondria, where it can trigger apoptotic events in cooperation with other death agonists of the Bcl-2 family [26].

Clearly, apoptosis has evolved great intricacy, and its outcome is very much dependent on the organism or cell type, and the environmental stimulus applied. It is important that the cellular response to these stimuli is elicited in a manner, which is beneficial to the organism. Death is often not the appropriate response, and equally important cell survival pathways and death inhibitory molecules have evolved in parallel.

I.4. Survival signaling via cell membrane receptors

I.4.1. The TNF receptor in cell protection

The binding of TNF to the TNF-R1 does not result in cell death in every cell type, unlike CD95L-receptor binding. Indeed the death signal is often only brought about with a concomitant blockage of protein synthesis, indicating there may be pre-existing cellular proteins which can block the apoptotic stimulus after TNF stimulation. As previously described, TNF ligand binding induces trimerisation of the receptor and subsequent binding of the adapter molecule TRADD.



In survival signalling, TRADD functions as a platform adapter that attracts several adapter molecules to the activated receptor: The binding of TRAF2 (TNFR-associated factor-2) and RIP (receptor-interacting protein) [14] stimulate pathways leading to the activation of NF-κB and JNK/AP-1 [27], as opposed to the death pathway engaged by FADD binding. TRAF2 and RIP activate NIK (NF-κB-inducing kinase), which in turn activates the IκB (inhibitor of κB) kinase complex, IKK [28] [29]. IKK phosphorylates IκB, leading to IκB ubiquitination and subsequent degradation, thereby liberating NF-κB and allowing it to translocate to the nucleus where it is able to activate gene transcription [30]. The transcriptional targets of NF-κB include the Bcl-2 pro-survival homologues Bcl-xL, Bfl1/A1 and Nrl3, as well as many transcription factors, growth factors and cytokines [31].

Fig.I-2: Survival and death signalling pathways from the TNFR1. (For details see text). (Mod. [14])

The pathway leading from TRAF2 and RIP recruitment to JNK activation occurs through a different sequence of events than that resulting in NF- κ B activation. The signal is transduced via a cascade involving the MAP (mitogen-activated protein) 3 kinases MEKK1 (MAP/Erk kinase kinase-1), JNKK (Jun N-terminal Kinase Kinase), and the nuclear shuttle kinase JNK [32] [33]. MEKK1 is related to NIK, and has been implicated in this pathway because a dominant negative MEKK1 has been shown to block TNF mediated JNK activation. JNK is typically activated by a wide variety of stimuli, including physical and chemical stress, as well as TNF and other cytokines [34].

Interestingly however, of the two JNK Kinases MKK4 and MKK7, only the latter is activated in response to TNF stimulation [35]. In addition to MEKK1, MKK4 and MKK7 are targeted by other members of the MAP3K (MAP Kinase Kinase Kinases): Amongst these are ASK-1 (apoptosis signal-regulating kinase) [36], TAK-1 (TGF- β -activating kinase) [37], and MLK3 (mixed lineage kinase 3) [38]. Accordingly, the pathway leading from TNF-R1 to JNK might include at least TRADD, TRAF 2, and a MAP3K. The signal is transmitted via JNK to the nucleus, where the regulation of novel gene expression takes place through the phosphorylation of transcription factors belonging to the AP-1 family. The phosphorylation takes place within their activation domains, leading to an increased transcriptional activity possibly through enhanced stability of AP-1 factors [39]. The transcriptional targets for NF- κ B and AP-1 include the Bcl-2 pro-survival homologues Bcl-xL, Bfl1/A1 and Nrl3, as well as many transcription factors, growth factors and cytokines c-IAP1, c-IAP2, TRAF1 and TRAF2 [31] [40].

I.4.2. Receptor tyrosine kinase signalling

The RPTK (receptor protein tyrosine kinase) family is a diverse group of transmembrane proteins with ligand stimutable PTK (protein tyrosine kinase) catalytic activity through tyrosine auto/trans-phosphorylation. Catalytic activity is either intrinsic to the receptor or is mediated through associating molecules. Upon ligand binding, many cytoplasmic signalling proteins containing SH2 (Src homology-2) and PTB (protein tyrosine-binding) domains congregate at the receptor, initiating a cascade of signalling events. A great deal of interest has been focused on both the receptor and cytosolic PTKs since many are known oncogenes. The outcome of signal transduction through RPTKs very much depends on the ligand and receptor type [41]. In PC12 cells for example, EGF/EGFR binding results in proliferation, whereas NGF binding to Trk receptors leads to differentiation, both events taking place through RPTK-Ras-MAPK signalling

[42]. For a long time it was believed that the contribution that these proteins made to oncogenesis was by disregulating mitogenic signalling, via Ras-Raf-MEK-ERK, leading to increased proliferation. However, RPTKs have been shown to contribute to these plethora of cytoplasmic PTKs recruited either directly or via adapter proteins [43]. Of particular interest was the revelation that such signalling events could also lead to the activation, or neutralisation of certain key apoptotic molecules such as BAD or Bcl-2 through phosphorylation via downstream effectors such as Raf and PI3K [44] [45]. This goes beyond orchestrating the transcriptional up-regulation of anti-apoptotic genes, providing a further advantage to the cell in terms of repelling any attempt at apoptosis.

I.4.3. Interleukin-3 and its receptor

IL-3 is capable of inducing growth and differentiation of both multipotential haematopoietic stem cells and macrophages, erythrocytes and lymphoid cells, but can also support the proliferation of murine cell lines with the properties of multi-potential progenitors. Unlike RPTKs however, the cytoplasmic regions contain no detectable catalytic domain. Nevertheless, evidence suggests that the signal transduction from IL-3 receptors involve tyrosine phosphorylation. The IL-3 receptor consists of an α and a β subunit, and signalling is achieved by recruiting numerous and varied tyrosine or serine/threonine kinases, adapter/docking proteins, eventually leading to the activation of transcription factors. Examples of the latter are the JAKs (Janus kinases), which phosphorylate tyrosines on the receptor thereby allowing a transcription factor, termed STAT (signal transducers and activators of transcription) to be recruited. The STATs bind at the phosphorylated receptor tyrosines, becoming themselves phosphorylated by JAKs, subsequently dissociating and initiating the transcription of genes controlling proliferation and survival [46] [47].

In an analogous fashion with the RPTKs, IL-3 receptor signalling also results in the activation of classical mitogenic pathway [48], as well as the Src-PI3K-Akt pathway [49] [50] [45]. Upon stimulation, tyrosine phosphorylation on the β chain leads to SHC recruitment via its PTB domain. SHC and Gb2 form a ternary complex allowing the guanine nucleotide exchange factor Sos to bind. The signal is then passed on via Ras to the mitogenic kinase cascade. The PI3K also binds at the β chain region where Ras is recruited, probably via an alternative adapter molecule, where it can transmit the signal to Akt after IL-3 binding [46]. This receptor system can also enhance the survival potential of the cell by influencing the function of apoptosis

regulatory molecules, mediated in particular by Raf and Akt, both directly at the mitochondria and via transcription [44] [45].

I.5. Anti-apoptotic molecules

The signalling pathways that regulate cell survival can directly and indirectly target molecules, which are capable of halting the death process by its teeth. Much of our understanding of these molecules, and their mechanisms of direct caspase inhibition, come from observations made during virus infection. As a means of defence against virus infection, cells commit suicide and die via apoptosis in order to benefit the whole organism. Some viruses, in the meantime, have themselves developed effective means of self-preservation [51]. In the genome of the *baculovirus*, an insect virus, two independent genes coding for proteins that can directly inhibit host caspases have been identified. The proteins, named P35 [52] and IAP (inhibitor of apoptosis protein) [53], are able to inhibit the caspases of many organisms including nematodes, flies and mammals. Additionally, the cowpox virus has a gene coding for the cytokine response modifier (crmA), a serpin which not only blocks host apoptosis by impeding caspase-8 activity, but is also capable of interfering with the host inflammatory response by binding to caspase-1 [54]. Although all three of these proteins can exert their effects in many different species and cell types, only one is conserved throughout evolution.

I.6. The inhibitor of apoptosis proteins

Since the discovery of the first IAP in baculoviruses, a multitude of related proteins have been described in virtually all eukaryotes, as well as in other viruses. In addition to their presence in these organisms, their scope of function and activity has also diversified with evolution. The investigation of their importance in cell survival signalling has intensified greatly in recent years with the observation that in humans, IAP malfunction contributes to various diseases.

The identifying characteristic of the IAP family members lies not singularly in their ability to prevent apoptosis, but rather in the presence of a key domain within their structure. This novel domain, termed the baculovirus IAP repeat (BIR), has a core presence and spacing of cysteine and histidine residues (Cx₂Cx₆Wx₃Dx₅Hx₆C) at the N-terminus, which has been

identified as a novel zinc-binding fold [55]. Membership of this family requires the presence of at least one of these domains, although several IAPs contain as many as three. In addition to the BIR domain, a number of IAPs contain a carboxyl-terminal RING zinc finger domain. Some IAPs also possess a caspase recruitment domain (CARD), also present in many of the adapter molecules controlling apoptosis signalling.

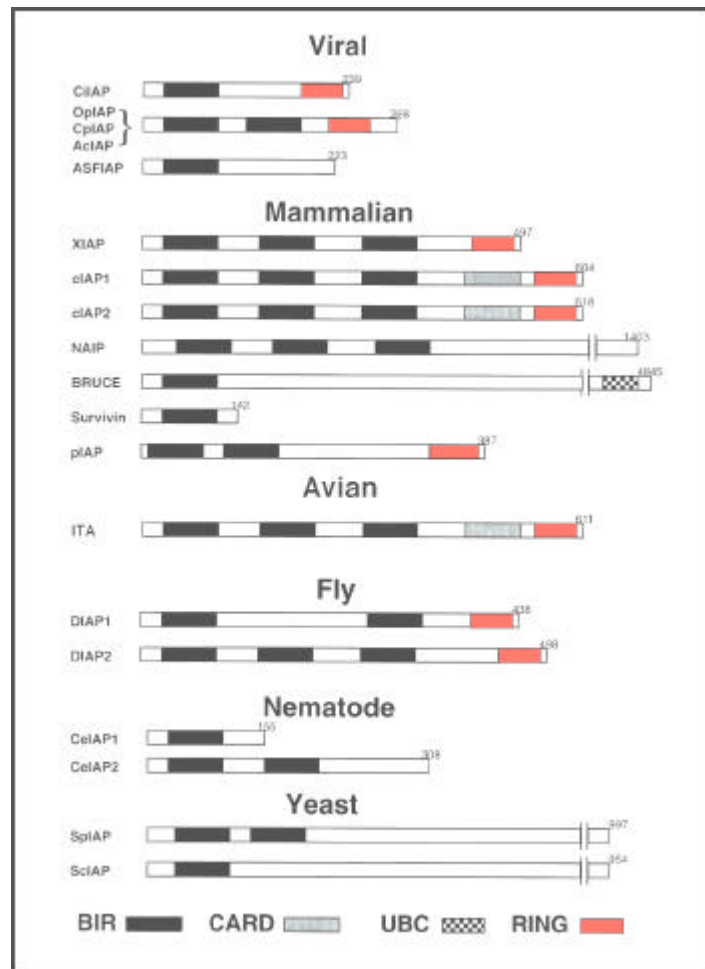


Fig.I-3: Structures of the IAP /BIR containing protein family. IAP proteins from many species are represented, and their various domains are highlighted. The BIR is shaded black, the CARD grey, the RING red, and the ubiquitin-conjugating domain (UBC) is chequered. The amino acid length is indicated on the top right of each protein. (mod. [56]).

At least seven human IAPs have been described already, as well as several mammalian homologues, an avian homologue ITA (inhibitor of T-cell apoptosis), two *Drosophila* IAPs (DIAP1 and DIAP2), two *Caenorhabditis elegans* members (CeIAP1 and CeIAP2), one from each of the fission yeast *Schizosaccharomyces pombe* and the budding yeast *Saccharomyces*

cerevisiae (SpIAP and ScIAP) [56]. Such is the abundance of these molecules that constant stream of new IAP members continue to appear in the literature.

I.6.1. Regulation of IAP expression

As previously described, TNF-R1 triggers NF- κ B activation upon TNF ligand binding, leading to nuclear translocation and transcription of important cell survival molecules. The expression of at least two of the human IAPs, c-IAP1 and c-IAP2, is transcriptionally regulated via the TNF-R1-NF- κ B pathway [57]. Interestingly TRAF1 and TRAF2, which play a very important role in TNF cell survival signalling, are also gene targets of NF- κ B, and must be expressed with c-IAPs 1 and -2 to prevent TNF mediated apoptosis [40]. The tissue distribution of c-IAP1 and c-IAP2 appear to be similar, found most highly expressed in kidney, small intestine lung and liver, and only weakly expressed in the central nervous system [58]. The neuronal IAP (NAIP) also shows a restricted expression, detectable only in liver, placenta and brain [6]. In contrast, the X-linked IAP (XIAP) appears to be expressed at the RNA level in virtually every adult and foetal tissue examined, except peripheral blood leukocytes [59]. Very recently however, closer inspection revealed the regulation of XIAP protein expression to be more complex than that of IAPs 1 and 2, being controlled at the level of translation initiation. There is a 162-nucleotide internal ribosomal entry site (IRES) sequence located in the 5' untranslated region (UTR) of XIAP mRNA, and this sequence is essential for cap-dependent translation of XIAP [60]. Furthermore, the IRES-mediated translation of XIAP mRNA is resistant to repression of protein synthesis that accompanies cellular stress such as serum deprivation or γ irradiation [60]. This suggests that the modulation of XIAP expression is beneficial for the cell during apoptotic signalling.

Although the expression of IAP proteins in cancer has only recently been touched upon, a picture is emerging of erroneous IAP expression playing a significant role in the survival of malignant cells. For example, higher levels of XIAP protein has an adverse prognostic significance for patients with acute myeloid leukaemia (AML) [61], and the expression of Survivin in oesophageal cancer seems to correlate with poor prognosis and responsiveness to treatment [62]. The opposite may also be true e.g. in degenerative diseases, where a lack of IAP can contribute to disease. In the inherited disease spinal muscular atrophy (SMA), NAIP was identified as a candidate gene by virtue of its deletion together with another gene *smn*, resulting in enhanced neuronal death possibly through unchecked caspase activity [6].

I.6.2. IAP involvement in signal transduction

The human c-IAP1 and c-IAP2 were originally cloned through their association with TNF-R2 receptor complexes [58] [63]. The proteins responsible for recruiting the IAPs are TRAF1 and TRAF2, which form heterocomplexes, since the IAPs do not interact directly with the receptor. The TNF-R1 also binds TRAFs 1 and 2, and it would be reasonable to assume that the IAPs play a role in survival signalling via both these receptors. As already noted, these molecules are NF- κ B target genes via signalling from the TNF-R1. Furthermore, overexpression of c-IAP2 can also lead to NF- κ B activation [57]. The observation that these c-IAP2 activities can be blocked by a dominant form of I- κ B which is resistant to TNF mediated degradation, would tend to suggest that a positive feedback loop exists via the TNF-R1-NF- κ B signal cascade and IAP gene transcription [40]. Interestingly, although TNF can activate caspase-8 via the TNF-R1, this rarely leads to cell death unless protein synthesis inhibitors are applied, suggesting that only in the absence of NF- κ B target gene translation is TNF cytotoxic.

Further evidence linking IAPs to NF- κ B came with the observation that in endothelial cells, XIAP overexpression leads to NF- κ B activation, increased p65 nuclear localisation, and enhanced I κ B degradation [64]. In dissecting this observation, it seems that XIAP activates IKK2, via a pathway requiring NIK but not MEKK1, and moreover involving the MAP3K TAK1. This last observation complemented earlier findings that IAP family members can play an additional role in signalling cascades unrelated to the TNF pathway.

XIAP can act as a mediator of bone morphogenic protein (BMP) signalling, by linking the intracellular domain of the BMP-receptor 1A to the signalling modulator TAB1 which subsequently recruits and activates TAK1 [65]. This activity is well conserved, since one of the earliest findings described the *Drosophila* IAPs, dIAP-1 and dIAP-2/dILP, as TkV-interacting (Thickveins) proteins in a *two-hybrid* screen. TkV is a type I serine-threonine kinase receptor homologous to the BMP type I receptor [66]. Another study also showed that XIAP could play a role in MAPK signal transduction. In this case, overexpression of XIAP led specifically to the activation of JNK1, and not JNK2 or any other MAPK, and that this activation was necessary to block procaspase-1 mediated apoptosis [67]. This accumulation of evidence strengthens the case for IAPs as multifunctional proteins, manoeuvring the cell away from apoptosis through multiple signal transduction pathways, whilst also capable of directly neutralising the cell's death effectors.

During the preparation of this dissertation, a thrilling new report highlighted exactly this dexterity of XIAP. This report placed XIAP at a central location for co-ordinating signalling from

the TGF- β type I receptor for the activation of transcription, as well as for the activation of both JNK and NF- κ B. The introduction of a dominant negative mutant of Smad4, a key player in TGF- β signalling, completely abolished these activities. However, the introduction of this Smad4 mutant had no effect on XIAP anti-caspase activity [68]. Some of the pathways in which IAPs play an important role are summarised in Fig.I-4.

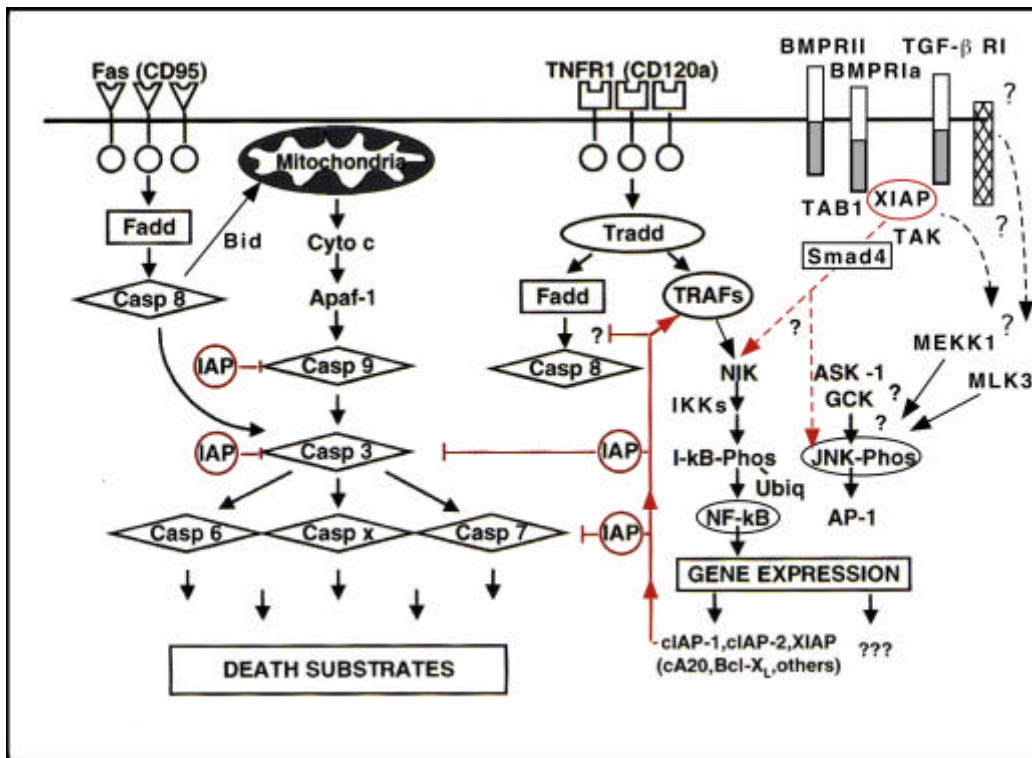


Fig.I-4: The possible IAP interactions within the cell and involvement in apoptosis regulating signal transduction pathways. Many human and *Drosophila* IAPs have been shown to directly block caspase 3, 7 and 9 activity. IAPs may also influence NF- κ B and JNK signal transduction pathways through TNFR1- and TNFR2-type cytokine receptors. Very recently, XIAP has been shown to be involved directly with TGF- β - and BMPR-signalling, both in humans and *Drosophila*. Many of these assigned functions are however preliminary, and require verification. (Mod. [56])

I.6.3. IAPs and direct caspase inhibition

The original discovery of the *baculovirus* IAP as an apoptosis inhibitory molecule naturally led to extensive investigation to determine at which level this inhibition took place. It soon became clear that the IAPs were a major modulator of caspase activity. One of the earliest observations characterised XIAP as a molecule that could not only inhibit caspase activity but also bound caspases 3 and 7 directly *in vitro* [69]. The growth in knowledge about XIAP function occurred hand in hand with an increased understanding of the cellular death machinery, in particular the

circumstances under which the caspases are activated. Many recent discoveries illustrate the complexity and the fine balance required in maintaining tissue homeostasis.

Whilst c-IAP1 and c-IAP2 have been shown to prevent binding and activation of caspase 8 to the TNF receptor [40], they can also bind to and inhibit the effector caspases. Similarly, although XIAP is a bridging protein at the receptor level in TGF- β and BMP receptor signalling, it too inhibits effector caspases. Indeed, XIAP, cIAP-1, cIAP-2 and even Survivin have been shown to bind and potently inhibit caspases 3,7 and 9 [69] [70], but not caspases 6, 10 or 8, making the IAPs the only known cellular inhibitor of caspases which target the enzymes directly, rather than indirectly affecting their activation. The specific regions responsible for this caspase binding have also recently been solved by crystal structure analysis. Interestingly, binding to caspases 3 and 7 requires BIR2 and the flanking 'linker' region of XIAP [71] [72], whilst caspase 9 recruitment takes place via BIR3 [55].

As already mentioned, apoptosis signalling via the mitochondrial pathway involves formation of the apoptosome, containing a number of different molecules, including cytochrome c, dATP/ATP, Apaf-1, and caspase-9. The intimate involvement of XIAP with caspases made it somewhat unsurprising that the process of caspase inhibition could also take place at the apoptosome. Beyond the aforementioned molecules, XIAP was also found within the apoptosome, in association with processed caspases-9 and -3. Furthermore, XIAP was shown to interact directly with Apaf-1, and was partially responsible for maintaining active caspase-3 within the complex [73]. These observations shed further light on the effectiveness of IAP mediated caspase inhibition, since by keeping the active effector caspases imprisoned within the apoptosome, cell destruction cannot take place.

I.6.4. Regulation of IAP function

Insights gained from the *Drosophila* system suggested that IAPs are subjected to regulation by cellular proteins. The *Drosophila* IAPs, DIAP-1 and DIAP-2, as well as the *baculovirus* IAPs OpIAP and CpIAP have been shown to interact with a number of cell death proteins. These include the aptly named Reaper (RPR), GRIM, HID and DOOM [74] [75]. Expression of these genes promotes apoptosis that can be suppressed by coexpression of the viral or *Drosophila* IAPs. Indeed RPR, HID and GRIM all contain a 14 amino acid sequence necessary and sufficient for inducing apoptosis and for binding IAPs. This suggests that it is the binding and subsequent neutralisation of IAPs by these death molecules that allows apoptosis to proceed unhindered [76].

It is possible to envisage a mechanism whereby these death molecules capture IAPs allowing the IAP inhibitable molecules such as caspases to carry out their task unopposed.

Although these *Drosophila* molecules are equally deadly in mammalian cells, the homologues thereof have yet to be identified. Very recently however, two groups of researchers simultaneously discovered the putative functional human and mouse homologues of these *Drosophila* regulators. Smac/DIABLO is a protein which resides in the mitochondrial intermembrane space (IMS), and is cleaved and subsequently released into the cytosol during apoptosis [18] [19]. Once in the cytosol it is able to compete for the caspase binding domains of the IAP proteins, and thereby antagonises IAP anti-caspase function in much the same way as the *Drosophila* death-inducing proteins. Specifically, this binding takes place at BIRs 2 and 3 of XIAP, through a tetrapeptide motif at the N-terminus of Smac/DIABLO (AVPI) which is also present on processed caspase-9 (ATPF) [77] [78] [79]. In concordance with RPR, HID and GRIM, Smac/DIABLO is also able to induce cell death when overexpressed in cells. The authenticity of Smac/DIABLO as a functional analogue was hotly contested very recently, when another group could show that Smac/DIABLO exists as multiple splice variants (Smac β , Smac γ , Smac δ), and that even a variant lacking the IAP-binding domain was able to potentiate apoptosis to the same extent as Smac. Although it seems clear that Smac/DIABLO does play an important role in regulating IAP function, its main pro-apoptotic function may be due to a mechanism other than IAP binding [80].

I.6.5. The IAP RING domain.

The BIR domains of IAP proteins have received the greatest attention in regard to understanding their functional relevance. However, the RING finger domain, present in most IAP members, also makes an important contribution to their cellular roles. Until recently, no specific function had been ascribed to RING finger domains, other than an involvement in dimerisation, although a large number of unrelated proteins possess such a domain. This changed with the realisation that RING finger proteins play critical roles in mediating the transfer of ubiquitin (Ub) both to heterologous substrates as well as to the RING finger proteins themselves. Protein ubiquitination involves the sequential action of Ub activating enzyme (E1), a Ub conjugating enzyme (E2), and a Ub protein ligase (E3), leading to the transfer of Ub, and formation of multi-Ub chains on proteins. These multi-Ub chains are potent targeting signals for protein degradation in proteasomes [81]. Indeed, the RING domains of XIAP, c-IAP1 [82] and c-IAP2 [83] have been

show to catalyse their own ubiquitination, indicating that they may also play an important role in self-regulation of their abundance and activity. Whether IAPs are also able to catalyse the ubiquitination of other molecules, and what these substrates may be, is still unclear.

In addition to this Ub ligase activity, the RING finger domain is important in mediating an alternative signalling event. XIAP was identified in connection with BMP signalling, by virtue of its interaction with the intracellular domain of the BMPR-1A in a two-hybrid screen. Since this interaction took place via the RING domain of XIAP, there is clearly more to it than solely ubiquitination. Furthermore, binding via the RING domain enabled TAB1 to bind to the BIR domains forming a bridging complex recruiting the signal transducer TAK1 [65]. The functional versatility of the RING domain clearly suggests a broader spectrum of potential targets still awaits discovery.

1.7. The Bcl-2 family in apoptosis regulation

Another group of proteins important in the regulation of apoptosis is the Bcl-2 family. These proteins also regulate an ancient cell death pathway, present in nematode worms, *Drosophila* and mammals. This diverse protein family can be divided into three distinct groups. Bcl-2 and its close relatives inhibit apoptosis whereas structurally similar relatives such as BAX, and more distant members such as BAD, are arbiters of cell death. These opposing groups govern the commitment of a cell whether to undergo apoptosis or not, with their focus of activity mainly at the mitochondria. The Bcl-2 family is one of the major groups of proteins, which determine whether the apoptosome can assemble.

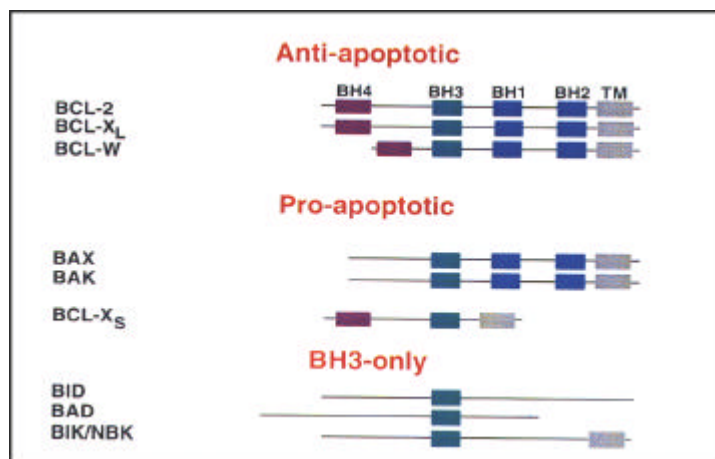


Fig.I-5: A cross section of some of anti-apoptotic and pro-apoptotic Bcl-2 members. Bcl-2 homology regions (BH1-4) are denoted, as is the carboxyl-terminal hydrophobic transmembrane (TM) domain. (Mod. [85])

Although the mechanism is not entirely clear, Bcl-2 family members appear to play a role in maintaining or disrupting mitochondrial membrane integrity. Again, protein domains contribute significantly to this: The Bcl-2 and Bax subfamilies share three of the four BH (Bcl-2 homology) sequence motifs, and can assume a similar conformation, whereas members of the third subfamily share only the BH3 domain. Some members of the Bcl-2 family and the domains they contain are described in Fig.I-5. These domains and Most members of the Bcl-2/Bax family possess a hydrophobic C-terminal segment which facilitates their interaction with the endoplasmic reticulum (ER), nuclear envelope, and in particular the outer mitochondrial membrane. The anti-apoptotic members normally reside at the mitochondria, and most others assemble during the process of apoptosis.

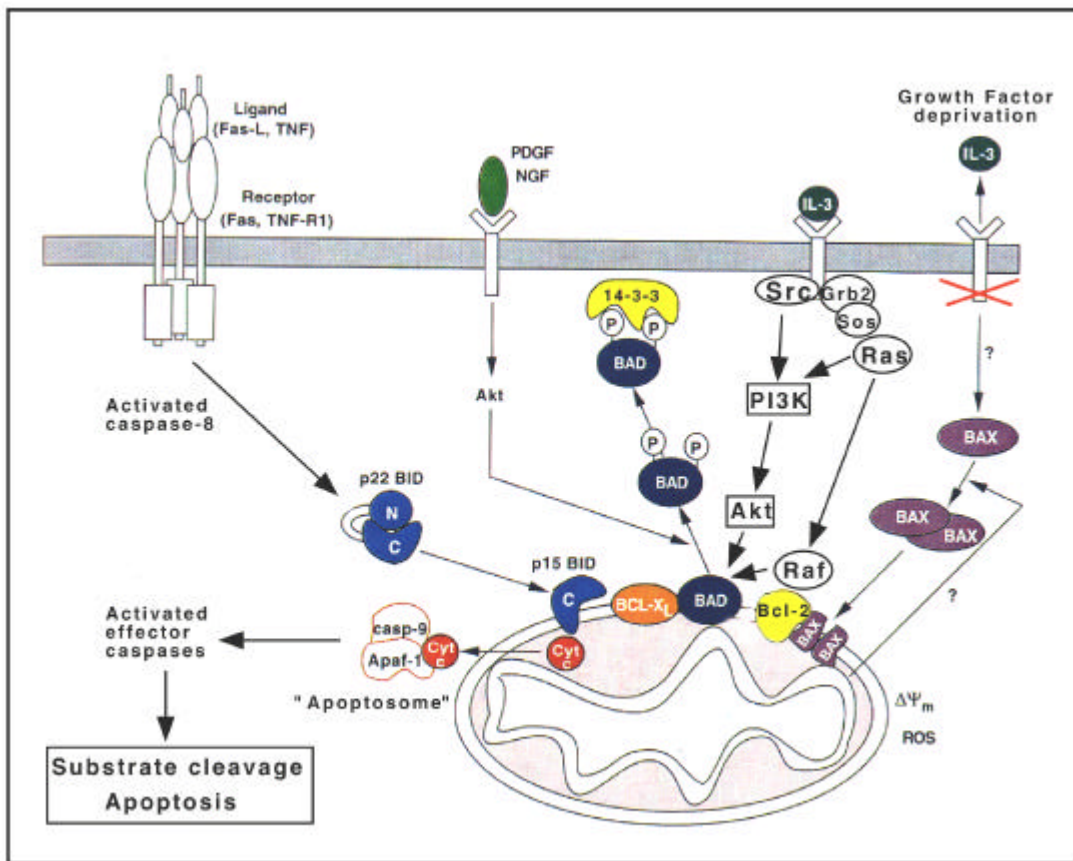


Fig.I-6: A model of apoptotic and growth factor survival signalling pathways involving the Bcl-2 members. Activation of the TNF α /Fas cell surface receptor leads to activation of caspase-8, which in turn cleaves BID. The p15 BID subsequently translocates to the mitochondria resulting in the release of cytochrome c. Cytochrome c release sets off a set of events leading to apoptosome formation and ensuing caspase cascade activation. Activation of growth factor receptors such as the NGF, PDGF and IL-3 receptors mediates the activation of signalling molecules such as Raf and Akt, which are in turn able to phosphorylate BAD. This removes BAD from the mitochondria, where it usually exerts its pro-apoptotic effects. Withdrawal of the growth factor returns BAD and induces the translocation of BAX to the mitochondria. (Mod. [85]).

Bcl-2 overexpression is able to prevent mitochondrial disturbances associated with apoptosis, such as pH change, membrane permeability and outer membrane integrity, and thereby prevent the escape of apoptogenic molecules from the IMS and subsequent downstream apoptosome formation [84] [85].

An important means of controlling some of the pro-apoptotic elements relies on signal transduction via growth factor/ cytokine receptors, described in earlier chapters. As mentioned in previous sections, phosphorylation of BAD at the mitochondria by the Raf kinase neutralises its function by allowing the adapter molecule 14-3-3 to bind and abrogate its pro-apoptotic capability [44]. Similarly, Activated AKT initiates 14-3-3 binding by phosphorylating BAD at serines-136 and -112, at consensus sites bearing the motif RXXRXXS/T, in stimulated cells [86] [45]. Denial or deprivation of the GF however has dire consequences for the cell, allowing BAX and BAD to promote cell death [46]. Depicted in Fig.1 is a summary of some of the signalling pathways which converge on the mitochondria, highlighting the interplay between these cascades and Bcl-2 proteins. It is clear that many signalling events are important in determining cell fate [87], and certainly Raf and AKT may be capable of targeting other mitochondrial associated proteins (V. LeMellay, personal communication). One useful model cell system often employed in the study of GF deprivation is the 32D promyeloid leukaemic cell line. These cells may be maintained undifferentiated in cell culture by supplementation of the medium with the essential growth factor Interleukin-3 [88]. However, GF withdrawal results in induction of apoptosis, which can be delayed by forced expression either of the anti-apoptotic Bcl-2 proteins, or by molecules involved in the signal transduction events [89] [90].

I.8. NRAGE and the p75 neurotrophin receptor

Neurotrophins exert their effect by binding two types of cell surface receptors: The Trk receptors are receptor tyrosine kinases, whereas the second type of neurotrophin receptor belongs to the TNF receptor superfamily and is known as the p75 neurotrophin receptor (p75NTR). Although there is a certain amount of cooperation between the two receptors, the precise physical arrangement of the p75NTR with the Trk receptors is unknown, and both receptors co-distribute on cell surfaces. Whereas the Trk receptors are predominantly involved in survival, proliferation and differentiation signalling, the evidence suggests that the p75NTR tends to elicit cell death signals, as several studies have shown *in vitro* and *in vivo* [91] [92]. However, the mechanism by

which this occurs is generally unknown. In accordance with other TNF receptors, signalling via the p75NTR also results in JNK and NF- κ B activation, and although the mechanism is again rather vague, the involvement of TRAF molecules has been hinted at [93]. Further efforts aimed at defining the effector molecules of p75NTR apoptotic signalling revealed BAX [65], some caspases and the Fas-associated phosphatase-1 [94]. New data has also shown the recruitment of the RhoA GTPase to the pseudo-death domain of p75NTR [95].

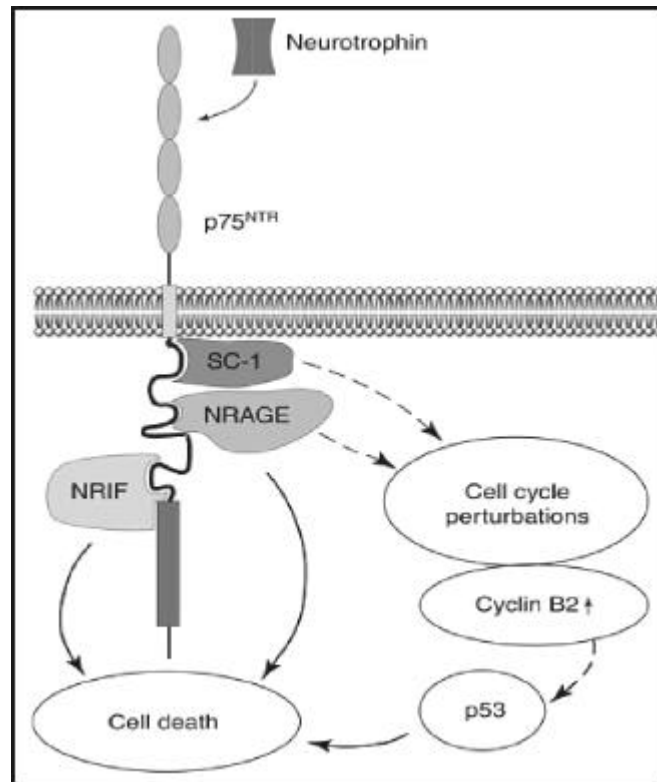


Fig.I-7: p75NTR apoptotic pathways. The intracellular part of the receptor consists of the juxtamembrane region (black line) and the death domain (grey rectangle). SC-1, NRIF and NRAGE have been identified as directly binding to the receptor, and have been shown to play role in NGF-p75NTR mediated apoptosis. The solid arrows represent experimental observations, whilst the broken arrows are hypothetical. (from Trends in Neuroscience)

Another line of experimental evidence puts forward the possibility that apoptosis is a secondary effect caused by the interference with cell cycle progression. Retinal neurones overexpress cyclin B2 after NGF stimulation *in vitro*, and re-enter the cell cycle before any cell death occurs [96]. A possible link between cyclin B2 and death is the tumour suppresser gene p53, which has been shown to mediate p75NTR induced apoptosis [97]. Further evidence for this line of thought comes from a newly described p75NTR-interacting protein. SC-1 was shown to interact with the intracellular domain of the p75NTR, and translocated to the nucleus after NGF binding [98]. Whilst SC-1 had no effect on apoptosis, the newly identified neurotrophin receptor

interacting factor (NRIF), a zinc finger protein, actively participated in cell death [99]. It has not been determined however, if this involves cell cycle disruption or not.

Late last year came the identification of NRAGE, the neurotrophin-receptor interacting MAGE homologue, in a two-hybrid screen with the receptor's intracellular domain (see Fig.1-7). Reconstitution experiments using the sympato-adrenal MAH cell line, which does not express Trk, p75NTR or NRAGE, showed that the formation of p75-NRAGE and p75NTR-TrkA complexes are mutually exclusive, and that the expression of both p75NTR and NRAGE were necessary to convey the apoptotic signal after NGF stimulation. Interestingly, NRAGE did not bind the death domain, but rather an 80 amino acid juxtamembrane domain. Furthermore, stimulation of PC12nr5 cells (a mutant cell line lacking Trk receptors) with NGF resulted in a shift of endogenous NRAGE to the plasmalemma cell fraction, although the expression in cytosol and nuclear fraction remained constant. In addition, transient overexpression of NRAGE in HEK293 cells also seemed to strongly retard cell cycle progression [100]. Thus NRAGE was shown as a novel link between receptor signalling and apoptosis pathways.

I.9. Experimental design and aim of the project

At the beginning of my doctoral thesis, very little was known about how IAPs performed their death-inhibitory roles. The early indications were that IAPs could effectively neutralise caspase activity via direct binding [69]. Observations made in our group indeed showed that the expression of ITA, the avian IAP homologue, could prevent TNF induced apoptosis in PC12 cells, albeit by an unknown mechanism [101]. This showed that despite the species disparity, IAP proteins maintain a very strong functional conservation, in addition to a high structural similarity. This had been previously indicated for *Drosophila* and viral IAPs [75]. A more unexpected finding was that ITA also blocked NGF mediated differentiation in these cells [101]. This implicated IAPs in a previously undescribed cellular function. Furthermore, ITA co-immunoprecipitated with Raf, a key player in the mitogenic signal transduction cascade. That Raf and ITA did not interact in the two-hybrid system suggested other molecules might be important in these processes.

In order to understand at what level ITA interfered with these processes, a yeast two-hybrid screen was the chosen method. This technique had proved invaluable in identifying novel protein interactions and discovering new genes. Since the observations from our group indicated that ITA could intercept cellular signals in PC12 cells, the library chosen for the screen was derived from a PC12 cells [101]. It is of course possible, at least in part, to predict the outcome of such a screen given the available knowledge on IAP-interacting proteins [58] [102] [69] [101]. The most interesting interactions are however those which are unpredictable. The result of this screen and subsequent analyses of novel IAP-interacting proteins, their roles in apoptosis signalling, and their influence on cell death will be described in the following chapter.

RESULTS

II-1 The identification of a novel IAP interacting protein

The yeast two-hybrid screen is a very useful tool for identifying novel interactions, but this is only if certain criteria are met. It is therefore important to optimise three conditions that lead to a successful screen. Firstly, the expression of a large exogenous protein in yeast cells can lead to cytotoxicity, even if the protein itself is under normal circumstances non-toxic. In this case, Gal4DB-ITA was found not to be toxic, and yeast cells were able to grow unhindered by the expression of the "bait" construct (data not shown). Secondly, the Gal4DB-ITA fusion protein should not autonomously activate any of the reporter genes in the yeast cells, either when expressed alone or when co-expressed with the "prey" vector. The transformed yeast were unable to grow under -LEU-TRP-HIS selection conditions when singly expressing the fusion protein or when the prey vector was co-expressed (data not shown). Finally, it is critical that the bait fusion protein is expressed in the yeast cells after transformation with the plasmid DNA. Yeast protein lysates transformed with Gal4DB-ITA or Gal4DB were subjected to SDS-PAGE, transferred to nitrocellulose, and immunoblotted with an α ITA antibody. Fig. II-1 shows the expression of the Gal4DB-ITA fusion protein in the yeast strain HF7c. This yeast strain has a weak promoter in the reporter genes, reducing the likelihood of non-specific reporter gene activation. Therefore the initial criteria were met to confidently proceed with a two-hybrid screen (Clontech).

The result of the screen is described in table II-1. The analysis of these clones, i.e. their identification, their authenticity as IAP-binding proteins, and their functional relevance will be described in this section of the dissertation.

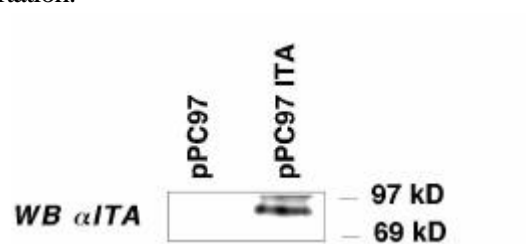


Fig. II-1: The Gal4DB-ITA fusion protein is expressed in yeast Yeast were transformed with either pPC97 or pPC97-ITA, and grown in selective culture media for 48 hrs, then lysed and electrophoresed on a 10% denaturing polyacrylamide gel and then transferred to nitrocellulose. The membrane was probed with an α ITA antibody. A band representing Gal4DB-ITA can be seen in pPC97-ITA expressing yeast but not pPC97 containing yeast.

II-1.1 The result of the two-hybrid screen

Reporter yeast-strain:	HF7c
Source of the cDNA Library:	Mitotic rat PC12 cells
Bait-vector:	pPC97 ITA
Cotransformation efficiency:	500 cfu / μ g DNA
Amount of Library-plasmid used:	2400 μ g
Number of screened clones:	3.6×10^6
Number of times through library:	0.5
HIS-positive clones (diameter > 2mm):	32
β -Gal-positive:	8
Positives after elimination of false positives:	3

Table II-1: The yeast two-hybrid screen results in 3 genuine positive clones. HF7c yeast strain was transformed first with the bait plasmid, and then with the library plasmids, at an efficiency of 500cfu/ μ gDNA. 3.6×10^6 independent clones were screened, from a library with a complexity of roughly 7.5×10^6 independent clones, indicating that roughly half the library was screened. 32 clones were able to grow on the triple nutrient marker deficient plates, and of these 8 were β -gal positive. Finally, after retransformation, 3 genuine positives remained.

The yeast two-hybrid screen resulted in 32 -Leu-Trp-His positives colonies. Of these, 8 turned blue in the β -galactosidase assay. The „prey“ plasmids from these β -galactosidase positive clones were then recovered by picking the yeast colonies still containing both plasmids and growing in liquid culture with TRP1 deficient media. This causes redundancy and therefore loss of the Leu2 nutrient marker-containing bait vector. The plasmids were then isolated and restriction analysis was performed to distinguish the prey vectors from the residual bait vector. These were then retransformed into the yeast in parallel with control transformations. This procedure further eliminated 5 false positives, leaving 3 genuine positive interactions from the screen that interacted specifically with ITA, and not with the bait vector. These cDNA clones were then amplified in bacteria, re-isolated, and subjected to sequence analysis.

Upon receipt of the DNA sequences, each clone was translated into its corresponding amino acid sequence. The correct reading frame was derived from the reading frame of the Gal4AD, since these prey clones should code for fusion proteins without any termination signals between the AD and the first amino acid of the protein of interest. All three clones were found to contain full open reading frames (ORFs). These results were obtained using the Lasergene Navigator software package. Next, the cDNAs could be identified using the National Center for

Biotechnology Information (NCBI) Basic Local Alignment Search Tool (BLAST) program. BLAST is a powerful analytical tool which compares a given nucleotide sequence against other nucleotide sequences stored in a database. The first search using the non-redundant database containing previously identified cDNAs proved negative for all three clones. This suggested that none of the interacting cDNAs had been previously described. The sequences were then submitted to a database containing "expressed sequence tags" (ESTs), which are collections of sequences of short reverse transcribed mRNAs, randomly generated and sequenced. This database returned several hits for each clone, indicating that all three cDNAs were previously undescribed, but nevertheless genuinely expressed genes.

```

                20          30          40          50          60
DN  GCTAGTCCCAGAGTTCACAGCCCCCAACTGCCAATGAGATGGCTGACATTCAGGTTCA 68
    A  S  P  Q  S  S  Q  P  P  T  A  N  E  M  A  D  I  Q  V  S
    A  S  P  Q  S  S  Q  P  P  T  A  N  E  K  A  D  T  E  V  S
THC GCTAGTCCCAGAGTTCACAGCCCCCAACTGCCAATGAGAAGGCTGATACTGAGGTTTCA 252
    200          210          220          230          240          250

    70          80          90          100          110          120
DN  GCAGCTGCCGCTAGG---CTAAGTCAGCCTTTAAAGTCCAGAATGCCACCACAAAAGGCC 125
    A  A  A  A  R  L  2  S  A  F  K  V  Q  N  A  T  T  K  G  P
    A  A  A  A  R  K  3  T  G  F  K  A  Q  N  T  T  T  K  G  P
THC GCAGCTGCTGCCAGGCCTAAG--ACAGGCTTTAAGGCCCAGAATACCACCACAAAAGGGGC 310
    260          270          280          290          300

```

Fig. II-2: A short excerpt of the identity between THC179960 and DNRAGE. TIGR clone THC179960 (THC) shows a very high (>95%) identity with the Δ NRAGE (Δ N) two-hybrid clones.

The Institute of Genomic Research (TIGR) also provides an Internet based search tool incorporating the information about sequenced ESTs. They took this data a step further in that they assembled overlapping ESTs in order to form a tentative human consensus (THC) "electronic clone". One such clone, THC179960 showed a very high identity with each of the three cDNAs, a short excerpt of which is shown in Fig.II-2. THC179960 was later identified as NRAGE, and therefore the two-hybrid clones are given the nomenclature Δ NRAGE followed by their molecular weight on SDS-PAGE. This provided two very important pieces of information. Firstly, this showed that the three clones from the two-hybrid screen belong to one gene. Secondly, it meant that these were incomplete parts of a larger cDNA, as represented in Fig.II-3. Furthermore, since the two-hybrid clones were pulled out of a rat library, and showed very high

identity with the human THC179960, it is also probable that this gene is conserved amongst mammals.

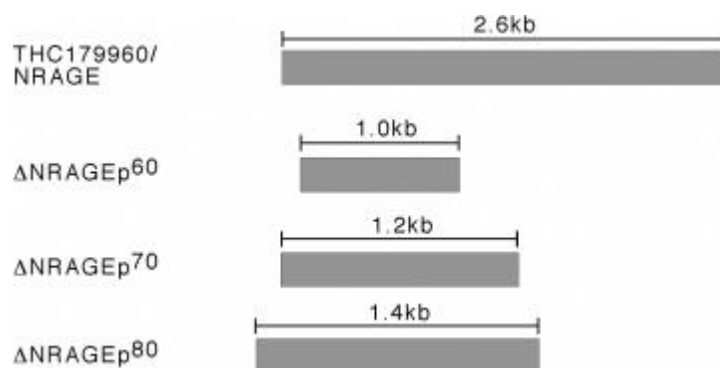


Fig. II-3: Schematic representation of the three overlapping two-hybrid clones compared with THC179960.

II-1.2 direct yeast two-hybrid tests

The IAP family comprises many proteins, with varying degrees of identity between the individual proteins. c-IAP1, c-IAP2 and XIAP bear the greatest identity with ITA. It was therefore interesting to see whether these IAPs also interact with the Δ NRAGE clones. In addition, the neuronal IAP, NAIP, was also tested. Interestingly, all three two-hybrid clones interacted with human XIAP, but not with human c-IAP1, c-IAP2, and neither with murine NAIP. The bait vector was added as a negative control. This indicated that the Δ NRAGE truncated proteins showed specificity for ITA and XIAP, as depicted in table II-2, strengthening their case as IAP interacting proteins.

<i>Cotransformants</i>	<i>Relative intensity of b-Gal test</i>
Δ NRAGE + ITA	+++
Δ NRAGE + c-IAP1	-
Δ NRAGE + c-IAP2	-
Δ NRAGE + XIAP	+++
Δ NRAGE + NAIP	-
Δ NRAGE + Gal4DB	-

Table II-2. Δ NRAGE also interacts with human XIAP. The three two-hybrid clones interact with XIAP with the same β -gal intensity as ITA in direct two-hybrid tests, but not with any of the other mammalian IAPs. The given cDNAs were cotransformed in yeast and spread onto -LEU/-TRP plates and subsequently streaked out on membranes and placed onto -LEU/-TRP/-HIS plates. After 48hrs Xgal tests were performed, and the relative intensities noted after 4hrs.

II-1.3 Mammalian two-hybrid test

The experiments described until now have been performed solely in yeast cells. It was important that these results were repeated under more physiological conditions. For this reason, the "mammalian two-hybrid test" was employed (Clontech). This allowed the interaction to be tested in higher eukaryotic cell types, which normally express XIAP and Δ NRAGE [69] [100].

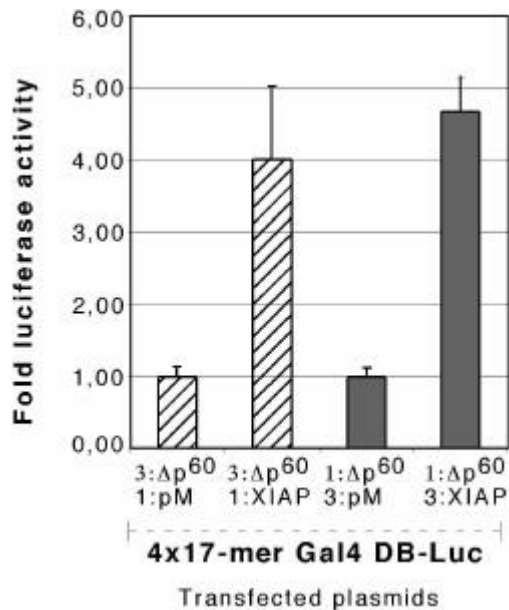


Fig. II-4: XIAP and Δ NRAGEp60 interact in the mammalian two-hybrid system HEK 293 cells were transiently transfected with VP16- Δ NRAGEp60 (Δ p⁶⁰) and either the Gal4DB-vector (pM) or the Gal4DB-XIAP (XIAP), together with a 4x17-mer Gal4DB-Luciferase reporter construct, and a CMV- β Galactosidase to control transfection efficiency. After 24hrs, the cells were lysed and luciferase activity was measured. Values were standardised using protein concentration and ONPG activity of the β gal construct. The values represent two experiments performed in duplicate. The hatched boxes represent a 3:1 DNA ratio of VP16- Δ NRAGEp60:pM/XIAP, whereas the solid boxes represent a 1:3 DNA ratio VP16- Δ NRAGEp60:pM/XIAP. The fold induction of luciferase activity in each test is measured against the baseline activity of pM with VP16- Δ NRAGEp60. The error bars denote standard deviation.

The activation of a luciferase reporter gene can only occur when the Gal4DB and VP16 transcriptional activator assemble together to form a complex with this reporter construct, analogously with the yeast system (Clontech). In Fig.II-4 the luciferase activities are standardised on the vector control, and given in fold activity induced by XIAP- Δ . This resulted in a 4-5 fold induction of luciferase activity suggesting Δ NRAGE p⁶⁰ can be recruited to the reporter construct by XIAP. This induction is also independent of the relative ratios of transfected DNA of VP16- Δ NRAGE p⁶⁰:pM/pMXIAP. The outcome of this experiment provided the evidence to suggest that this interaction was indeed as genuine for the mammalian system as it was for the yeast environment.

II-2 The molecular cloning of the complete *nrage* cDNA

The largest two-hybrid clone was 1.4 kb in length, contained an uninterrupted ORF, and did not contain a polyadenylation signal. Furthermore, the electronic clone THC179960 had a predicted length of 2.6 kb. Taken together, this suggested that even the largest two-hybrid clone contained merely a truncated cDNA. Therefore it was of the utmost importance to obtain the full cDNA of this gene for further functional analysis.

II-2.1 Expression and screening for *nrage* in S194 plasmacytoma

There are many methods available to obtain full cDNAs from incomplete sequences. These include standard PCR, RACE PCR (rapid amplification of cDNA ends) or library screening. In order to assess whether these were an option, an initial Northern blot was performed. Fig.II-5 shows that these transcripts are highly expressed in the murine NIH 3T3 fibroblast cell line also in the murine S194 plasmacytoma cell line.

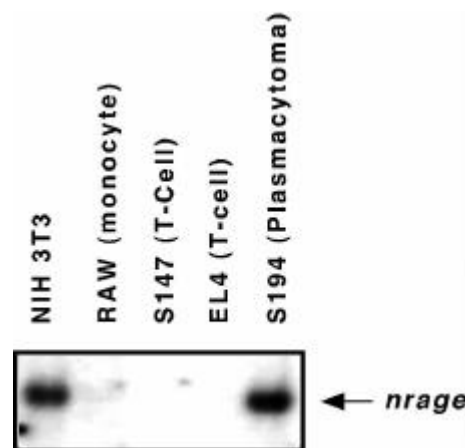


Fig. II-5: the *nrage* mRNA is highly expressed in NIH 3T3 cells and in the S194 murine plasmacytoma cell line. 10 μ g total RNA from various cell lines was separated on a denaturing 1% agarose gel, and Northern blot analysis was performed with radioactively labelled *Dnragep80* probe. Strong signals were only observed with NIH 3T3 and S194 RNA.

The high transcript expression in S194 cells indicated that a bright option for obtaining the complete cDNA would be through screening a bacterially expressed S194 cDNA library available at our institute. The complete cDNA was thus isolated from the library by colony hybridisation after several amplification rounds, using the largest two-hybrid insert as a radioactively labelled probe. The original positive colonies are shown in Fig.II-6, and were

derived from a single clone. The resultant clone was 2.6 kb in length, with a putative translation initiation sequence at its 5' as well as a polyadenylation signal at its 3', and a polyadenylation tail.

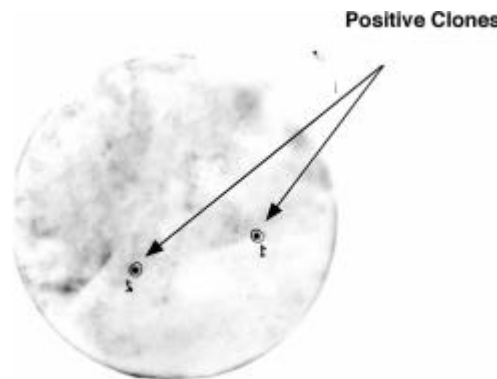


Fig. II-6: The full length *nrage* cDNA is successfully cloned from an S194 cDNA library. 1×10^6 bacterial colony forming units were plated out on 160mm agar plates, and colony hybridisation was performed using an $[\alpha\text{-}^{32}\text{P}]\text{dCTP}$ labelled ΔNRAGEp^{80} probe, and finally an Xray film was overlaid on the membranes. The two initial positive clones shown above were subjected to several rounds of enrichment until single positive bacterial clones could be easily identified

II-2.2 Analysis, modification and expression of the complete *nrage* cDNA

The complete cDNA was sequenced through twice, with ambiguous or unreadable stretches re-examined to determine whether these required further sequencing with alternative primers. The sequence information was put together using the Lasergene Navigator software system, and a consensus sequence incorporating the data from each sequence reaction was established. The DNA consensus sequence was then translated into the predicted amino acid sequence, shown in Fig.II-8A. Closer inspection revealed a number of translation termination codons. The first appeared at amino acid 29, and was followed by a potential translation initiation codon at position 47, indicating that this stop codon possibly belonged to the 5' untranslated region of the gene and was therefore legitimate. In the carboxyl-terminal region, a cluster of termination codons appeared from amino acid 792, which also appeared to be legitimate. Surprisingly however, the triplet 1140-1142 (responsible for $\alpha\alpha 381$) was also a stop codon. This stop codon was not present in the corresponding region of the clones identified in the two-hybrid screen. This suggested that it was either a mutation specific for the S194 cell line, or that this was a DNA polymerase proof-reading error caused during the amplification of the cDNA library [103]. In order to resolve this question, S194 mRNA was reverse transcribed (RT), and then the region of the cDNA where the stop codon appeared was amplified with specific primers, utilising the polymerase chain reaction (PCR), and then sequenced. The results of these DNA analyses are

shown in Fig.II-8B, and clearly indicate that the stop codon is due to a single base exchange at position 1141. In the original cDNA clone, position 1141 is an adenine, flanked by 5' by a thymine and 3' by a guanine. In the NRAGE ORF this mutation (TAG) leads to a translation termination signal. In the RT-PCR S194 mRNA however, position 1141 is a guanine nucleotide, which changes the code to a TGG, resulting in the amino acid tryptophan. This would suggest that a proof reading error by the DNA polymerase during the amplification of this cDNA library is responsible for the mutation.

It was therefore necessary to undo this erroneous nucleotide exchange, since this would result in the translation of a truncated protein. Site directed mutagenesis was the method chosen to return the adenine to a guanine nucleotide. As seen in Fig.II-8B, this technique was successful in re-introducing the guanine to position 1141. Since this process also involved PCR amplification, the resultant cDNA was sequenced once again to ensure there were no further proof-reading errors created.

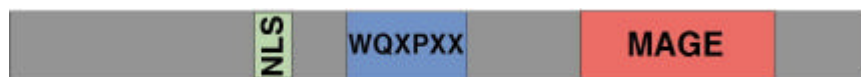


Fig. II-7: The primary structure of the NRAGE protein highlighting the domains of interest. The full cDNA was translated into the corresponding amino acid sequence in order to identify possible known protein motifs. The information from several database searches is summarised in this figure. A potential nuclear localisation signal (NLS), a 25×WQXPXX domain repeat, and a melanoma-associated antigen (MAGE) domain is represented.

Having obtained the full coding sequence of this previously undescribed gene, this was then resubmitted to the BLAST database, in order to see if the new sequence information would provide some further clues as to whether this protein had any known relatives. The results of this new search showed that indeed the NH₂-terminal part of the protein bore a high homology to a large protein group known as the MAGE (melanoma associated antigens) family. Disappointingly however, despite awareness of these proteins for over a decade, hardly any information was available regarding their physiological role in cell function. Most of the investigative work centred on the finding that without exception, these genes and the many splice variants thereof, show a highly restricted expression pattern. The only terminally differentiated tissue in which some of these genes are expressed are testes, whereas many tumours are known to harbour these proteins. To such an extent that they are regarded as targets for anti-tumour therapy [104]. This new protein contained a unique domain however, and was significantly larger than any of the MAGE proteins, which suggested it may not belong to the classical MAGE family, but perhaps shares a functional MAGE domain. This new domain consists of an almost perfect

II-2.3 Protein expression of NRAGE confirms successful site directed mutagenesis

In addition to the sequencing evidence, to be certain that the *nrage* cDNA has been correctly mutagenised at nucleotide 1141, and that no further termination signals occurred as a result of this, the cDNA was cloned into the eukaryotic expression vector PCSM2+. The two-hybrid clones and the original cDNA were also placed in this vector, which expresses the protein with 6 c-Myc epitopes, and then transfected into HEK293 cells. The cells were lysed after 48 hrs, and 20µg protein from each of these lysates was subjected to SDS-PAGE, transferred to nitrocellulose and probed with a α -Myc antibody.

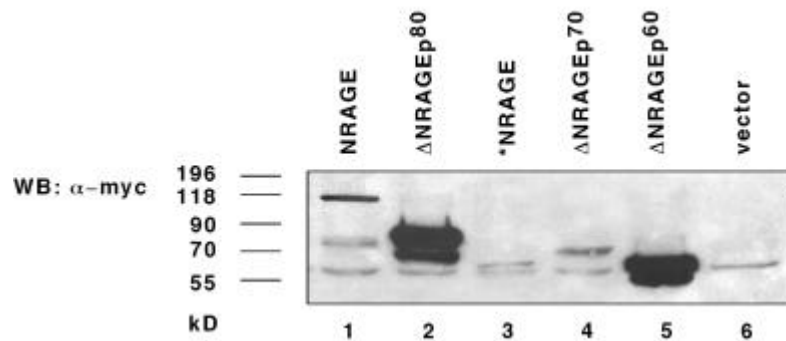


Fig.II-9: Confirmation *in vivo* of the sequence data by Western blot analysis of translated proteins. The original *NRAGE cDNA, together with the mutagenised NRAGE version and the original two-hybrid Δ NRAGE clones, were inserted into a mammalian expression vector in-frame with a myc epitope and transfected into HEK 293 cells. The cells were lysed after 48hrs, and 20µg protein was loaded on an SDS-PAGE transferred to a nitrocellulose membrane, and immunoblotted with a α Myc antibody.

The result is shown in Fig.II-9, and clearly demonstrates the truncated protein in lane 3 running just above the unspecific band at about 55kD, whilst the protein resulting from the cDNA with the nucleotide exchange at position 1141 runs much slower at around 110kD in lane 1. The two-hybrid clones can also be seen expressed as predicted from their uninterrupted ORFs in lanes 2, 4 and 5. Lane 6 shows the vector transfected negative control, with an unspecific crossreacting band at 55kD.

II-2.4 Distribution of expression pattern of *nrage* transcripts in adult mouse tissue

The only clue so far as to the type of family to which NRAGE belonged came from the sequence comparison data using the BLAST program. This showed a high identity between the Carboxyl-

terminus of NRAGE and the MAGE group of proteins. In order to find out if the expression pattern of *nrage* corresponded with that of the *mage* family, a multiple tissue Northern blot was constructed from the organs of inbred mice. This was then hybridised with a radiolabelled full-length cDNA NRAGE probe. In Fig.II-10A the result of this Northern blot is shown.

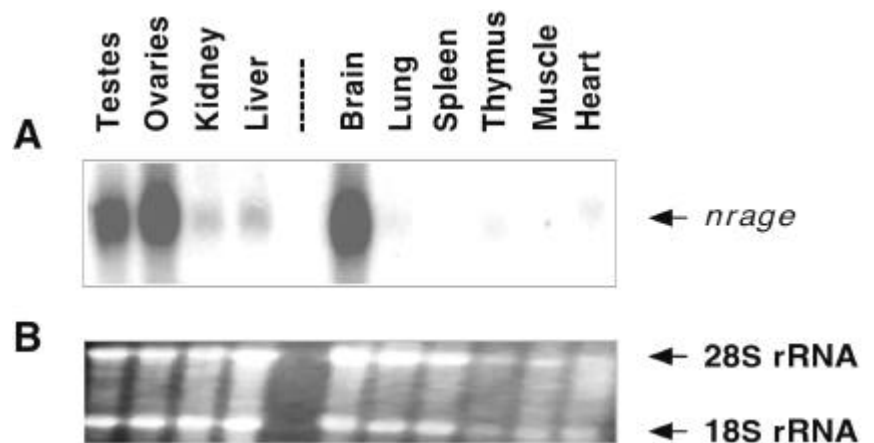


Fig.II-10: The *nrage* transcript is expressed in many adult mouse tissue types. 20 μ g total RNA from various adult mouse tissues was loaded onto a denaturing formaldehyde agarose gel, blotted onto a membrane and cross-linked with UV light. For panel A, the complete NRAGE cDNA was labelled with [α - 32 P] dCTP by random primer labelling, and hybridised O/N with the membrane. A photographic film was exposed to the membrane for two weeks, and then developed. In panel B the RNA was visualised with ethidium bromide prior to blotting to shown equal loading.

As with other MAGE domain containing proteins, there is indeed a high level of *nrage* expression in testis. In contrast with all previously identified *mage* genes however, this novel transcript is also expressed in many other terminally differentiated adult tissue types [104]. Most notable is the very high expression in brain and ovary, but expression is also detected in various other organs including kidney, liver, lung thymus and heart. Expression was not detectable in spleen or thymus tissue. This indicates that *nrage* still shows a restricted expression pattern, but much broader than that of any other previous *mage* gene, suggesting therefore that NRAGE is an important protein in normal tissues. It remains to be seen whether NRAGE also plays a role in tumours. Another observation made from this experiment was that *nrage* transcripts were of uniform length, unlike many of the *mage* genes which are often expressed in multiple splice forms [104].

II-3 Investigation of the IAP-NRAGE binding in co-immunoprecipitation experiments

Although the results of the mammalian two-hybrid system in section II-1.3 gave a good indication that the interactions observed in the yeast two-hybrid system were genuine, confirmation was required with more detailed examination.

II-3.1 ITA interacts with NRAGE via its RING zinc-finger domain

To independently confirm the ITA-NRAGE two-hybrid interaction, co-immunoprecipitations were performed. A Flag epitope was fused to in frame with the full coding sequence of NRAGE by PCR, and then cloned into the mammalian expression vector PGEZ-IEG5. HEK293 cells were then cotransfected with HA-tagged ITA, HA-ITA deletion mutants, and Flag-NRAGE. The results are shown in Fig.II-11.

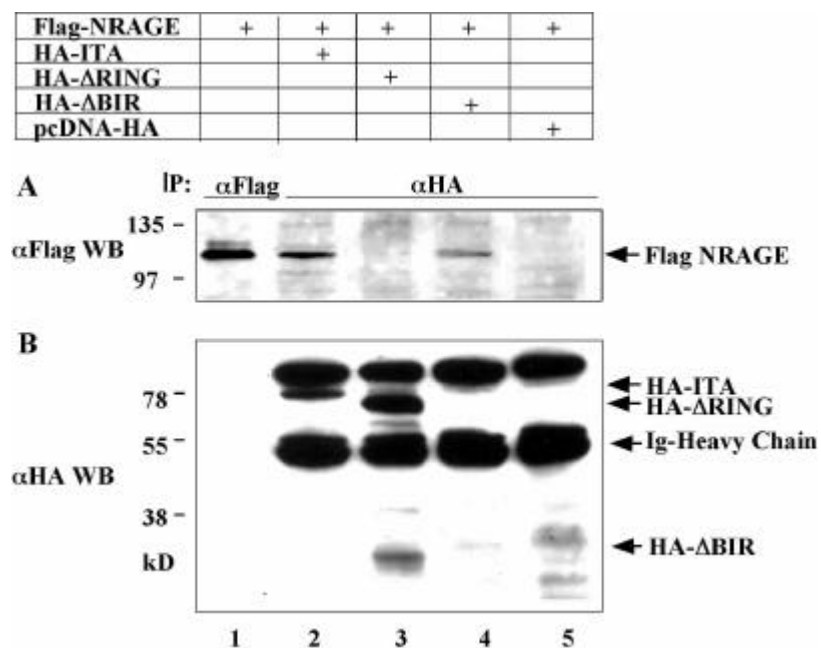


Fig.II-11:ITA coprecipitates with NRAGE in mammalian cells via its RING domain. In panel A, Flag-NRAGE is shown to coprecipitate with HA-ITA and HA-ΔBIR in mammalian cell lysates (lanes 2 and 4), but not with HA-ΔRING (lane 3). HEK 293 cells were transfected and proteins were immunoprecipitated after preclearing, with anti-HA antibody as indicated, washed twice with high salt NP40 and detected after SDS-PAGE with goat polyclonal anti-Flag antiserum. Lane 1 shows the positive NRAGE control, lane 5 the negative vector control. The immunoblot was stripped and reprobed with the 12CA5 anti-HA antibody to show the HA-ITA proteins (Fig. 2B).

NRAGE was immunoprecipitated and subsequently immunoblotted using a goat anti-Flag antibody (Fig.II-11A, lane 1) as a positive control. NRAGE was detectable after immunoprecipitation with the 12CA5 HA antibody using lysates from HA-ITA expressing lysates (Fig.II-11A lane 2), but not from control cells (Fig.II-11A, lane 5). Furthermore, NRAGE co-immunoprecipitated with an ITA deletion construct containing only the RING domain (Fig.II-11A, lane 4), but not with the deletion construct containing only the BIR domains of ITA (Fig.II-11A, lane 3). These interactions were able to withstand high stringency washes with 500mM NaCl. In Fig. II-11B the presence of the immunoprecipitated ITA proteins used in the co-precipitation experiments (lanes 2-5) was confirmed by stripping and reprobing the same membrane with the 12CA5 monoclonal antibody. These experiments demonstrate that ITA interacts with NRAGE with high affinity, and that this interaction occurs probably via ITA's carboxyl-terminal RING zinc-finger domain.

II-3.2 XIAP binds to NRAGE

The same strategy was applied to confirm the XIAP-NRAGE binding. HEK293 cells were transiently transfected with vectors expressing Flag-NRAGE and GST-XIAP, or Flag-NRAGE and GST only. In Figure II-12A NRAGE is co-precipitated with GST-XIAP (lane 2), whereas no coprecipitated protein was detected in the control sample (lane 3). NRAGE was immunoprecipitated and immunoblotted as a positive control (lane 1). The blot was stripped and reprobed using the rabbit polyclonal XIAP antibody to visualise GST-XIAP in the lower panel.

In Fig.II-12B, the reverse experiment was performed. GST-XIAP was co-immunoprecipitated with NRAGE (lane 2). Once again, this interaction was stable enough to withstand high salt washing conditions (500mM NaCl). Immunoprecipitated and immunoblotted GST-XIAP was used as the positive control (lane 2) while GST containing lysate was used as a negative control in this experiment (lane 3). The blots were stripped and reprobed using the Flag antibody to detect tagged NRAGE. These experiments confirm NRAGE as a novel XIAP interacting protein, with a strong binding affinity.

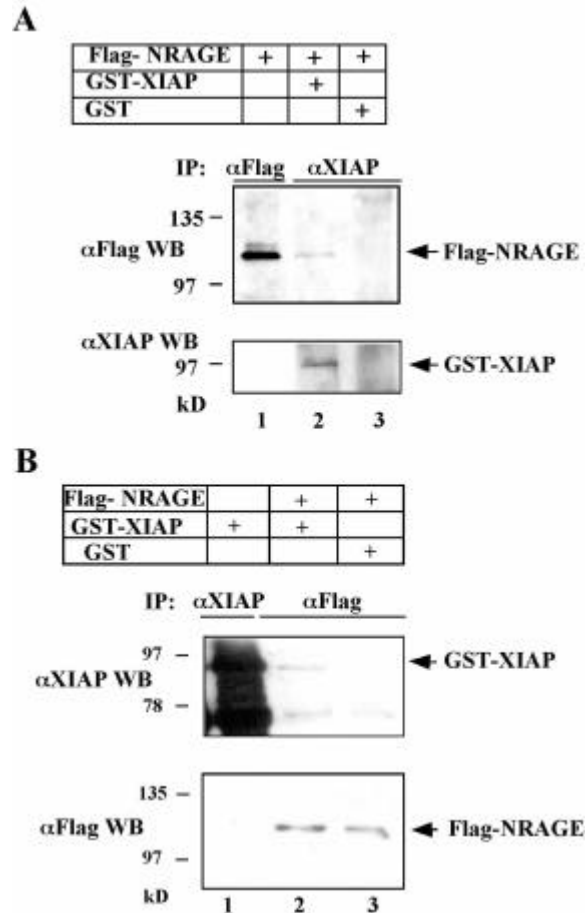


Fig.II-12: XIAP coprecipitates with NRAGE in mammalian cells. GST-XIAP or GST was transfected together with Flag-NRAGE in HEK293 cells as depicted. In Fig.II-12A, Flag-NRAGE coprecipitates with GST-XIAP in precleared cell lysates, after immunoprecipitation with a rabbit polyclonal anti-XIAP antibody, washing twice with high salt NP40, and subsequently detecting with goat anti-Flag antiserum (lane 2). Lane 1 shows the positive NRAGE control, lane 3 the negative GST control. The blot was stripped and reprobbed with anti-XIAP antibody. In Fig.II-12B, GST-XIAP coprecipitates with Flag-NRAGE in precleared transfected lysates, after immunoprecipitating with anti Flag M2 monoclonal antibody and washing with high salt NP40 (lane 2). The immunoprecipitates were subjected to SDS-PAGE and electroblotting, then detected with anti XIAP antibody. Lane 1 shows the positive control GST-XIAP, and lane 3 the GST negative control. The blot was stripped and reprobbed with goat anti-Flag to detect Flag-NRAGE.

II-4: The influence of NRAGE on apoptosis in 32D cells upon IL-3 withdrawal

IL-3 dependent 32D cells have been well studied with regard to the process of apoptosis induced by growth factor withdrawal [88] [105]. IL-3 is essential for survival of 32D cells mediated through many different signalling events, linking the receptor to cytosolic modulators of apoptosis, making this cell system a useful model to study apoptosis [46].

II-4.1 NRAGE expression in the IL-3 dependent 32D cell line augments factor withdrawal induced apoptosis

NRAGE and vector stably transduced cell lines were established to examine the contribution of NRAGE to this process. NRAGE expression was determined by Western blotting (Fig.II-13B). The proliferation rate of these cells was not affected by the stable integration of the retroviral vector or NRAGE protein expression (data not shown). Cell survival after IL-3 withdrawal was measured by trypan blue exclusion. As shown in Fig.II-13A the vector transduced cells behave identically to the parental cells. In contrast, expression of NRAGE had a dramatic effect on the kinetics of cell death in 32D cells. The survival curves for NRAGE and the vector/parental lines diverge very early on (12hrs) and this trend continues throughout the experiment.

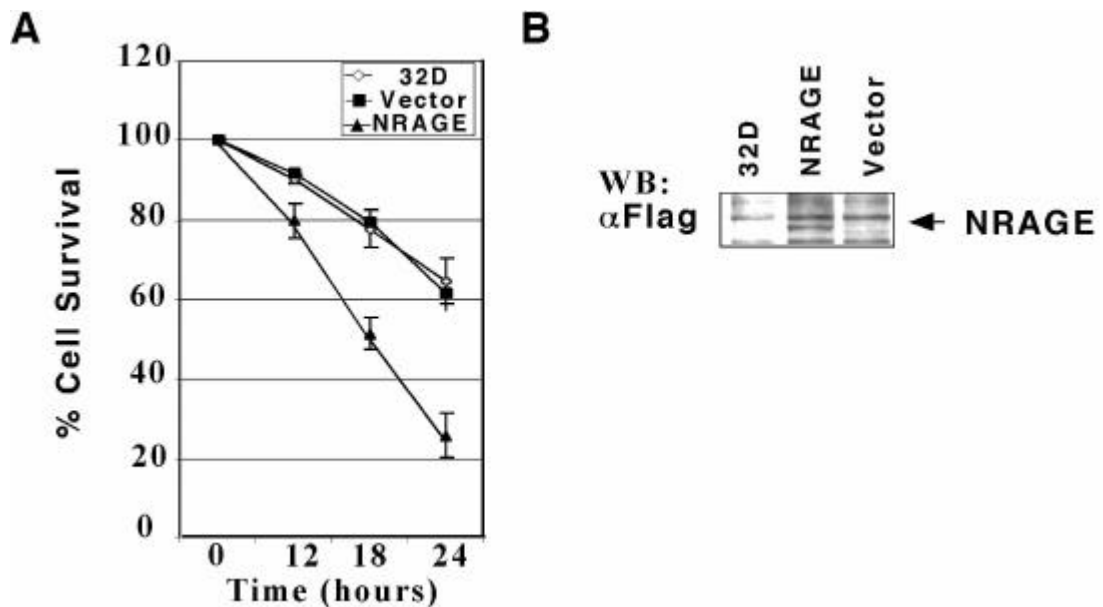


Fig.II-13: Stable NRAGE expression greatly reduces the viability 32 D cells after IL-3 withdrawal. (A) 32D parental, empty vector, and NRAGE transduced cells were seeded (0.5×10^6) in medium lacking IL-3 into the wells of a 24 well plate, and cell viability measured at the time points indicated by trypan blue exclusion. Fig.II-13A is representative of 5 experiments, each performed in duplicate, with the points of the curves being taken from two of these experiments, measured in duplicate. Between 150-250 cells are counted per measurement. Mean values and standard deviation (error bars) are shown. In Fig.II-13B, the expression of Flag-NRAGE in the stable NRAGE cells is confirmed. 20 μ g proteins from the lysates of each cell type were subjected to Western immunoblotting with a Flag antibody.

At the 24hr timepoint about three times as many dead cells were observed with the NRAGE expressing cell pool. This indicates that NRAGE greatly accelerates the cell death process upon growth factor withdrawal in this IL-3 dependent promyeloid cell line.

II-4.2 NRAGE binds XIAP *in vivo* upon IL-3 withdrawal in 32D cells.

Over a 24 hour period the interaction of NRAGE with endogenous XIAP was analysed in 32D cells. The binding of NRAGE with XIAP is undetectable in proliferating 32D cells, however, 8-12 hours after IL-3 withdrawal an induction of binding can be observed, trailing off thereafter, and becoming undetectable at 16 hours, as shown in Fig.II-14. In an earlier experiment, the induction was even observed after 4 hrs.

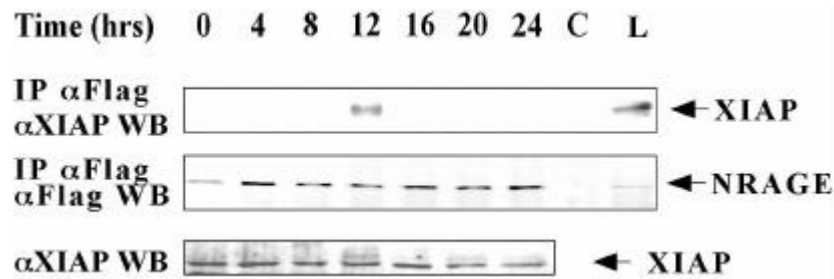


Fig.II-14: NRAGE binds inducibly to endogenous XIAP upon IL-3 withdrawal. NRAGE transduced cells were washed 3 times and seeded in 20ml medium lacking IL-3 (0.5×10^6 cells/ml) in T75 culture flasks, and lysed in NP40 buffer at 4°C at the indicated time points. A vector control was also taken at time 0 (C). NRAGE was immunoprecipitated O/N at 4°C using the monoclonal Flag antibody (M2) coupled to 30µl protein-G agarose from 500µg precleared lysate, and washed twice in high salt NP40. The IPs were subsequently immunoblotted with αXIAP to identify any coprecipitating endogenous XIAP. The blot was then stripped and reprobed with Flag antibody to detect NRAGE. 20µg lysate was also taken from each time point to determine XIAP expression levels. L denotes 20µg lysate from time 0 NRAGE expressing cells. The data is representative of two experiments, with the results from one being shown.

II-4.3 NRAGE overcomes Bcl-2 mediated cell protection

Forced Bcl-2 expression in 32D cells has been shown to be very effective in rescuing these cells from the induction of apoptosis by a variety of stimuli including withdrawal of essential growth factors [106]. It was interesting therefore to test whether Bcl-2 could also block the death enhancing activity of NRAGE. 32D cells stably expressing Bcl-2 were infected with either the retroviral control vector, or the retrovirus containing Flag-NRAGE, and selected as described in Materials and methods. 24 hours after IL-3 withdrawal, the 32D cells expressing Bcl-2 had

gained a 100% increase in survival compared with the wild type cells, and no significant difference was seen between the 32DBcl-2 vector transduced cells and the parental cells. However, the 32DBcl-2 cells expressing NRAGE showed a dramatic reduction in survival, completely abolishing any protection given by Bcl-2 (Fig.II-14A). This would suggest that NRAGE is a pro-apoptotic protein in spite of Bcl-2 expression, after growth factor withdrawal. The expression of the transduced proteins is shown in Fig.II-14B

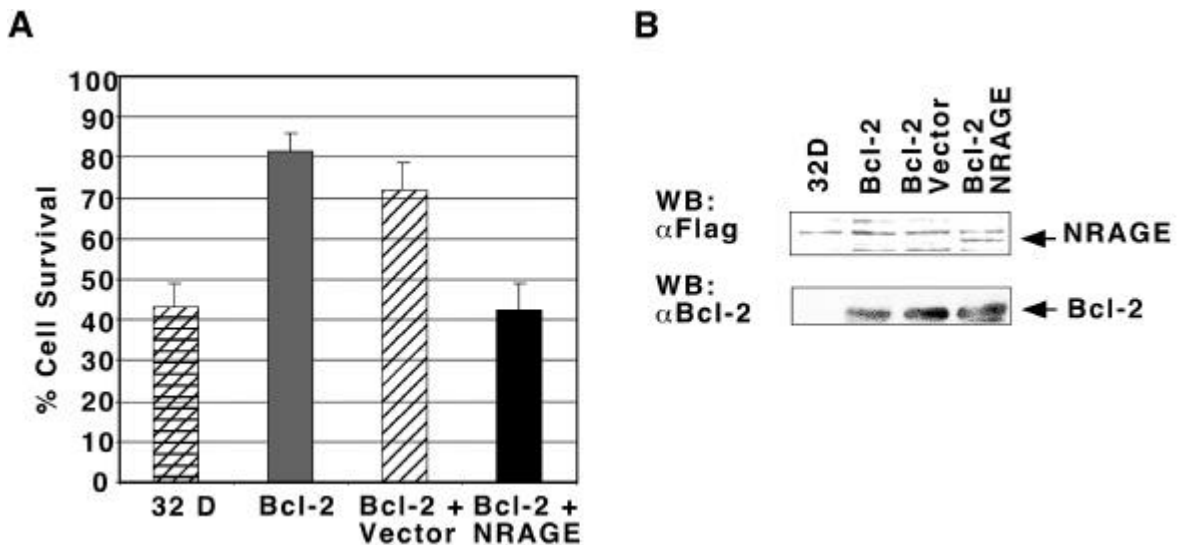


Fig.II-15: The effect of NRAGE on 32D cells protected from IL-3 withdrawal by the expression of Bcl-2 was investigated. 32D parental cells, Bcl-2, Bcl-2 + empty vector, and Bcl-2 + NRAGE stably expressing cells were seeded as above and cell viability was measured after 24 hours. The results shown in Fig.II-5 are representative of 4 experiments each performed in duplicate, after 24 hours IL-3 withdrawal, measured as previously described. The results from two of these experiments are depicted in the figure; mean values and standard deviations (error bars) are shown.

II-5 The participation of NRAGE and XIAP in signalling pathways

Previous reports had indicated that XIAP could influence MAPK signalling pathways via an unknown mechanism [67]. It would therefore be unsurprising if NRAGE was involved in this avenue of IAP function. Indeed NRAGE was cloned as a protein which interacts with a receptor potentially involved in MAPK signal transduction [100].

II-5.1 NRAGE and XIAP cooperate in JNK signalling

When overexpressed in HEK293 cells, XIAP was able to specifically activate JNK1, but not any other MAPK member, and that this played a role in XIAP mediated cell death prevention [67].

Therefore it was interesting to see whether NRAGE could influence this signal pathway. XIAP, NRAGE and MLK3, a known JNK1 activator [107], were transfected together with JNK1 in various combinations in HEK293 cells. JNK1 was then immunoprecipitated, and incubated with its substrate c-Jun, in an immune-complex kinase assay, the results of which are shown in Fig.II-16. In lane 1 the expression of XIAP weakly activates JNK1, which is not affected by the co-expression of NRAGE (lane 2). NRAGE itself had no detectable effect on JNK1 activity, as seen in lane 6. Overexpression of wild-type MLK3 results in a slightly enhanced JNK1 activity, which is not greatly influenced by the co-expression of XIAP. However, when NRAGE is included with XIAP and MLK3, a dramatically enhanced JNK1 activity is observed (lane 5). This is only comparable with the activation observed after 60 minutes of arsenite stimulation, a classical stress inducing agent (lane 7), and potent inducer of JNK activity [108].

GST-XIAP	+	+		+	+		
Flag-MLK3			+	+	+		
myc-NRAGE		+			+	+	
HA-JNK1	+	+	+	+	+	+	+

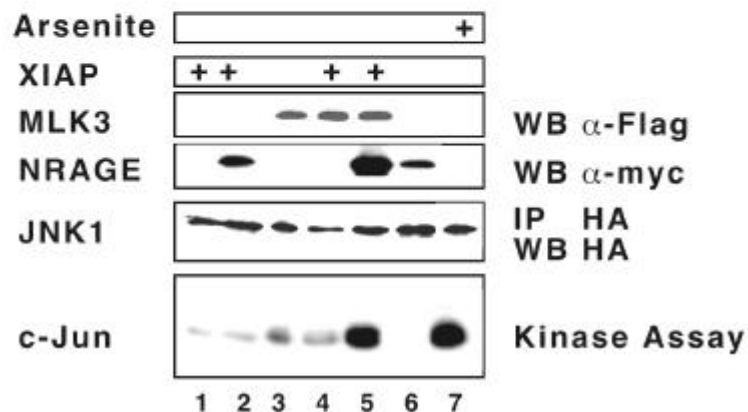


Fig.II-16: NRAGE and XIAP cooperate to greatly enhance MLK3 mediated JNK activation. HEK 293 cells were transfected with the constructs denoted, the amount of DNA being standardised where necessary with empty vectors. The cells were starved for 48hrs and then lysed. HA -JNK1 was immunoprecipitated from 500µg protein lysate, and an immune-complex kinase assay was performed with GST-c-Jun as a substrate. An X-ray film was exposed O/N, and the membrane probed with HA to show equal loading. The lysates were also probed for MLK3 and NRAGE. Lane 7 shows cells stimulated with arsenite for 60 minutes as a positive control for JNK activity.

This suggests that although it is highly unlikely that either XIAP or NRAGE possess intrinsic catalytic activity, they may nevertheless influence kinase signalling pathways upon binding.

Preliminary data underway to determine the role of NRAGE in cell signalling suggests that NRAGE is itself a potential a target for phosphorylation. Probing immunoprecipitated

NRAGE from lysates of cells treated with various stimuli, utilising phosphotyrosine antibodies, suggested that certain factors found in FCS may induce a rapid tyrosine phosphorylation in NRAGE (data not shown). The significance of these observations is not clear, and certainly requires further investigation. Another indication that NRAGE could be a target for phosphorylation came from a software program available on the Internet. The NetPhos 2.0 WWW server, (<http://www.cbs.dtu.dk/services/NetPhos/>), produces neural network predictions for serine, threonine and tyrosine phosphorylation sites in eukaryotic proteins. A summary of the predicted phosphorylated residues on NRAGE, with a probability of >0.90, is shown in FigII-17. The predictions are based on the analysis of neighbouring amino acids, which although by no means definitive, certainly provide some further preliminary indications. Interestingly, only one tyrosine residue is given a probability of >0.9 of being phosphorylated.

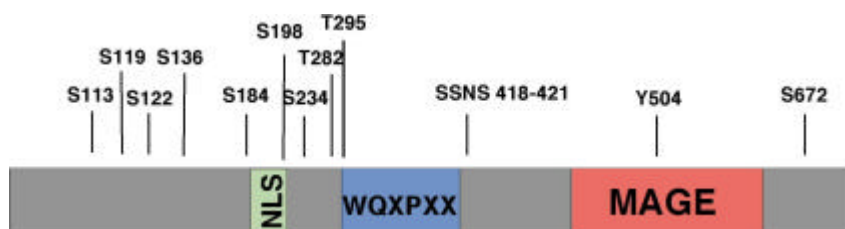


Fig.II-17: NetPhos predicts that NRAGE is phosphorylated on many serines, threonines and tyrosines. A summary of the predicted phosphorylatable residues, with a probability of >0.90, are superimposed on the primary structure of NRAGE. Other residues showing a probability of between 0.70-8.9 are not depicted.

II-6 Cellular localisation of NRAGE and DNRAGE mutants

Another consideration important in determining the function of a protein is its localisation within the cell. Many proteins occupy different subcellular positions depending on the status of the cell, or the environmental stimulus. Many cellular proteins also contain domains, which allow them to travel between different compartments. One such domain is the NLS, which allows docking with certain nuclear pore proteins, thereby facilitating nuclear import [109]. A potential NLS located in the NH₂-terminal part of NRAGE, slightly upstream of the WXQXXP repeat region. It was therefore of interest to examine the functionality of this domain. The largest and smallest two-hybrid clones, Δ NRAGE^{p80} and Δ NRAGE^{p60}, as well as the full length NRAGE were transiently transfected in HEK 293 cells, and analysed for their cellular localisation.

Surprisingly, the two-hybrid clones localised to entirely different cellular compartments. $\Delta\text{NRAGE}^{\text{P}60}$ was located exclusively in the nucleus (Fig.II-21A), whilst $\Delta\text{NRAGE}^{\text{P}80}$ could only be observed in the cytoplasm (Fig.II-21B). Furthermore, the wild-type NRAGE was located mostly in the cytoplasm (Fig.II-21C), but could also be seen in the nucleus of a small proportion of cells (Fig.II-21D). This would imply that although the NLS is present in all clones, $\Delta\text{NRAGE}^{\text{P}80}$ and the full NRAGE might contain other domains through which they are retained in the cytoplasm, by other cytosolic proteins.

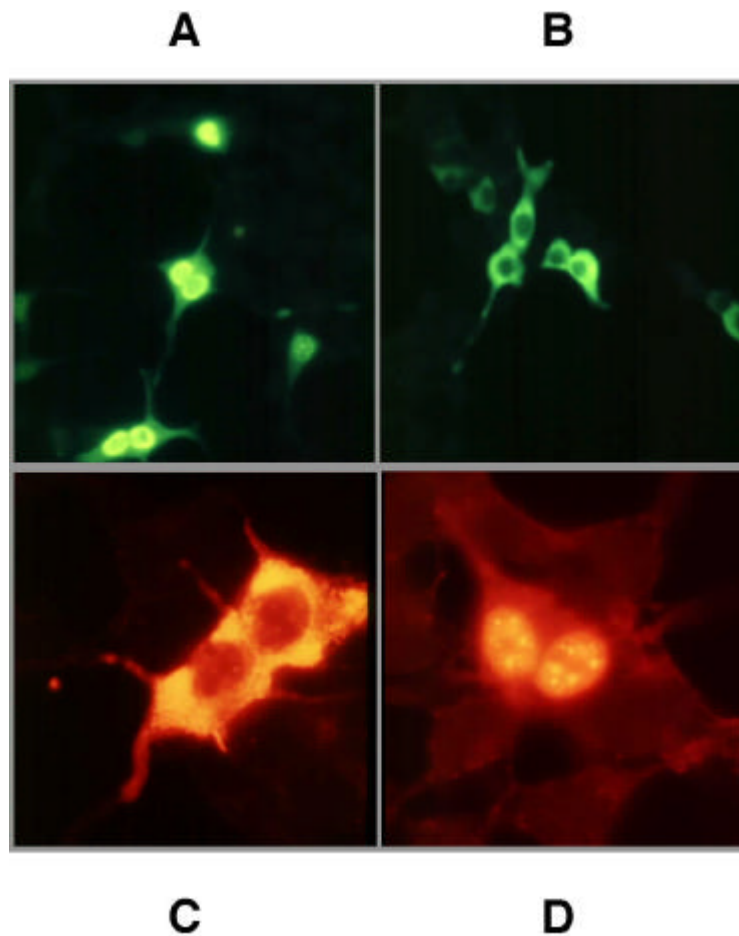


Fig.II-21: NRAGE is located in many cellular compartments. HEK 293 cells were transfected with the $\Delta\text{NRAGE}^{\text{P}60}$ and $-\text{P}80$ truncated isoforms, as well as the complete cDNA, and the expression of each was measured by immunofluorescence: After 48hrs culture in 10% FCS, the cells were fixed in 4% formaldehyde, and permeabilised with 0,5% Triton-X-100. The cells were then incubated with the primary antibody and then with the appropriate FITC or Cy3 conjugated secondary antibody. The Myc- $\Delta\text{NRAGE}^{\text{P}60}$ and Myc- $\Delta\text{NRAGE}^{\text{P}80}$ constructs were detected using the 9E10 Myc monoclonal antibody, followed by a secondary FITC conjugated rabbit anti-mouse antibody. The Flag-NRAGE protein was visualised using the primary monoclonal Flag (M2) antibody followed by a goat anti-mouse Cy3 conjugated secondary antibody. Panels A and B are at 20 \times magnification, whilst panels C and D are at 100 \times magnification. Panel A shows Myc- $\Delta\text{NRAGE}^{\text{P}60}$ located exclusively in the nucleus, in contrast to panel B which shows the larger Myc- $\Delta\text{NRAGE}^{\text{P}80}$ solely expressed in the cytoplasm. The location of the wild-type NRAGE is however, not as conclusive. Panel C shows NRAGE clearly located in the in the cytoplasm of the cell, with a slightly speckled distribution. Panel D on the other hand shows NRAGE present only in the nucleus of the cell, highly concentrated at certain structures. In the majority of cells though, NRAGE is cytoplasmic (data not shown).

DISCUSSION

III-1. The discovery of a novel IAP-binding protein

Apart from the Bcl-2 proteins, the IAP family members constitute the largest group of pro-survival molecules. Members of this heterogenous family are defined by the presence of up to three NH₂-terminal BIR domains, and their ability to suppress apoptosis. Many contain additional domains such as a Carboxy-terminal RING zinc-finger domain [56]. BIR domains are thought to mediate caspase binding and inhibition, and are both necessary and sufficient for the anti-apoptotic function of IAP proteins [70]. Many IAP-inhibiting molecules also compete for BIR-binding such as RPR and Smac [110] [78], and further evidence suggest homo-oligomerisation even takes place at the BIRs [111] whilst very little is known about the function of the RING domain.

The mode of action of Bcl-2 members is well understood [85]. In contrast very little is known about the mechanisms by which they pursue their anti-apoptotic function [56]. In an attempt to define such regulators, a yeast *two-hybrid* screen was performed in a PC12 library using the avian IAP, ITA, as a bait. Three truncated overlapping cDNAs were identified as genuine positive interacting clones. They represented the NH₂-terminal part of an unknown protein (Fig.II-3), which was later isolated independently by another group. The allocation of nomenclature to this undescribed gene is discussed in the next section, and will be designated as NRAGE. This interaction with NRAGE was also seen with XIAP, a human IAP member, in direct *two-hybrid* tests (Table II-2). At least when considering amino acid sequence identity, an interaction with c-IAP1 or c-IAP2 might have been expected, since these show a greater similarity with ITA[112]. However, since the exact role of ITA in the physiological context is unclear, or indeed which functional IAP isoform it represents[113] [114], it can be concluded that XIAP is a relevant mammalian IAP for the interaction with NRAGE. The neuronal IAP member NAIP did not interact with NRAGE. This observation could at least be clarified through subsequent experiments, which found the RING domain of IAP proteins necessary for the NRAGE-IAP interaction (fig.II-11). NAIP is one of the IAP members which along with Survivin and the yeast BIR proteins, does not possess a Carboxy-terminal RING domain [115] [6].

To validate these two-hybrid data required further experiments were performed. This binding was tested in a more appropriate higher eukaryotic cell system, the HEK293 cell system, by two independent techniques. In the first instance, XIAP was demonstrated to interact with the

Δ NRAGEp⁶⁰ in the mammalian two-hybrid system. This showed the interaction indirectly via the activation of a reporter gene, which could only occur when XIAP and Δ NRAGEp⁶⁰ bound together. They are thus recruited to the reporter construct Gal4 binding motif by the Gal4DB-XIAP thereby allowing the VP16- Δ NRAGEp⁶⁰ to transactivate the luciferase gene. This result extends the yeast *two-hybrid* test. This observation, taken together with the yeast two-hybrid results, also suggested that the NH₂-terminal part of NRAGE was responsible for the interaction with ITA and XIAP.

Of great interest was the capability of the complete NRAGE wild-type protein to bind with ITA and XIAP. To investigate this, the same HEK 293 cell system was utilised, but this time the interaction was appraised in co-immunoprecipitations. With this technique, the binding between proteins can be visualised by Western blotting. The optimal lysis buffer is a relatively mild one, containing no SDS detergent, and relatively low amounts of salt. The elimination of unspecific binding was achieved through raising the stringency of the washing conditions, in this case by increasing the concentration of salt. The results showed that the complete NRAGE protein indeed interacts with ITA and XIAP. This is clearly important, since NRAGE has been demonstrated so far as being expressed *in vivo* as a complete protein, and not as truncated proteins such as those identified in the *two-hybrid* screen. These results also indicated that the RING region of ITA appears to be necessary for this interaction (Fig.II-11).

Until now, the function of the RING domain had been mostly overlooked in favour of the more unique BIR domains. RING domains are more ubiquitous than BIR domains, and have been identified in many proteins as important protein-protein, or protein-DNA interacting regions. They consist of conserved patterns of cysteine and histidine residues, which bind two Zinc atoms. [116]. The course of research undertaken in this dissertation led to the identification of NRAGE as the first intracellular non-receptor protein to interact with this specific domain. Since many other proteins contain a RING domain, it could also be possible that NRAGE binds to the RING domain of other proteins. A BLAST search with the RING and linker region of XIAP revealed a number of non-IAP cellular proteins with significant homology. One such RING containing protein, the MIR (myosin regulatory light chain interacting protein), also showed homology with XIAP in the region adjacent to this domain. Indeed, this protein was cloned as the result of a search for novel IAP proteins. Furthermore, overexpression of MIR in PC12 cells was able to block neurite outgrowth after NGF stimulation, downstream of Trk phosphorylation [117].

The understanding of the IAP RING domain function had previously been limited to the knowledge that it could be a target for ubiquitination [82] [83], a function common to the RING domains of many other proteins [81]. The binding of NRAGE at this region might therefore result in one of three events: One possibility is that this could lead to the catalysis of NRAGE ubiquitination and subsequent degradation: Another possibility concerns speculation that the ubiquitination of XIAP is an indirect method of caspase degradation [118]. Since both IAP ubiquitination and caspase activation occur after apoptotic stimuli, it might be possible that by binding activated caspases, XIAP targets them for degradation. Therefore, NRAGE binding the RING domain could prevent IAP ubiquitination, thus prolonging XIAP survival and increasing the half-life of active caspases [82]: Or finally, that the binding of NRAGE to the RING domain would perform some role in an unrelated, as yet undiscovered function for the IAP RING domain. This may include sequestration of XIAP by NRAGE to a compartment of the cell where it may no longer be active. The results from section II-4, where NRAGE function in 32D cells was investigated, shed some light on which of the hypotheses is likely to be the case. In figure II-14, the level of expression of overexpressed NRAGE is unaffected over a time period of 24hrs of IL-3 withdrawal. This would indicate that the first hypothesis is not relevant in this system. The second is however possible, since over the same time course the level of expression of endogenous XIAP also seems to be constant. If NRAGE does prevent the ubiquitination of XIAP, and thereby prolong XIAP half-life, then it would appear that the enhanced stability of the protein may not necessarily be advantageous in terms of preventing cell death caused by growth factor deprivation in 32D cells. If indeed XIAP-NRAGE heterodimers were still able to bind activated caspases, but this complex was no longer targeted for degradation, it could be true that the half-life of the activated caspases is also increased [73]. It would of course be equally necessary to monitor the expression of XIAP in non-NRAGE expressing cells, and to compare the expression and activity of the caspases in this environment. The third possibility cannot be excluded, since so little is known about the relevance of this RING domain, other than the singular observation that XIAP can act as a bridging protein in BMP signalling [65].

Another point to consider is whether the binding of NRAGE to this region could sterically hinder or obscure alternative docking areas, most notably the BIR domains, for other cellular proteins. The recently identified IAP inhibitor molecule Smac/DIABLO is thought to compete directly with caspases for IAP-binding at the BIR [79]. Thus, the cellular balance between life and death could be tilted either way, depending on the availability of IAP substrates. Without competition from other sources, IAPs can effectively stave off cell death by directly binding

caspses [69]. The introduction of competing non-caspase IAP-BIR-binding molecules, such as Smac/DIABLO, RPR, HID or GRIM, could however reverse or neutralise this death inhibitory mechanism, tilting the balance once again towards apoptosis [119] [18] [19]. It was observed that NRAGE expression augments cellular death after initiation of apoptosis in 32D cells, and that there is induced binding between NRAGE and endogenous XIAP. An alternative explanation for this phenomenon, would see NRAGE obscuring the XIAP-caspase docking sites, and thus neutralising the endogenous XIAP anti-caspase function. Since it is also clear that NRAGE may have its own intrinsic death-promoting activity [100], it cannot be ruled out that NRAGE itself further influences apoptosis in an IAP-independent mechanism.

The expression of Bcl-2 has been shown to protect 32D cells from growth factor withdrawal [120] [105]. The ability of Bcl-2 to block apoptosis is however very much dependent on the cell type and stimulus, or indeed the mode of apoptosis [121] [122]. Whilst Bcl-2 was able to block IL-3 deprivation induced apoptosis, this was not the case when an alternative stimulus such as TNF was employed as a death-inducing agent [106]. It was therefore of great interest to see whether the accelerated death caused by NRAGE expression could be abrogated by Bcl-2. As depicted in fig.II-15, Bcl-2 cell protection was drastically reduced in the NRAGE expressing cells. This could indicate that NRAGE is capable of augmenting cell death even in the presence of Bcl-2. The pathways leading to apoptosis have been separated into two distinct groups, based on cell type. In Type I cells e.g. SKW (B-cell lymphoma), CD95 triggering leads to strong caspase-8 activation at the DISC, which bypasses the mitochondria, and results in activation of downstream effector caspases. With type II cells on the other hand e.g. Jurkat T-cells CD95 activation causes a weak DISC formation, leading to the activation of the mitochondria, in turn resulting in cleavage of caspase-3 and caspase-8 downstream of the mitochondria [121]. Thus blocking activation of the mitochondria by Bcl-2 or Bcl-xL inhibits receptor induced apoptosis only in type II cells [121]. It is also likely however that a certain amount of cross-talk exists [26]. Since NRAGE is able to overcome the protection given by Bcl-2 at the mitochondria, this suggests that NRAGE might either interfere with Bcl-2 directly at the mitochondria, or the enhanced death in NRAGE/Bcl-2 cells is due to an alternative pathway. NRAGE has been shown to interact with the p75NTR, and that the apoptotic signal required NRAGE recruitment upon NGF binding. Furthermore, NRAGE translocated to the cell membrane after stimulation of this pro-apoptotic pathway [100]. These observations were however based on a very narrow set of conditions, and it is likely that the link between the receptor-NRAGE binding, and the downstream effectors of apoptosis, may take place in a more diverse set of systems. Perhaps

NRAGE could even interact with death receptors other than the p75NTR, as is seen with molecules such as the TRAF, which bind many of these receptors [123]. Indeed, the TRAF2-p75NTR interaction was shown to enhance cell death [93]. It may therefore be possible that NRAGE translocates to the cell membrane with alternative apoptotic stimuli, where it may influence an NGF independent pathway. It may also be possible that the induction of apoptosis, together with the unphysiological overexpression of NRAGE, is sufficient to engage the pathway downstream of NRAGE. This pathway may be independent of mitochondrial apoptosis, since NRAGE expression could bypass of the cellular protection gained by Bcl-2 expression. The result described in Fig.II-15 would suggest that NRAGE does not compete with or antagonise Bcl-2 function at the mitochondria.

The protection afforded by Bcl-2 is not permanent or complete, but simply delays the onset of cell death[105]. Although the expression of NRAGE abolishes the protective effects of Bcl-2, after 24 hours in the absence of IL-3 Bcl-2/NRAGE expressing cells exhibited the same level of viability as wild-type 32D cells. In contrast, 32D cells expressing just NRAGE showed a marked reduction in cell viability compared with wild-type cells. The reason for this could be that the expression of Bcl-2 dampens mitochondrial mediated apoptosis that possibly occur at later stages.

In summary, the results from sections II-3 and II-4 suggest that NRAGE binds the IAP proteins ITA and XIAP, with a strong affinity. This binding seems to require the RING domain. Furthermore, NRAGE potentiates cell death upon stimulation of apoptosis, by a mechanism involving an induced binding with the potent cellular caspase inhibitor XIAP. The enhanced apoptosis takes place via a pathway which is not inhibited by the expression of Bcl-2, and may therefore involve a pathway independent of the mitochondria, at least in the early stages of apoptosis. Further, NRAGE may neutralize XIAP anti-caspase function by sequestration or by interfering with its caspase binding ability.

III-2 NRAGE is a novel MAGE-like member with unique characteristics

With the identification of a novel gene, one of the first tasks is to ascribe the gene an appropriate nomenclature, which should reflect the physiological function of the gene. Prior to any such functional data being available, my personal choice had been BONUS (Bearer Of a New and Unusual Structure), and throughout the duration of my doctoral research, other groups independently identified the same or orthologous genes as MAGE-D [124], snerg-1 [125], Dlxin-

1 [126] and the neurotrophin interacting MAGE homologue, NRAGE [100]. The first group to publish this new gene [124] were concerned solely with the identification of MAGE genes, which until then had been entirely tumour and germ-line specific proteins coding for antigens recognised by T cells, whose cellular function was virtually unknown [104]. Lucas *et al.* confirmed the results of section II-2.4 that this new MAGE variant was expressed in many more terminally differentiated adult tissues than simply testis. Furthermore, they showed that Mage-D did not code for any previously known MAGE antigenic peptides [124]. This raises the question as to whether in fact NRAGE belongs to the MAGE family, or is a functionally distinct protein that contains a MAGE domain.

With the rapidly increasing amount of genome sequence information available, and the strides made improving the software for analysing this Data, it is clear that a number of other NRAGE-like genes exist. These include the hepatocellular carcinoma associated gene (JCL-1) (Genbank entry AAD00728), and the breast cancer associated gene protein (BCG-1) (Genbank entry AF126181), which also show a high homology with NRAGE outside the MAGE domain. Other proteins which contain a MAGE domain, but show no homology outside this domain include members of the Magphinin (Genbank entry AF241245) and Trophinin family. Trophinin is a completely unrelated protein important in trophoblast-endometrial epithelial cell adhesion in the mouse uterus [127]. In addition, the platelet derived growth receptor alpha (PDGFRA) possibly contains a truncated MAGE domain adjacent to its tyrosine kinase catalytic domain (domain architecture retrieval tool (DART) at NCBI, ref: XP011186). The similarities between some of the recently identified MAGE/MAGE-like proteins and NRAGE are described in Fig.III-1.

The evidence suggests that NRAGE is a MAGE relative, albeit more distant than the classical MAGE antigens, rather than simply a MAGE domain containing protein. However, the fact that it possesses the unique 25(WQXPXX) domain, its existence as a single splice form (Fig.II-5 and Fig.II-10), and that it does not show the usually recognised MAGE antigens [124] would lead to the conclusion that particularly regarding its function, NRAGE and not MAGE-D, is the most appropriate nomenclature for THC179960. This also concurs with the nomenclature given to other MAGE-like families which are named BAGE, GAGE, LAGE etc. [104].

Understanding the function of NRAGE in normal cellular physiology may thus shed some light on the importance of MAGE and MAGE domains in tumours. The discovery that NRAGE binds the p75NTR [100], and XIAP (this dissertation), two human proteins important in

regulating apoptosis, should stimulate research aimed at investigating whether this interaction is common to other MAGE proteins in malignancies.

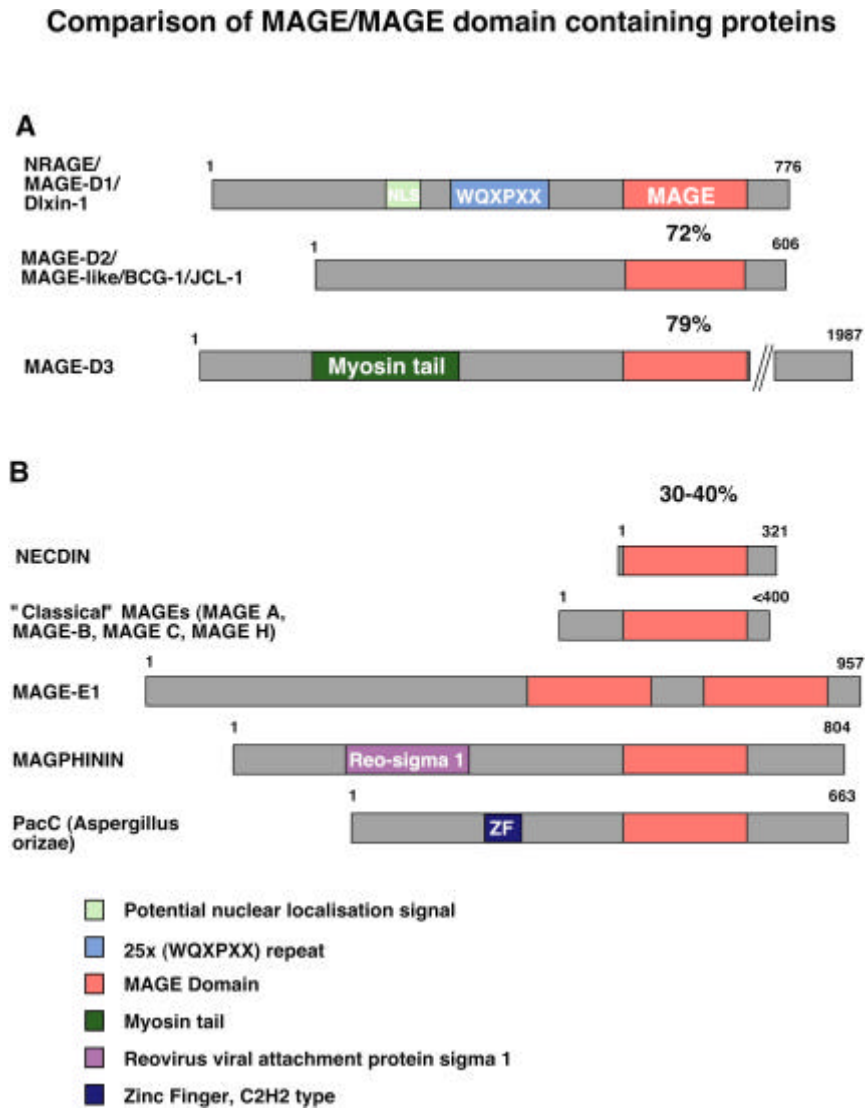


Fig.III-1: Primary protein structures of MAGE/MAGE domain proteins compared with NRAGE. In part A, the MAGE proteins with the highest homologies to the NRAGE MAGE domain are shown, with relative percentage indicated between the MAGE domains. In part B, the less homologous members of the MAGE/NECDIN protein family are shown. The relative identities between these MAGE domains and the NRAGE MAGE domain vary between 30-40%. Grey regions indicate lower homology regions. The additional putative domains/structures are indicated by coloured boxes, described at the bottom of the figure. Amino acid length is indicated above each protein. Human MAGE proteins are shown unless otherwise indicated. The primary structure of the "classical" MAGE members is represented by a single protein for simplicity. Domains are predicted by the NCBI DART program.

The one exception amongst the MAGE proteins is Necdin, for which a significant amount of research has been dedicated to resolving its cellular function. It was identified in 1991 from a

neurally differentiated embryonic carcinoma cell line [128]. It appeared to be a nuclear protein which seemed to be important in brain/neural tissue, specifically in post-mitotic neurons, and could arrest the cell cycle [129]. More explicitly, it was shown that Necdin interacts with viral cell cycle regulators such as the SV40 large T, adenovirus E1A, and the transcription factor E2F1, as well as the tumour suppresser p53 [130] [131]. Interestingly, Necdin is also a possible candidate gene for Prader-willi syndrome (PWS), since its chromosomal location is one often deleted in PWS [132]. Since this was the only information available about MAGE function, and taking its neuronal expression into account, it may readily be thought that NRAGE could also function in a cell cycle-influencing fashion. Indeed the investigators who identified NRAGE suggested as much, based on Necdin/NRAGE structural similarity and on experiments where transiently overexpressed NRAGE resulted in a reduction of cell cycle progression. They pointed to a shared mechanism for Necdin and NRAGE in mediating cell cycle effects [100].

The results presented in this dissertation would indicate that the function of NRAGE lies not primarily in cell cycle arrest/interference, since this would preclude the stable overexpression of NRAGE in 32D cells (section II-4.1) and indeed even in PC12 cells (data not shown), where NRAGE is already expressed as an endogenous protein [100]. However, since a successful selection process requires proliferating cells, it could be that in the stably transduced NRAGE cells are low expressers of the protein. The experiments performed by Salehi *et al.* took place in transient overexpression conditions in HEK 293 cells, where high levels of protein can be achieved. There are however many MAGE proteins other than Necdin which show a greater structural identity with NRAGE. Using the BLAST sequence alignment program from NCBI, Necdin scores 140 points when compared with NRAGE, whereas MAGE-E1b, Maged3, Maged2, and MageB3 score 412, 354, 311 and 171 respectively (NRAGE against NRAGE scores 1406). Since the MAGE proteins are expressed in tumours and malignancies, cell populations which characteristically undergo genetic changes, it could be possible that under these conditions cell cycle interference may be of benefit to the tumour [104]. It would also be of great interest to see if other MAGE proteins also interact with XIAP, and what consequence this interaction would have in tumour or melanoma progression and apoptosis resistance in chemotherapy [133]. It might also be possible that homo- or hetero-dimerisation also important in NRAGE, as it is with IAPs [111].

The relevance of the MAGE domain is unknown, but it would appear that other domains additionally present in the atypical MAGE proteins may have a significant influence on the precise function of these proteins. Identifying the function of the MAGE domain would however

go a long way towards understanding the MAGE family as a whole. Strangely, in more than 10 years of research, no mutational analysis or characterisation of this domain has been described.

III-3 The influence of NRAGE and XIAP on signal transduction

One of the more recent observations involving IAP function was the participation of XIAP in the activation of the MAPK JNK1 [67]. Furthermore, our group identified ITA as being able to interfere with differentiation in PC12 cells [101], a process governed by MAPK signalling [134]. It was therefore interesting to examine the role of NRAGE in MAPK signalling. Described in section II-5 is the first revelation that NRAGE is a novel signal transduction protein. Although the protein itself has no catalytic domain, this does not preclude the possibility that NRAGE may facilitate the transmission of a signal via alternative means. XIAP had previously been shown to act as a bridging molecule, linking the BMP receptor to the downstream effectors of signal transduction, however the exact mode of action is unknown [65] [64] [68]. Adapter molecules have been shown previously to induce a signal when overexpressed, independently of ligand-receptor binding [135].

The results shown in Fig.II-16 confirm that the overexpression of XIAP gives rise to a limited JNK1 activation [67]. In confirmation with Sanna et al, no effect was seen on the mitogenic cascade, or the MKK6/p38 pathway, when XIAP was overexpressed with NRAGE or an upstream member of either cascade (data not shown). NRAGE did not cause any such activation when coexpressed with JNK1, but did not significantly effect the level of XIAP mediated JNK1 activation either. MLK3, a known upstream kinase of JNK1 [107, 136] also led to a weak JNK1 activation, that was not significantly effected by the coexpression of XIAP. However, when NRAGE was coexpressed with MLK3 and XIAP, the level of JNK1 activity was greatly increased, although the level of MLK3 expression was equal in each case. The level of activity was comparable to that after 60 minutes arsenite stimulation, which is sufficient to maximally activate JNK1 [108]. This observation is all the more stunning since the cells were starved unstimulated, and a kinase with only basal activity was co-transfected. This suggested that NRAGE and XIAP may act upstream of MLK3 in JNK signalling, and that all must be expressed together in order to exert a maximal JNK activity.

MLK3 is a MAP3K, and XIAP had been previously shown to activate the MAP3K TAK1 [64]. Furthermore, p75NTR signalling is thought to be mediated in part via MEKK1-JNK i.e. MAP3K signalling [137] [97]. Bearing these reports in mind, and since NRAGE binds directly

with the p75NTR [100] as well as with XIAP (B.W.M. Jordan *et al.* submitted), it would be conceivable that that NRAGE could also influence MAPK signalling upstream of MAP3K. The interpretation of the significance of JNK activation via XIAP or via the XIAP/NRAGE/MLK3 coexpression is clouded by the abundance of evidence linking the activation of JNK to both cell survival and cell death fates [39]. Interestingly however, MLK3 expression has been shown to induce apoptosis in PC12 cells and sympathetic neurons, whilst a dominant negative form of the kinase blocked both this pathway, and the death signal induced by NGF withdrawal [138]. Therefore it could be that NRAGE mediates part of its apoptotic signal via the enhancement of MLK3 activity, modulated by the coexpression of XIAP, possibly linking the death receptor to an unknown upstream activator. The activation of MAPK pathways during apoptosis/differentiation in PC12 cells requires a fine balance between ERK and JNK activation, which can be more accurately investigated using endogenous levels of proteins [139] [140]. In direct *two-hybrid* tests, neither NRAGE nor XIAP interacted with MLK3 (data not shown). Whilst the downstream targets of MLK3 are well known, Rac1 and CDC42 are the only described upstream activators of MLK3, and it would also be interesting to examine whether NRAGE or XIAP are themselves influenced by these proteins [141] [142].

In order to identify the cause of the inducible interaction between XIAP and NRAGE, one possible clue came from the Internet version of the Netphos program. This suggested that several serine, threonine and tyrosine residues on NRAGE were phosphorylatable. Since IL-3 receptor signalling involves the phosphorylation of many different targets, on serines, threonines and tyrosines, it would also be worthy to speculate that the inducible binding between NRAGE and XIAP after IL-3 withdrawal is influenced by phosphorylation/dephosphorylation events [46]. Preliminary data indicate NRAGE is constitutively tyrosine phosphorylated in 32D cells, up to 20 hrs after IL-3 withdrawal (data not shown). This does not exclude that other serine, threonine or indeed other tyrosine phosphorylation/dephosphorylation may take place during this time. Although the 32D cells are deprived of IL-3 during these investigations, they are stimulated with 10% FCS. Further investigation revealed in HEK 293 cells that serum stimulation leads to a rapid tyrosine phosphorylation of NRAGE (data not shown). This observation brought to light the fact that NRAGE function may be influenced by more than simply the p75NTR [100] and perhaps receptor tyrosine kinases. Another indicator that other NRAGE-like Mage proteins are possible substrates for kinases came from a small report which identified several casein kinase I (CKI) substrates. Amongst these was MAGE/Necdin-like (accession Z98046) [143], a putative 606 amino acid protein which shares a 67% identity with NRAGE C-terminal and 30% identity with

the NRAGE N-terminal part. CKI is a serine/threonine kinase, whose function is poorly characterised. Interestingly, CKI has been shown to associate with and phosphorylate the p75 TNFRI [144].

Indeed, another group independently cloned NRAGE as Dlxin-1, a protein that was able to bind to Dlx5, a protein which is specifically expressed in bone structures [126]. Dlx5 is a positive regulator of the mouse osteocalcin gene, however this is subject to some controversy [145] [146]. Interestingly, osteocalcin is regulated by FGF2, a transmembrane RPTK involved in signal transduction through a variety of pathways, including the classical mitogenic pathway [147] [148]. Dlxin-1 was thus identified in the very specific context of osteoblast regulation, giving strong evidence of the cell/tissue type dependent role of this multifunctional protein [126]. Finally, the last group to have identified this gene named it snerg-1, later MAGE-D [125]. Transcripts of this gene were detected in healthy tissue, and the levels of these transcripts were regulated by follitropin, lutropin and prolactin in rat Sertoli and Leydig cells [125].

It is clear therefore from the work carried out during this dissertation, as well as from published reports, that NRAGE and XIAP may participate in many cellular responses involving varied signal transduction pathways. This undoubtedly includes direct phosphorylation of NRAGE, although from which receptors the signal originates, or the mechanisms that control this have yet to be identified.

One possible way in which the phosphorylation of NRAGE may alter its function would be through altering its cellular localisation, or by altering its binding ability with other proteins [149]. The cell localisation data gained from the immunofluorescence microscopy of the Δ NRAGE mutants reveals some noteworthy disparity. The exclusive localisation of Δ NRAGE⁶⁰ in the nucleus would seem to legitimise that the putative NRAGE NLS described Fig.II-7 is functional. Astonishingly, Δ NRAGE⁸⁰ appears solely in the cytoplasm of the cells. This would suggest that a 20kD region between the WQXPXX domain and the MAGE domain is responsible for binding to another cellular protein, which confines Δ NRAGE⁸⁰ to the cytosol. Intriguingly, the complete NRAGE protein is present in both the cytoplasm and the nucleus, although the majority of the cells express NRAGE in the cytoplasm (Data not shown). This is not unsurprising, since one would expect NRAGE to equilibrate within the cell to its optimal location for the cell, but that nevertheless a minority of cells may experience local fluctuations or disturbances, which could alter this distribution. The possibility that this cellular movement follows the engagement of signal transduction cascades gains credence from the observations of

Salehi *et al.*, and of Masuda *et al.*. The former observed a shift of endogenous NRAGE to the plasmalemma upon NGF stimulation in PC12nr5 cells, although expression remained relatively constant in nuclear and cytoplasmic fractions [100]. The latter group observed an interaction between Dlxin-1 and Dlx5 which is present in both the nucleus and the cytoplasm [150], and between Dlxin-1 and the nuclear transcription factor Msx2 [151] [126].

Clearly, as discussed in this dissertation there are many ambiguities to be clarified in order to fully understand the physiological consequences of these new discoveries. Taken together, the data provided in this thesis add a completely new dimension to the previously available information regarding IAP function. Furthermore, a previously undescribed gene was identified, whilst its function both dependent and independent of IAPs, has been highlighted.

MATERIALS AND METHODS

The methods described in this section are all based upon today's standard molecular and cellular biology techniques.

IV-1. Materials

IV-1.1. Instruments

Hardware

Bacterial incubator

Bacterial shaker

Cell culture incubator

Cell culture microscope

Cell culture Hood

Developing machine

DNA Sequencer

Electrophoresis power supply

Electrophoresis unit, small

Fine scale

Heat block

Homogenizer

Horizontal electrophoresis gel

Microlumat

Mega centrifuge

Mini centrifuge

pH meter

Phosphoimager

Shakers

Manufacturer

Heraeus B 6200

New Brunswick Scientific innova 4330

Köttermann

Carl Zeiss

HLB2472, BIO-FLOW Technik

Agfa

ABI PRISM 373, ABI

EPS600, Pharmacia

Bio-Rad Mini-Protean II

Scaltec SBC 21

Liebisch, Type 2099-DA

Polytron

MWG Biotech

EG&G, Berthold

J-6B, Beckman; Megafuge 1.0 R, Heraeus;

RC 5B plus, Sorval

5417R, Eppendorf

Biofuge 15, Heraeus

Microprocessor, WTW

Fujix BAS-2000 III, Fuji,

with plates BAS-MP 2040P, Fuji

Heidolph, Unimax 2010, Edmund Bühler

WS5

Scale	BP2100S, BP310S, Sartorius
Spectrophotometer	U-2000, Hitachi
Thermocycler	PE9600, Perkin Elmer
Vortex	Scientific Industries Genie-2
Water bath	GFL 1083, Amersham-Buchler

IV-1.2. Chemical reagents and general materials

Reagent	Purchased from
[α - ³² P]dCTP	Amersham
[γ - ³² P]dATP	Amersham
1 kb DNA ladder	Sigma
Acrylamide (30%)/Bisacrylamide (0,8%)	Roth
Adenosin-5'Triphosphate (ATP)	Sigma
Agarose, ultra pure	Life Technologies, Inc.
Ammonium Acetate	Sigma
Ammonium peroxydisulfate (APS)	Sigma
Ampicillin	Sigma
AntifoamA	Sigma
Aprotinin	Roth
Bacto-Agar	Roth
Bovine serum albumin (BSA)	Sigma
Bradford-reagent	Biorad
Bromphenolblue	Sigma
β -Mercaptoethanol	Roth
Calciumchloride (CaCl ₂)	Sigma
Chloroform	Roth
Circlegrow (GC)	Dianova
Deoxycholate (DOC)	Sigma
Diethyl pyrocarbonate (DEP)	Merck
Dimethylsulfoxide (DMSO)	Sigma

Dithiothreitol (DTT)	Sigma
D-Luciferin (free acid)	Applichem
dNTP	MBI
Ethylenediaminetetraacetic acid-disodium salt (EDTA)	Sigma
EGTA	Sigma
Ethanol	Roth
Ethidiumbromide	Life Technologies, Inc.
Formaldehyde	Roth
Formamide	Roth
Glutathion-sepharose	Pharmacia
Glycerol	Sigma
Guanidine thiocyanate	Roth
Hydrochloride (HCl)	Roth
IGEPAL (NP-40)	Sigma
Isoropyl-1-thio- β -D-galactopyranoside (IPTG)	Roth
Isopropanol	Merck
Leupeptin	Sigma
L-Arginine	Sigma
L-Lysine	Sigma
L-Methionine	Sigma
L-Phenylalanine	Sigma
L-Threonine	Sigma
L-Tryptophan	Sigma
Magnesiumchloride	Sigma
3-(N-morpholino)propanesulfonic acid (MOPS)	Sigma
Nitrocellulose BAS-85 membrane	Schleicher & Schüll
Ortho-nitrophenyl- β -D-galactoside (ONPG)	Applichem
Pefablock	Roth
Phenol	Roth
Phenol:Chloroform:Isoamylacohol	Roth
Phenol/Chloroform (TE saturated)	Roth

Ponceau S	Sigma
Potassium acetate (KAc)	Sigma
Potassiumchloride (KCl)	Sigma
Potassiumdihydrophosphate (KH ₂ PO ₄)	Merck
Protein A-agarose	Roche
Protein A-peroxidase	Amersham-Buchler
Protein marker (SDS-7B)	Sigma
SDS ultra pure	Roth
Sodium citrate	Merck
Sodiumdihydrophosphate (NaH ₂ PO ₄)	Merck
Sodiumhydrophosphate (NaHPO ₄)	Merck
Sodiumhydroxide (NaOH)	Sigma
sodium morpholineethanesulfonate (Na-MES)	sigma
Sodium orthovanadate	Sigma
Sonicated salmon sperm	Invitrogen
12-O-tetradecanoyl-phorbo1-13-acetate (TPA)	Sigma
TEMED	Roth
Tris-(hydroxymethyl)-aminomethane (Tris)	Roth
Triton-X100	Sigma
Tyrosine	Sigma
Uracil	Sigma
Whatman 3MM Paper	Schleicher & Schüll
X-gal	Sigma
X-ray film	Amersham-Buchler
Xylencyanol	Roth
Yeast extract	Life Technologies, Inc.

IV-1.3. Cell culture materials

Reagent

DMEM
 Foetal calf serum (FCS)
 Interleukin-3

 L-Glutamine
 Phosphate buffered saline (PBS)
 Penicillin /Streptomycin
 Puromycin
 RPMI 1640
 Trypsin-EDTA
 Trypanblue
 Zeocin TM
 Cell Freezing Medium: 70% Complete
 DMEM/RPMI 1640 (10% FCS, P/S), 20% Fetal
 Bovine Serum, 10% DMSO

Source

Life Technologies, Inc.
 PAA
 WEHI conditioned medium
 (MSZ)
 Life Technologies, Inc.
 Gibco
 Life Technologies, Inc.

 Life Technologies, Inc.
 Gibco
 Sigma
 Invitrogen
 MSZ

IV-1.4. Antibodies**Antibodies**

anti-Flag M2 (mouse monoclonal)
 anti-Myc (mouse monoclonal)
 anti-GST (rabbit polyclonal)

 anti-15CA5 (mouse monoclonal)

 anti-ITA (rabbit polyclonal)
 anti-XIAP (rabbit polyclonal)
 anti-Rabbit IgG conjugated peroxide

Antigens

Flag-epitope
 Myc epitope
 Glutathione-S-
 Transferase
 Haemagglutinin
 (HA) antigen
 peptide
 peptide

Source

Kodak-IBI (Integra)
 MSZ Würzburg
 MSZ Würzburg

 MSZ Würzburg

 [112]
 R&D Systems
 Amersham-Life
 Sciences

anti-Goat IgG conjugated peroxidase (POD)	Santa Cruz
anti-Mouse IgG conjugated peroxidase (POD)	Biotechnology Amersham-LifeSciences
Protein-A conjugated Agarose-beads	Roche
Protein-A conjugated Peroxidase	Roche
Protein-G conjugated Agarose-beads	Roche

IV-1.5. Enzymes

Items	Source
Calf Intestinal Phosphatase (CIP)	New England Biolabs
Pfu polymerase	Stratagene
RNase	Roche
T4 Ligase	New England Biolabs (NEB)
Restriction Endonucleases	AGS, Fermentas, Boehringer Mannheim,

IV-1.6. Kits

Items	Source
ECL Western blotting detection reagents	Amersham
QIAEX II Gel Extraction Kit	Qiagen
QIAGEN Plasmid Kit (Midi, Maxi)	Qiagen
QIAquick PCR purification Kit	Qiagen
Quick Change TM Site Directed Mutagenesis Kit	Stratagene
<i>rediprime</i> TM II random prime labelling system	Amersham Pharmacia Biotech

IV-1.7. cDNA libraries and plasmid DNA

cDNA libraries and plasmids

Mitotic PC12 (rat) cDNA library in the yeast two-hybrid vector pPC86HA

Mouse S194 plasmacytoma cell library in pRCMV2

pRCMV2-*NRAGE

pPC97

pPC86

pPC86HA-ΔNRAGEp⁶⁰

pPC86HA-ΔNRAGEp⁷⁰

pPC86HA-ΔNRAGEp⁸⁰

pPC97-ITA

pPC97-c-IAP1

pPC97-c-IAP2

pPC97-XIAP

pPC97-NAIP

pCFG5 IEGZ

pCFG5 IEGZ-NRAGE

pCMV Flag-MLK3

pCDNA3

pCDNA3-HAJNK1

pCDNA3-*NRAGE

pCNDNA3-NRAGE

pCS2+MT

pCS2+MT-ΔNRAGEp⁶⁰

pCS2+MT-ΔNRAGEp⁷⁰

Source

A.Kalmes (MSZ)

T.Wirth (Ulm)

B.W.M.jordan

D.Nathans (Howard Hughes Medical Institute, Baltimore)

D.Nathans (Howard Hughes Medical Institute, Baltimore)

B.W.M.jordan

B.W.M.jordan

B.W.M.jordan

L.Wixler

L.Wixler

L.Wixler

L.Wixler

L.Wixler

D.Lindemann (Institute of Virology)

B.W.M.jordan

J.Hartkamp

Invitrogen

A. Kieser (München)

B.W.M.jordan

B.W.M.jordan

R.Rupp

B.W.M.jordan

B.W.M.jordan

pCS2+MT-ΔNRAGEp ⁸⁰	B.W.M.jordan
pCS2+MT-NRAGE	B.W.M.jordan
pCS2+MT-*NRAGE	B.W.M.jordan
4x17-mer GAL4DB-Luciferase	Clontech
pM	Clontech
pMGal4BD	Clontech
pVP16	Clontech
pM-XIAP	B.W.M.jordan
pVP16-ΔNRAGEp ⁶⁰	B.W.M.jordan

IV-1.8. Oligonucleotides

Primer name	Sequence
Forward kozak-Flag-NRAGE	5'- gcgaattctgccaccatggactacaagaaggacgatgagatgat gacaaactggaacctccag-3'
Reverse kozak-Flag-NRAGE	5'-gcgctcgcagttactcaaccagaagaagccaatg-3'
Forward mutagenesis	5'-cctggc ccaattgtctggccaaaccaatggcc-3'
Reverse mutagenesis	5'-ggccattgggtttggccagacaattgggccagg-3'

IV-1.9. Cell lines, yeast and bacterial strains

Cell lines:	Source:
HEK 293	Human embryonic kidney, transformed with adenovirus.
293T	HEK293 cells transformed with the SV40 Large T Antigen
32D	Mouse transformed promyeloid leukaemia cell line, IL-3 dependent [88] [105]
32D-Bcl-2	32D cells stably transduced with human Bcl-2 [106]
Yeast strains:	Source
HF7c, Y190	Clontech. Contain <i>HIS3</i> and <i>lacZ</i> reporter genes

Bacterial strains:DH5 α

BL21

Source:

Bethesda Research Laboratories. Optimised for DNA transformation and replication

Stratagene. Optimised for DNA transformation and protein translation

IV-2. Solutions and buffers**IV-2.1. Bacterial medium and DNA isolation buffers****LB (Luria-Bertani) medium**

10g/L Bacto-tryptone

10g/L NaCl, 5g yeast extract

Adjust pH to 7.5 with NaOH

For plates, add 15 g Bacto-agar

CG (Circle-Grow) medium

40g Circle Grow dissolved in 1L d.d. water

2x TY medium

16 g Bacto-tryptone

10 g Yeast extract

5 g NaCl

Adjust pH to 7.4 with NaOH and total volume to 1 litre with H₂O

For plates, add 15 g Bacto-agar

Buffer P1 (resuspension buffer)

50mM Tris-HCL

10mMEDTA

10 μ g/ml RNaseA

pH 8.

Buffer P2 (Lysis buffer)

10% SDS

200 mM NaOH

Buffer P3 (Neutralization buffer)

3 M potassium acetate, pH5.5

Buffer QBT (Equilibration buffer)

15% ethanol

0.15% Triton X-100

Buffer QC (Wash buffer)

2.0 M NaCl

50 mM MOPS, pH7.0

15% ethanol

Buffer QF (Elution buffer)

1.25 mM NaCl

50 mM Tris-HCl, pH 8.5

15% ethanol

IV-2.2. RNA buffers**SolutionD**

4M Guanidine thiocyanate

25mM Na-citrate

100mM β -Mercaptoethanol

0.5% Lauroylsacosine

0.1% AntifoamA

DEP-H₂O

20 μ l DEP to 100ml H₂O, leave 1hr before autoclaving.

STE

0.1M NaCl

20 mM Tris (pH 7.4)

10mM EDTA (pH8.0)

Probe buffer

50%(v/v) Formamide

17.5%(v/v) formaldehyde

5% (v/v) 20×MOPS

27.5% (v/v) DEP H₂O

TNEE buffer

10 mM Tris pH 7.5

1 mM EDTA

50 mM NaCl

5 mM EGTA

Phosphate buffer

89g NaH₂PO₄·2H₂O

4ml 85% Phosphoric acid

made up to 1L, pH 7.2

Hybridisation/prehybridisation buffer

7% SDS

0.5M Phosphate buffer

1mM EDTA

Washing buffer 1

40mM Phosphate buffer

1mM EDTA

5% SDS

Washing buffer 2

40nM Phosphate buffer

1mM EDTA

1% SDS

10[×] RNA gel loading buffer

See 10×DNA gel loading buffer.

IV-2.3. DNA buffers

1x CIP Buffer

50 mM NaCl

10 mM Tris-HCl

10 mM MgCl₂

1 mM dithiothreitol , pH7.9

10x DNA Gel Loading Buffer

40% (w/v) saccharose

0.25% bromphenolblue

0.25% xylencyanol, use as 1x solution

1x Tris-Acetate-EDTA (TAE)

40 mM Tris-HCl,

40 mM acetic acid,

2 mM EDTA; pH7.8

10x Tris-Buffered Saline (TBS)

1 mM Tris-HCl,

150 mM NaCl

IV-2.4. Protein analysis buffers**TBST**

1x TBS + 0.05% Tween

Blotting Buffer

39 mM Glycine

48 mM Tris

0.037% SDS

10% Methanol

Blocking Buffer

5% (w/v) of non-fat dry milk in TBST

Kinase Buffer

10 mM MgCl₂

25 mM HEPES, pH 7.5

25 mM β -glycerophosphate

1 mM Sodium vanadate

0.5 mM DTT

Luciferase Assay Buffer

125 mM Na-MES, pH 7.8

125 mM Tris-HCl, pH 7.8

25 mM magnesium acetate

2 mg of ATP per ml

Luciferin Solution

1 mM D-luciferin in 5 mM KH_2PO_4

Lysis Buffer (for cell culture)

50 mM Na-MES, pH 7.8

50 mM Tris-HCl, pH 7.8

10 mM DTT

2% Triton X-100

b-Gal Assay Buffer

100 mM Na-phosphate-buffer, pH7.4

10 mM KCl

1 mM MgSO_4

3.5 $\mu\text{l/ml}$ β -mercaptoethanol

ONPG-solution

4 mg/ml ONPG in 0.5 M Na-phosphate buffer, pH7.0

Phosphate-Buffered Saline (PBS)

136 mM NaCl

2.6 mM KCl

10 mM Na_2HPO_4 ,

1.5 mM KH_2PO_4 , pH7.4

NP40 lysis buffer

10 mM HEPES pH 7.4

145 mM KCl

5 mM MgCl_2

1 mM EGTA
0.2% IGEPAL
1 mM pefablock
1 mM sodium vanadate
5 mM benzamidine
5 µg/ml aprotinin
5 µg/ml leupeptin

TLB Buffer

20 mM Tris, pH 7.4
50 mM Sodium β-glycerophosphate
20 mM sodium pyrophosphated
500 mM NaCl
10 % (v/v) glycerol
0.1% Triton X-100
2 mM EDTA
1 mM pefablock
1 mM sodium orthovanadate
5 mM benzamidine
5 µg/ml aprotinin
5 µg/ml leupeptin

Running Buffer (for SDS-PAGE)

25 mM Tris
250 mM Glycine
0.1 % SDS

5x SDS-loading Buffer (for SDS-PAGE)

31 mM Tris HCl, pH6.8
1% SDS
5 % Glycerin
2.5 % Mercaptoethanol
0.05 % Bromphenoblue, 1x solution
Sodium Tris-EDTA Buffer (STE)

100 mM NaCl
10 mM Tris-HCl, pH 8.0
1 mM EDTA

IV-2.5. Yeast media and solutions

Amino acid dropout solution

0,2g arginine
0,1g Histidine
0,6g Isoleucine
0,6g Leucine
0,4g Lysine
0,1g Methionine
0,6g Phenyl alanine
0,5g Threonine
0,4g Tryptophan

Dissolve in 100ml d.d water, sterile filter, and store at 4°C. Omit the appropriate amino acid for the respective *dropout* solution.

Glucose

20 % (w/v) Glucose dissolve in distilled water and autoclaved. Stored at 4°C one open.

Selection Media (SD)

8g Difco yeast nitrogen base w/o amino acids
55mg Tyrosine
55mg Uracil
55mg Adenine
(for plates, 25g Agar)

Make up to 890ml distilled water and autoclave.

10ml appropriate 100× *dropout* solution, and 100ml glucose

Growth media (YEPD)

11g yeast extract
22g Bacto peptone
55mg Adenine

(For plates 24g agar)

Fill to 900ml with dist. water and autoclave. Cool to 50-60°C; add 100 ml 20% glucose

X-Gal stock solution

20mg/ml X-gal (5-Bromo-4-Chloro-3-Indolyl- β -D-Galactopyranosid) dissolved in DMF and aliquoted at -20°C in darkness.

Z buffer

16.1g/l Na₂HPO₄

5.5g/l NaH₂PO₄.H₂O

0.75g/l KCl

MgSO₄.7H₂O

Adjust to pH 7, autoclave and maintain at room temp.

Plate mixture

45% PEG (sterile filtered)

1M lithium acetate

1 M Tris-Cl (pH7.5)

0.5 M EDTA

Dissolved in dist. water and sterile filtered.

10⁻¹ TE

0,1 M Tris-HCL

10 mM EDTA (pH 7.5)

10⁻¹ LiAc

1 M lithium acetate

50% PEG

50 % (w/v) PEG dissolved in water and sterile filtered.

IV-3. Methods

IV-3.1. Bacterial manipulation

Plasmid transformed bacteria are selected on LB plates with the appropriate antibiotic for 24 hr. For overnight mini cultures, single colonies are picked and inoculated in LB medium with antibiotic and shaken overnight at 37°C. This preculture is then used for preparing frozen glycerine cultures, plasmid DNA or protein purification. For storage of bacteria, a glycerol stock culture is prepared by growing bacteria to an OD of 0.8 at a wavelength of 600nm in culture medium. 500µl bacterial culture is taken and added to 500 µl 80% glycerine and then mix thoroughly in a small 1.5ml tube. This stock solution is subsequently frozen at -80°C. To inoculate an overnight culture again, take out bacteria and hold at room temperature (RT) until surface is thawed. Pick a small amount of cells and mix into 25 ml culture medium and leave to grow for several hours at 37°C in a bacterial culture shaker. The frozen stock is immediately returned to the -80°C.

IV-3.1.1. Preparation of competent cells (CaCl₂ method)

On the first day, inoculate an overnight preculture from a single colony on a prestreaked plate (from glycerol stock) in 2ml LB or 2x TY media by incubation at 37°C and shaking to aerate. The second day, inoculate 1 ml of the preculture in 100ml fresh media and grow the culture at 37°C until OD at wavelength 600nm of the culture reaches between 0.2 and 0.3. Cool down the culture on ice for at least 15 min. (The following procedures should be carried out at 4°C in pre-cooled sterile tubes). Harvest the cells in a centrifuge at 5000 g for 5 min, and discard the supernatant. Resuspend the bacterial pellets thoroughly in a small volume of ice-cold 100mM CaCl₂. Dilute the suspension with the CaCl₂ solution to a final volume of 30-40 ml, and leave on ice for 25 min with occasional shaking. Spin down the cells as before, discard the supernatant carefully and resuspend the pellets in 5 ml glycerol/CaCl₂. The suspension can be aliquoted in 100 to 400 µl aliquots and stored at -70°C. The transformation efficiency of the bacteria prepared by this method should reach at least 10⁶.

IV-3.1.2. Transformation of competent bacteria

Thaw the competent bacteria from a desired origin on ice. Add a maximum of 20ng ligated DNA or purified plasmid-DNA to 100 µl competent cells in a cold 1.5 ml microfuge tube. Mix carefully and keep on ice for 20 min or longer. Heat-shock the bacteria then at 42°C for 90 sec, add 1 ml antibiotic-free LB medium, and aerate at 37°C for 30 min. Selection of transformed bacteria is done by plating 100 µl of the bacterial suspension on antibiotic containing agar plates. Only bacteria that have taken up the desired plasmids, which normally contain ampicillin

resistance cassette, can grow on the agar plates. A single colony can then be expanded in LB medium and used for DNA preparation.

IV 3.2. DNA methods

IV-3.2.1. Electrophoresis of DNA on agarose gel

Double stranded DNA fragments with lengths between 0.5 kb and 10 kb can be separated according to their lengths on agarose gels. Agarose is added to 1x TAE to obtain a final concentration between 0.7-2%. Boil the suspension in the microwave until the agarose is completely solubilised. Allow the agarose to cool down to around 50°C before adding ethidium bromide up to 0.5 µg/ml and pour into the gel apparatus. Add DNA gel loading buffer to the DNA sample and apply on the gel. Electrophorese in 1x TAE buffer at 100 volts. The DNA can be visualised under UV-light.

IV-3.2.2. Isolation of plasmid DNA from agarose (QIAEX II agarose gel extraction protocol)

This protocol is designed for the extraction of 40-bp to 50-kbp DNA fragments from 0.3-2% standard agarose gels in TAE or TBE buffer. DNA molecules are adsorbed to QIAEX II silica particles in the presence of high salt. All non-nucleic acid impurities such as agarose, proteins, salts, and ethidium bromide are removed during washing steps.

Excise the desired DNA band from the agarose gel under the UV light. Weigh the gel slice and add 3 volumes of Buffer QG to 1 volume of gel for DNA fragments 100-bp-4 kbp; for DNA fragments more than 4 kbp, add 2 volume of QG plus 2 volumes of H₂O. Resuspend QIAEA II by vortexing for 30 sec; add 10 µl (or 30 µl) of QIAEX II to the sample containing not more than 2 µg of DNA (between 2-10 µg). Incubate at 50°C for 10 min to solubilise the agarose and bind the DNA. Mix by vortexing every 2 min to keep QIAEX II in suspension. Centrifuge the sample for 30 sec and carefully remove supernatant with a pipette. Wash the pellet with 500 ml of Buffer QG and then twice with Buffer PE. Air-dry the pellet and elute the DNA in 10 mM Tris-HCL or H₂O and resuspend the pellet by vortexing. Incubate at RT for 5 min (or at 50°C for 5 min) for DNA fragments not more than 4 kbp (for DNA fragments between 4-10 kb). Centrifuge for 30 sec and carefully pipette supernatant into a clean tube.

IV-3.2.3. Purification of plasmid DNA (QIAquick PCR purification kit)

This protocol is designed to purify single- or double-stranded PCR products or DNA plasmids ranging from 100 bp to 10 kbp. DNA adsorbs to the silica-membrane in the presence of high salt while contaminants pass through the column. The impurities are washed away and pure DNA is eluted with Tris buffer or H₂O.

Add 5 volume of buffer PB to 1 volume of the contaminants and mix. Place a QIAquick spin column in a 2 ml collection tube. Apply the mixed sample to the QIAquick column and centrifuge 30-60 sec. Discard flow-through and place QIAquick column back into the same collection tube. Add 0.75 ml Washing Buffer PE to column and centrifuge 30-60 sec. Discard flow-through and place QIAquick column back into the same collection tube. Centrifuge column for an additional 1 min at maximum speed. Place QIAquick column in a clean 1.5 ml microfuge tube. Add 50 µl Elution Buffer EB or H₂O to the centre of the QIAquick column and centrifuge for 1 min. Store the purified DNA at - 20°C.

IV-3.2.4. Ligation of DNA fragments

1. Calf-intestinal-phosphatase (CIP) reaction (5' phosphorylation)

Alkaline phosphatase catalyses the removal of 5' phosphate groups from DNA, RNA and ribo- and deoxyribonucleoside triphosphates. For blunt end ligation, the 5' phosphate group of the vector must be removed by CIP reaction. This reaction is also used to prevent the re-ligation of the vectors. 2.5 µg of DNA fragments is phosphorylated at 37°C for 30 min in 100 µl of reaction volumes consisting of 1x CIP buffer and 1 µl of phosphatase. 5 mM EDTA is then added to the reaction and incubated with the reaction at 65°C for 15 min to inactivate the enzyme. The DNA fragments are purified by phenol and ethanol precipitation before ligation reaction.

IV-3.2.5. Cohesive-end ligation

Prepare the plasmid DNA or DNA fragment by cutting it with suitable restriction enzymes, which is followed by purification. 1:3 molar ratio of vector: insert DNA fragments together with 1 µl of T4 ligase are incubated in 1x Ligation Buffer in a total volume of 20 µl for 4 hr at RT or overnight at 16°C. Heat the mixture at 65°C for 10 min to inactivate the enzyme.

IV-3.2.6. Mini-preparation of plasmid DNA

Grow 3 ml overnight culture in LB, 2x TY, or GC media with 100 µg/ml ampicillin at 37°C overnight. Pellet the cells at 14,000 rpm for 1 min. Remove the supernatant and resuspend the pellets in 100 µl Buffer. Add 200 µl Buffer P2 (Lysis Buffer) and incubate at RT for 5 min. Add 150 µl ice-cold 3 M acidic KOAc (Neutralisation Buffer), mix by inverting the tubes for 6-7

times and incubate on ice for 5 min. Centrifuge at 15,000 rpm for 3 min. Transfer the supernatant to a fresh Eppendorf tube and add 900 μ l of pre-cooled 100% ethanol, precipitate at -70°C for 10 min. Centrifuge the pellet at 15,000 rpm for 10 min. Wash the pellet with 200 μ l 70% ethanol. Air-dry the pellet and resuspend it in 30-50 μ l 10 mM Tris-HCl, pH 7.8.

IV-3.2.7. Maxi-preparation of plasmid DNA

Grow culture in 50 ml GC media containing plasmids or recombinant plasmids overnight in a 37°C incubator with shaking at 220 rpm. Collect the bacteria and isolate DNA plasmids by using a Quiagen Plasmid Maxi Kit. This extraction method is based on Birnboim's alkali lysis principle. Resuspend the bacterial pellet in 10 ml of Buffer P1. Add 10 ml of Buffer P2, mix gently, and incubate at RT for 5 min. Add 10 ml of chilled Buffer P3, mix immediately, and incubate on ice for 20 min. Centrifuge at 4,000 rpm for 30 min at 4°C. Filter the supernatant over a prewetted, folded filter. Apply the supernatant to a equilibrated QIAGEN-tip 500 and allow it to enter the resin by gravity flow. Wash the QIAGEN-tip twice with Buffer QC. Elute DNA with 15 ml Buffer QF. These processes result in the isolation of a DNA-salt pellet, which is precipitated by 0.7 volumes (10.5 ml) of isopropanol and centrifuged further at 4000 rpm for 30 min. Washed the resulting pellet twice with 70% ethanol and air-dry at RT. The pellet is then carefully resuspended in TE buffer and used for transfection of cultured mammalian cells.

IV-3.2.8. Measurement of DNA concentration

The DNA concentration is determined by using an UV spectrophotometer at wavelength of 260 nm. The absorption of 1 at 260 nm corresponds to a concentration of 50 μ g/ml double stranded DNA. Identity, integrity and possible purity of the DNA can be subsequently analysed on an agarose gel.

IV-3.2.9. DNA Sequencing (Sanger Dideoxy Method)

DNA can be sequenced by generating fragments through the controlled interruption of enzymatic replication [152]. DNA polymerase I is used to copy a particular sequence of a single-stranded DNA. The synthesis is primed by complementary fragment, which may be obtained from a restriction enzyme digest or synthesised chemically. In addition to the four deoxyribonucleoside triphosphates (ddNTP), the incubation mixture contains a 2', 3'-dideoxy analogue of one of them. The incorporation of this analogue blocks further growth of the new chain because it lacks the 3'-hydroxyl terminus needed to form the next phosphodiester bond. A fluorescent tag is attached to the oligonucleotide primer, a differently coloured one in each of the four chain-terminating reaction mixtures. The reaction mixtures are combined and electrophoresed together. The

separated bands of DNA are then detected by their fluorescence as they pass out the bottom of the tube, and the sequence of their colours directly yields the base sequence.

1. Sequencing Reaction:

The "Taq Cycle Sequencing" is performed by using "PRISM™ Ready Reaction DyeDeoxy™ Terminator Cycle Sequencing Kit". Mix the following reagents in a 0.6 ml double-snap-cap microfuge tube:

Terminator premix*	9.5 µl
DNA template	1.0 µg
Primer	10 pmol
dH ₂ O	Adjust the final reaction volume to 20 µl

*A-Dye Terminator labelled with dichloro[R6G]

C-Dye Terminator labelled with dichloro[TAMRA]

G-Dye Terminator labelled with dichloro[R110]

T-Dye Terminator labelled with dichloro[ROX]

Place the tubes in a thermal cycler preheated to 96°C which is followed by 25 cycles of thermal cycling steps: 96°C for 15 sec; 48°C for 15 sec; 60°C for 4 min; and keep at 4°C after the reaction.

2. Removal of the excess dye terminators by using CENTRI-SEP Columns:

CENTRI-SEP Columns are designed for the fast and efficient purification of large molecules from small molecules.

Prepare the CENTRI-SEP columns according to the standard procedures (PRINCETON SEPARATIONS, INC.) Transfer the DyeDeoxy™ terminator reaction mixture to the top of the gel. Carefully dispense the sample gently onto the centre of the gel bed at the top of the column without disturbing the gel surface. Place the column into the sample collection tube and place both into the rotor. Maintain proper column orientation. Spin the column and collection tube at

750 g for 2 min. The purified sample will be collected in the bottom of the sample collection tube. Dry the sample in a vacuum centrifuge.

3. Preparation and Loading of the samples:

Resuspend the pellet in 4 μ l of the following reagent mixture containing 5 μ l deionized formamide and 1 μ l 25 mM EDTA with blue dextran (50 mg/ml). Centrifuge the solution to collect all the liquid at the bottom of the tube. Denature the samples at 95°C for 2 min and transfer them immediately on ice. The samples are then separated on polyacrylamide gel on the ABI PRISM 373 DNA Sequencer with the appropriate run module, DT {dR Set Any-Primer} mobility file, and matrix file.

DNA sequencing is done by R. Krug (MSZ, Würzburg).

IV-3.3. Extracting and handling RNA

IV-3.3.1. Isolation of RNA from tissue

RNA is extremely sensitive to degradation by RNases, and should therefore be handled where possible with RNase-free materials. Tissues can be taken fresh or stored at -80°C. Frozen or fresh tissues should be put in 8 ml Sol. D (in 50 ml Falcon tube). Homogenise in Polytron for 30 sec at speed "6"(speed "7" for bone). Repeat until adequately homogenised (the mechanical parts may heat up during this procedure, therefore avoid prolonged homogenisation, and keep on ice). Add 0.8 ml NaAc pH 4.0, 8.0ml Phenol (TE sat.) and 1.6 ml Chloroform. Mix on a Vortex for 25 sec then place on ice for 15 min. Centrifuge at 10,000 rpm for 15 min. Dissolve pellet in 2 ml TE/0.5% SDS. Add 7 ml Isopropanol and incubate O/N at -20°C. Transfer to a 10 ml polyallomer tube (Falcon) and add 2 ml Phenol/Chloform (10 \times TE sat.). Vortex for 10 sec and spin for 3 min at 3000 rpm. Add 1 ml 7.5M NH₄Ac and 8 ml 95% Ethanol, and incubate at -20°C for 15 min. Spin 5 min at 5000 rpm. Resuspend pellet in 100 μ l DEP-H₂O, measure concentration, and store at -20°C under 2.5 volumes ethanol.

IV-3.3.2. Isolation of RNA from cells

Harvest cells and wash twice in ice-cold PBS, and resuspend in 1 ml ice-cold PBS and transfer to Eppendorf. Spin for 10 sec, remove supernatant and resuspend in ice-cold TNEE buffer. Add 30 μ l of 5% NP40, vortex briefly and incubate on ice for 5 min. Spin at max. speed for 1 min. In the meantime prepare an Eppendorf containing 30 μ l 10% SDS and 200 μ l Phenol (TE buffered) (at room temperature). Transfer the supernatant from the last centrifugation step to the tubes containing SDS/Phenol, vortex 20 sec, and spin again for 1 min. Transfer the supernatant to a

tube containing 30 μ l 3M NaOAc and 1 ml ethanol. Incubate for 1 min at -70°C and then on ice for 10 min, and then centrifuge at full speed for 5 min. Dry pellet, take up in 400 μ l DEP-H₂O, measure concentration at OD₂₆₀, and store the rest under 2.5 volumes ethanol at -20°C.

IV-3.3.3. Running RNA samples on denaturing gels

Centrifuge 10 μ g RNA at full speed for 15 min, take off SN and air dry (usually requires 1 min, do not dry longer!). Reconstitute with 18 μ l probe buffer, pipetting up and down several times. Denature at 56°C for 10 min and add 2 μ l 10 \times loading buffer. Dissolve 1 g agarose in 77 ml DEP water, and boil. Allow cooling to 60°C and then add 5 ml 20 \times MOPS and 18 ml formaldehyde. Pour gel and allow to set. The gel is run in \times MOPS buffer. The RNA can be labelled using ethidium bromide, photographed, and then capillary blotted onto nitrocellulose.

IV-3.3.4. Northern blotting

Once the denatured RNA has been immobilised onto nitrocellulose, it is possible to radioactively label and hybridise a probe. The Northern blots described in this dissertation were probed with cDNAs labelled according to the RediprimeTM kit protocol from Amersham Pharmacia Biotech, which is based upon a standard Klenow based technique. The membrane was first incubated with prehybridising solution for 1 hr at 65°C. The solution was then changed and replaced with hybridisation solution containing the radiolabelled probe and incubated overnight at 65°C. The probe may be frozen, denatured and re-used for up to one week later. Following hybridisation, the membrane is then subjected to washing at 65°C. The membrane is washed once with washing buffer 1, followed by three times with washing buffer 2, each for 15 min. The membrane is then rinsed to remove excess SDS.

IV-3.4. Yeast two-hybrid methods

A modified Clontech MatchmakerTM yeast two-hybrid system was utilised in order to identify new IAP-binding proteins. This system was based on that of Stanley Fields and co-workers at the State university of New York at Stony Brook [Fields, 1989 #165]. The principle uses a simple growth selection and colourimetric assay which is based on reconstitution of a functional GAL4 transcriptional activator. This transcriptional activator is first separated into its DNA-binding domain (DB) and activation domain (AD), and then reconstituted *in vivo* in yeast cells. This reconstitution results in activation of a nutritional reporter gene (*HIS3*), as well as a colourimetric reporter (*LacZ*), under the control of a GAL4-responsive promoter. This method has yielded a great deal of information regarding previously unknown protein interactions [153] [102].

IV-3.4.1. The two-hybrid screen

ITA was cloned in frame into the pPC97 vector containing the GAL4 DB, resulting in a GAL4DB-ITA fusion protein, also designated '*Bait*', when transformed in yeast. Likewise, the PC12 cDNA library was cloned into the complementary pPC86 vector containing the GAL4AD, resulting in GAL4AD-PC12-LIBRARY fusions, also designated '*Prey*'. Each of the vector types also contains a nutrient marker, allowing the successfully transformed yeast to grow in the absence of the specific amino acid. Reconstitution of the GAL4-DB and -AD, brought about by an interaction between GAL4DB-ITA and a GAL4AD-PC12-LIBRARY fusion protein, results in the activation of a third nutrient reporter gene located in the yeast genome. Activation of this third reporter gene (*HIS3*) enables the yeast to grow on -His/-Leu/-Trp SD medium. To confirm the protein interaction, primary His⁺ transformants are tested for expression of the second reporter gene *LacZ* using a β -galactosidase colony filter assay.

Protocol: 2 μ g pPC97 ITA was transformed using the small scale transformation protocol, plated onto a -Leu SD plate, and incubated for 48hr at 30°C. Five colonies were inoculated in 0.5 ml -Leu SD medium, vortexed and transferred to a flask containing 150 ml -Leu SD medium. This was then grown O/N at 30°C shaking at 250 rpm to an OD₆₀₀ >1.5. This was then transferred to 1 L -Leu SD giving an OD₆₀₀ of 0.2-0.3 and incubated for 3 hr with shaking at 250 rpm. The cells were then centrifuged at 1000 \times g for 5 min at room temperature, the SN discarded, and the pellet resuspended in 8 ml freshly prepared sterile 1 \times TE/LiAc. 2.4 mg PC12 library DNA was added to the pellet and mixed well. 60 ml sterile 1 \times PEG/LiAc solution was added, vortexed, and incubated at 30°C for 30 min shaking with 200 rpm. Next, 8 ml DMSO (10% final concentration) was added and mixed gently by inversion. The cell suspension was heat shocked in a 42°C water bath for 15 minutes, swirling occasionally to mix. The cells were then chilled on ice and then pelleted by centrifuging for 5 min at 1000 \times g. The pellet was resuspended in 15 ml 1 \times TE buffer, plated out onto -Leu/-Trp/-His SD plates, and incubated for 5-9 days at 30°C.

The transformation efficiency and number of independent clones screened were determined in order to assess the effectiveness of the procedure. 1/10, 1/100 and 1/1000 dilutions of the cell suspension were made and then plated out onto -Leu/-Trp SD plates and allowed to grow 2-3 days. The number of colonies were counted for each dilution, and the cotransformation efficiency was calculated according to the following formula:

$$\frac{\text{cfu} \times \text{total suspension vol. } (\mu\text{l})}{\text{Vol. plated } (\mu\text{l}) \times \text{dilution factor} \times \text{amount DNA used } (\mu\text{g})} = \text{cfu}/\mu\text{g DNA}$$

To estimate the number of clones screened:

$\text{cfu}/\mu\text{g} \times \text{amount DNA used } (\mu\text{g}) = \# \text{ of clones screened}$

IV-3.4.2. Colony lift β -galactosidase filter assay

Due to the occurrence of false positives growing on the triple dropout (-Leu/-Trp/-His) plates, a second test is performed to determine which of the *HIS3* positive clones are also *LacZ*, by screening for blue colonies in a β -gal test. The colonies are transferred to filters and placed on selection medium. After incubation for 1-2 days at 30°C, the membranes are lifted out and the colonies assayed for β -galactosidase activity. A Z-buffer/X-gal mix is prepared by adding 500 μ l X-Gal stock (20 mg/ml) 27 μ l β -Mercaptoethanol to 10 ml Z-buffer. A sterile Whatman #5 filter was placed in a 100 mm plate and soaked with 1 ml Z buffer/X-gal buffer. The yeast were permeabilised by placing the membrane face up in a pool of liquid nitrogen. Using forceps, the membrane should be completely submerged for 10 sec, or until uniformly frozen. The membrane was then placed carefully, colony side up, on the presoaked filter. Genuine positives should develop a blue colour between 30 min-8 hr.

IV-3.4.3. Transforming *S. cerevisiae* with plasmids (small scale)

A single yeast colony is incubated O/N in 50 ml YEPD medium, shaking at 30°C in a water bath. One ml yeast culture per transformation is placed in an Eppendorf and spun for 5 sec. The SN can be discarded, leaving 50-100 μ l in the tube in which to resuspend the pellet. To this 2 μ l carrier DNA and \approx 1 μ g plasmid DNA is added and then vortexed. In addition, 0.5 ml plate mixture and 20 μ l DTT were added, the tube was vortexed again and incubated at room temperature for 6 hrs to O/N. after a 10 min heat shock at 42 °C, 200 μ l cells from the bottom of the tube were plated out on a selection plate. The yeast were grown for up to three days at 30°C.

IV-3.4.4. Direct two-hybrid tests

Using the above method it is possible to cotransform two complementary vectors to analyse a direct interaction between two proteins. After cotransformation, the yeast are plated first on -Leu/-Trp SD plates, before being transferred to -Leu/-Trp/-His SD plates to test *HIS3* and subsequently *LacZ* activity. This direct testing method is also employed to test the specificity of a library screen interaction, since it is possible to examine whether potential *prey* clone is able to autonomously activate the reporter genes with or without the empty *bait* vector.

IV-3.4.5. Plasmid isolation from yeast cells

In order to identify prey plasmids from a library screen, 1,5 ml of an overnight culture is spun at 14,000 rpm for 5 sec, and the pellet resuspended in 100 µl STET buffer. To this, 100 µl glass beads are added and shaken violently for 5 min on a vortexer, in order to mechanically break the cell membranes. Add another 100µl STET and incubate at 100°C for 3 min. Chill on ice and centrifuge at 4°C for 10 min, then aspirate 100µl supernatant and transfer to an Eppendorf containing 50µl 7,5M ammonium acetate. Incubate at -20°C for 30 min, then centrifuge (12,000 × g) at 4°C. 100µl supernatant is then added to 400µL 100% ethanol, incubated for 5 min on ice, and centrifuged at 12,000 × g. After the DNA pellet is dry, resolve in 20µl TE and transform in DH5α bacteria. The *bait* and *prey* plasmids should be distinguished by restriction digest of overnight cultures from colonies picked. The *prey* plasmid can then be sequenced, retransformed in yeast and tested for interaction with the *bait* plasmid/empty vector in direct *two-hybrid* tests.

IV-3.4.6. Protein extraction from yeast

Centrifuge 1,5 ml overnight culture for 30 sec, remove supernatant and add 30 µl 2 × laemmli buffer, boil for 2 min and fill to fluid level with glass beads. Vortex for 1 min, then add another 70µl laemmli. Vortex again for 1 min, boil for 2 min then place on ice for 5 min. add a further 30µl laemmli, pipette the liquid and transfer to a new Eppendorf. Centrifuge for 30 sec, place the SN in a new Eppendorf, and run on SDS-PAGE.

IV-3.5. Protein methodologies

IV-3.5.1. Immunoprecipitation

For immunoprecipitation of cellular proteins, protein G sepharose is employed for monoclonal antibodies and goat antisera, whereas protein A sepharose is used for rabbit antibodies. 20 µl sepharose was incubated with 0.5-4 µg of antibody, 500 µg precleared lysate and the volume made up to 1 ml in an Eppendorf tube using lysis buffer. Lysates are first precleared for 1 hr with the relevant beads. Samples are incubated on a nutator for at least 2 hr at 4 °C and then washed with appropriate wash buffers, depending on the stringency required. The choice of wash buffer should insure low background and maximum preservation of complexed proteins. When analysing novel interactions, a mild wash buffer like NP40 buffer is used in order to insure that interactions between proteins of interest are not destroyed. The immunoprecipitated proteins are boiled in Laemmli buffer and subjected to SDS PAGE and Western blotting, or their activity can be analysed in *in vitro* kinase assays.

IV-3.5.2. *In vitro* kinase assay

The kinase activity of an enzyme can be measured *in vitro* by the uptake of [γ - 32 P] ATP radioactivity by its substrate. The immunoprecipitated kinases are washed twice with both lysis buffer and kinase buffer. For MLK3 kinase assays, SDS must be omitted from all buffers. Add 5 μ Ci [γ - 32 P] ATP, 2-5 μ g of substrates, 0.1 mM ATP, and 20 μ l kinase buffer, incubate the mixture at 30°C for 20 min. The reaction is then stopped by adding SDS-loading Buffer and incubated at 95°C for 5 min. The proteins are separated by SDS-PAGE, and then blotted onto nitrocellulose membranes. The membrane is placed in a lightproof cassette together with x-ray film to detect the γ -radiation. Equal loading of the immunoprecipitated kinase is subsequently controlled by immunoblotting with specific antibodies.

IV-3.5.3. Measurement of Protein concentration (Bio-Rad protein assay)

The Bio-Rad Protein Assay is based on the observation that when Coomassie Brilliant Blue G-250 binds to the protein, the absorbency maximum shifts from 450 nm to 595 nm [154]. Equal volumes of cell lysate containing 1-20 μ g of protein is added to diluted Dye Reagent and mixed well (1:5 dilution of Dye Reagent Concentrate in ddH₂O). After a period of 5 min to 1 hr, the absorption at wavelength 595 is measured versus reagent blank (which contains only the lysis buffer).

IV-3.5.4. Sodium dodecyl sulfate polyacrylamide gel electrophoresis (SDS PAGE)

Proteins can be easily separated on the basis of mass by electrophoresis in a polyacrylamide gel under denaturing conditions. Cells are harvested, washed, lysed, and where possible protein content is measured. Cell debris is cleared by centrifugation. 5x SDS-loading Buffer is used to denature 20-50 μ g of precleared cell extracts, whilst for IPs an equal amount of 2x SDS-loading is added, and then heated at 95°C for 5 min. SDS is an anionic detergent that disrupts nearly all noncovalent interactions in native proteins. β -Mercaptoethanol is also included in the sample buffer to reduce disulfide bonds. The SDS complexes with the denatured proteins are then electrophoresed on a polyacrylamide gel in the form of a thin vertical slab. Vertical gels are set in between 2 glass plates with an internal thickness of 1.5 mm between the two plates. In this chamber, the acrylamide mix is poured and left to polymerise for at least 30 min at RT. The gels are composed of two layers: a 615% separating gel (pH 8.8) that separates the proteins according to size; and a lower percentage (5%) stacking gel (pH 6.8) that insures the proteins simultaneous entry into the separating gel at the same height.

	Separating gel	Stacking gel
Tris pH 8.8	2.5 ml.	1.25 ml
Acrylamide/bisacrylamide 29:1 (30%)	2.0-5.0 ml	1.7 ml
10% SDS	0.1 ml	0.1 ml
ddH ₂ O	5.4-2.4 ml	6.8 ml
10% APS	0.1 ml	0.1 ml

The separating gel is poured in between two glass plates, leaving a space of about 1cm plus the length of the teeth of the comb. Isopropanol is added to the surface of the gel to exclude air. After the separating gel is polymerised, the isopropanol is removed. The stacking gel poured on top of the separating gel, the comb inserted, and allowed to polymerise. The samples are loaded into the wells of the gel and running buffer is added to the chamber. A cover is then placed over the gel chamber and 45 mA are applied. The negatively charged SDS-proteins complexes migrate in the direction of the anode at the bottom of the gel. Small proteins move rapidly through the gel, whereas large ones migrate slower. Proteins that differ in mass by about 2% can be distinguished with this method. The electrophoretic mobility of many proteins in SDS-polyacrylamide gels is proportional to the logarithm of their mass.

IV-3.5.5. Immunoblotting

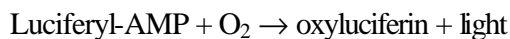
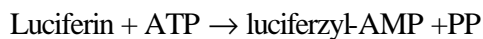
After the cell extracts are subjected to SDS-PAGE, the proteins are transferred by electroblotting to nitrocellulose BAS-85 membrane. SDS-PAGE gels are electroblotted at 400 mA in blotting buffer for 45 min. Ponceau S fixative dye solution (containing Ponceau S, trichloroacetic acid, and sulfosalicylic acid) is used to check if the transfer has occurred. Stain for 5 min and wash with de-ionised water. For Western blot analysis, incubate the membranes in blocking buffer for 1 hr at RT. or overnight at 4°C on a shaker. Dilute the first antibody in BST/5% milk (unless otherwise indicated), add to the membrane, and incubate O/N at 4°C. Wash the membrane three times with BST, each time for 10 min. Dilute the appropriate peroxidase-conjugated secondary antibody in TBST (or according to manufacturers instructions), add to the membrane, incubate at RT for 45 min, and wash. This step is followed by the standard enhanced chemiluminescence reaction (ECL-system): incubate the membrane in a 1:1 mix of ECL solutions 1 and 2. This reaction is based on a peroxidase catalysed oxidation of Luminol, which leads to the emission of light photons that can be detected on X-ray film. Thus the peroxidase conjugated secondary antibodies bound to the primary antibody detect the protein of interest.

IV-3.5.6. Immunoblot stripping

The removal of primary and secondary antibodies from a membrane is possible, so that it may be reprobed with alternative antibodies. To make 50 ml stripping buffer, mix 3.125 ml of a 1M Tris solution, 5 ml of a 20% SDS solution, 0.35 ml of 4.3M β -Mercaptoethanol, and make up to 50ml with 42ml distilled H₂O. Incubate the membrane in stripping buffer for 30 min at 50°C. The membrane should be washed at least 5 times with PBST or TBST. The membrane can then be reprobed as described above.

IV-3.5.7. Luciferase reporter gene assay

Bioluminescence is characterised by light emission catalysed by an enzyme. Firefly luciferase, catalyses the release of light upon addition of luciferin and ATP. The luciferase activity is assayed and quantified by measurement of light production. The photon production by catalytic oxidation of beetle luciferin occurs from an enzyme intermediate, luciferyl-AMP.



Luciferin is first activated by addition ATP. The activated luciferin reacts with oxygen to form dioxetane. Dioxetane decomposes and excites the molecule, which transfers to its ground state by emission of fluorescence light.

The transfected cells are harvested and lysed in 100 μ l of lysis buffer, mixed well, and incubated on ice for 30 min. The crude cell lysates are precleared by centrifugation at maximum speed for 1 min. 50 μ l of precleared cell extract is added to 50 μ l of Luciferase Assay Buffer. The activity is measured after injection of 50 μ l of D-luciferin solution, and the reaction is monitored in a Berthold luminometer for 5 sec. The luciferase activities are normalised against the β -galactosidase activity of co-transfected 1 μ g Rous sarcoma virus LTR β -gal vector in the β -galactosidase assay. Results are presented as luciferase units normalised to protein concentration. Each experiment is performed in duplicates or triplicates. The mean and standard deviations of two independent experiments are shown in the figures.

IV-3.5.8. β -galactosidase assay

The β -galactosidase assay is performed according to a standard protocol (Sambrook, J., Fritsch, E.F., and Maniatis, T. 1989: Molecular cloning: A laboratory Manual 2nd Ed., Cold Spring Harbor Laboratory Press, New York). 20 μ l (approximately 15-20 μ g of total protein concentration) of precleared cell lysate is added to 500 μ l of β -gal Assay Buffer and 100 μ l

ONPG-solution. This is incubated at 37°C until the solution begins to turn yellow (between 4 hr to overnight). 250 µl of 1 M Na₂CO₃ is added to stop the reaction. The absorption of the solution at wavelength 420 should be measured within the next 30 min.

IV-3.6. Cell culture techniques

IV-3.6.1. Cell maintenance

The human embryonic kidney cell line HEK293 and 293T derived virus packaging cells were cultured in Dulbecco's modified Eagle's medium (DMEM) supplemented with 10% (v/v) foetal calf serum (FCS), 100 U penicillin and streptomycin per ml, and 2 mM L-glutamine, at 37°C in humidified air with 6% CO₂. The 32D cells were obtained from Dr. J.S. Greenberger and grown in RPMI 1640 (Gibco) supplemented with 10% heat inactivated (45 min., 56⁰C) foetal calf serum, 100 U penicillin and streptomycin per ml, 2 mM L-glutamine and 15% of WEHI-conditioned medium at 37⁰C, 5% CO₂ and 90% humidity. 32DBcl-2 cells were obtained from J.Reed.

IV-3.6.2. Transient transfection of 293 cells (Calcium phosphate method)

Cells were transfected by a calcium phosphate coprecipitation method according to a modified Stratagene protocol. For each 10 cm plate, 5-10 µg DNA was made up to 450 µl with Sigma endotoxin-free water, and mixed with 50 µl 2.5M CaCl₂. Then 500 µl 2×BBS (pH6.97) was added dropwise while vortexing, and left at room temperature for max. 20 min. The transfection mix was then added carefully to the cells and incubated for 6hr-O/N at 37°C, 7% CO₂. After the incubation, the cells were washed at least 3× with 1×PBS prewarmed to 37°C. HEK293 cells were starved in DMEM with 0.3% (v/v) FCS for 48h after transfection, whereas the 293T derived lines were maintained in 10 % (v/v) FCS throughout. Transfection efficiency was monitored via the GFP expression from the pCFG5-IEGZ.

IV-3.6.3. Establishment of stable cell lines

70% confluent 293T derived virus-packaging cells were transfected in a single well of a flat bottom six-well tissue culture plate with 2.5 µg of purified DNA following the above CaPO₄ protocol. 24 hours after transfection cells were refed with 2 millilitres of fresh medium for overnight. The following day tissue culture supernatants were cleared from cells by centrifugation (800×g, 5 minutes at 20⁰C) and sterile filtered through a 0.45 µm filter attached to a syringe. 32D cells to be infected were seeded at 0.5x10⁶ cells per ml to which 1 ml of the virus supernatant, 250 µl WEHI conditioned medium and 1 µg polybrene/ml were added. 24 hours

later the infection was resupplied with 2 ml fresh 32D cell culture medium. Selection of cells carrying the pCF5 IEGZ expression constructs was started by adding 600µg Zeocin/ml. Selection medium was changed every other day.

IV-3.6.4. Cell survival assays

For the analysis of cell survival and intracellular signalling pathways cells were washed three times in tissue culture medium without WEHI cell supernatant. 0.5×10^6 cells in a total volume of 1 ml were dispensed into a single well of a flat bottom 24 well tissue culture plate. Cell viability was routinely assessed by staining the cells in trypan blue (Sigma).

IV-3.6.5. Immunofluorescence

HEK 293 cells were seeded on cover slips in 6-wells and transfected the next day according to the above protocol. 48hr after transfection, the cells were washed 2× with 1×PBS, and fixed in 3,7% Formaldehyde in PBS for 10 min. The cells were washed again twice with 1×PBS, and permeabilised for 10 min with 0,5% Triton-X-100. To prevent non-specific antibody binding, the cells were then blocked in 1% BSA/1% serum (from the species where the secondary antibody was derived from) for 30 min. The first antibody was diluted in 1% BSA according to the manufacturers recommendations and incubated for 45 min. The unbound antibody was washed away by incubating three times for 5 min with 1×PBS. The fluorescence-conjugated secondary antibody was then diluted appropriately in 1% BSA and incubated for 45 min protected from light. The cells were then washed three times in 1×PBS to remove excess antibody and carefully mounted on a glass slide using 50% glycerol. The cover slip can then be mounted more permanently by applying nail varnish to the edges.

N.B. Some antibodies cross-react with BSA or with serum proteins, therefore always check the manufacturers guidelines before use. All steps are carried out at room temperature. The cell nuclei may also be stained after the incubation with the second antibody by rinsing with 200 mM KCl and applying a 1:1000 dilution of a 5µg/ml DAPI in PBS for 15 min.

REFERENCES

1. Vogt, C., *Untersuchungen über die Entwicklungsgeschichte der Geburtshelferkrote (Alytes obstetricans)*. 1842: JU Gassman. 130.
2. Kerr, J.F., A.H. Wyllie, and A.R. Currie, *Apoptosis: a basic biological phenomenon with wide-ranging implications in tissue kinetics*. Br J Cancer, 1972. 26(4): p. 239-57.
3. Ellis, H.M. and H.R. Horvitz, *Genetic control of programmed cell death in the nematode C. elegans*. Cell, 1986. 44(6): p. 817-29.
4. Strasser, A., et al., *Novel primitive lymphoid tumours induced in transgenic mice by cooperation between myc and bcl-2*. Nature, 1990. 348(6299): p. 331-3.
5. Watanabe-Fukunaga, R., et al., *Lymphoproliferation disorder in mice explained by defects in Fas antigen that mediates apoptosis*. Nature, 1992. 356(6367): p. 314-7.
6. Roy, N., et al., *The gene for neuronal apoptosis inhibitory protein is partially deleted in individuals with spinal muscular atrophy*. Cell, 1995. 80(1): p. 167-78.
7. Strasser, A., L. O'Connor, and V.M. Dixit, *Apoptosis signaling*. Annu Rev Biochem, 2000. 69: p. 217-45.
8. Magnusson, C. and D.L. Vaux, *Signalling by CD95 and TNF receptors: not only life and death*. Immunol Cell Biol, 1999. 77(1): p. 41-6.
9. Liepinsh, E., et al., *NMR structure of the death domain of the p75 neurotrophin receptor*. Embo J, 1997. 16(16): p. 4999-5005.
10. Huang, B., et al., *NMR structure and mutagenesis of the Fas (APO-1/CD95) death domain*. Nature, 1996. 384(6610): p. 638-41.
11. Fesik, S.W., *Insights into programmed cell death through structural biology*. Cell, 2000. 103(2): p. 273-82.
12. Hofmann, K., P. Bucher, and J. Tschopp, *The CARD domain: a new apoptotic signalling motif*. Trends Biochem Sci, 1997. 22(5): p. 155-6.
13. Qin, H., et al., *Structural basis of procaspase-9 recruitment by the apoptotic protease-activating factor 1*. Nature, 1999. 399(6736): p. 549-57.
14. Ashkenazi, A. and V.M. Dixit, *Death receptors: signaling and modulation*. Science, 1998. 281(5381): p. 1305-8.
15. Tsujimoto, Y., *Role of Bcl-2 family proteins in apoptosis: apoptosomes or mitochondria?* Genes Cells, 1998. 3(11): p. 697-707.

16. Adrain, C. and S.J. Martin, *The mitochondrial apoptosome: a killer unleashed by the cytochrome seas*. Trends Biochem Sci, 2001. 26(6): p. 390-7.
17. Susin, S.A., et al., *Molecular characterization of mitochondrial apoptosis-inducing factor*. Nature, 1999. 397(6718): p. 441-6.
18. Du, C., et al., *Smac, a mitochondrial protein that promotes cytochrome c-dependent caspase activation by eliminating IAP inhibition*. Cell, 2000. 102(1): p. 33-42.
19. Verhagen, A.M., et al., *Identification of DIABLO, a mammalian protein that promotes apoptosis by binding to and antagonizing IAP proteins*. Cell, 2000. 102(1): p. 43-53.
20. Saleh, A., et al., *Cytochrome c and dATP-mediated oligomerization of Apaf-1 is a prerequisite for procaspase-9 activation*. J Biol Chem, 1999. 274(25): p. 17941-5.
21. Green, D.R. and J.C. Reed, *Mitochondria and apoptosis*. Science, 1998. 281(5381): p. 1309-12.
22. Hu, Y., et al., *WD-40 repeat region regulates Apaf-1 self-association and procaspase-9 activation*. J Biol Chem, 1998. 273(50): p. 33489-94.
23. Thornberry, N.A., *Caspases: key mediators of apoptosis*. Chem Biol, 1998. 5(5): p. R97-103.
24. Cain, K., et al., *Caspase activation involves the formation of the aposome, a large (approximately 700 kDa) caspase-activating complex*. J Biol Chem, 1999. 274(32): p. 22686-92.
25. Li, H., et al., *Cleavage of BID by caspase 8 mediates the mitochondrial damage in the Fas pathway of apoptosis*. Cell, 1998. 94(4): p. 491-501.
26. Luo, X., et al., *Bid, a Bcl2 interacting protein, mediates cytochrome c release from mitochondria in response to activation of cell surface death receptors*. Cell, 1998. 94(4): p. 481-90.
27. Tartaglia, L.A. and D.V. Goeddel, *Two TNF receptors*. Immunol Today, 1992. 13(5): p. 151-3.
28. Malinin, N.L., et al., *MAP3K-related kinase involved in NF-kappaB induction by TNF, CD95 and IL-1*. Nature, 1997. 385(6616): p. 540-4.
29. Regnier, C.H., et al., *Identification and characterization of an IkappaB kinase*. Cell, 1997. 90(2): p. 373-83.
30. DiDonato, J.A., et al., *A cytokine-responsive IkappaB kinase that activates the transcription factor NF-kappaB*. Nature, 1997. 388(6642): p. 548-54.
31. Pahl, H.L., *Activators and target genes of Rel/NF-kappaB transcription factors*. Oncogene, 1999. 18(49): p. 6853-66.

32. Liu, Z.G., et al., *Dissection of TNF receptor 1 effector functions: JNK activation is not linked to apoptosis while NF-kappaB activation prevents cell death*. Cell, 1996. 87(3): p. 565-76.
33. Natoli, G., et al., *Activation of SAPK/JNK by TNF receptor 1 through a noncytotoxic TRAF2- dependent pathway*. Science, 1997. 275(5297): p. 200-3.
34. Song, H.Y., et al., *Tumor necrosis factor (TNF)-mediated kinase cascades: bifurcation of nuclear factor-kappaB and c-jun N-terminal kinase (JNK/SAPK) pathways at TNF receptor-associated factor 2*. Proc Natl Acad Sci U S A, 1997. 94(18): p. 9792-6.
35. Moriguchi, T., et al., *A novel SAPK/JNK kinase, MKK7, stimulated by TNFalpha and cellular stresses*. Embo J, 1997. 16(23): p. 7045-53.
36. Ichijo, H., et al., *Induction of apoptosis by ASK1, a mammalian MAPKKK that activates SAPK/JNK and p38 signaling pathways*. Science, 1997. 275(5296): p. 90-4.
37. Shirakabe, K., et al., *TAK1 mediates the ceramide signaling to stress-activated protein kinase/c-Jun N-terminal kinase*. J Biol Chem, 1997. 272(13): p. 8141-4.
38. Whitmarsh, A.J., et al., *A mammalian scaffold complex that selectively mediates MAP kinase activation*. Science, 1998. 281(5383): p. 1671-4.
39. Davis, R.J., *Signal transduction by the JNK group of MAP kinases*. Cell, 2000. 103(2): p. 239-52.
40. Wang, C.Y., et al., *NF-kappaB antiapoptosis: induction of TRAF1 and TRAF2 and c-IAP1 and c-IAP2 to suppress caspase-8 activation*. Science, 1998. 281(5383): p. 1680-3.
41. Tan, P.B. and S.K. Kim, *Signaling specificity: the RTK/RAS/MAP kinase pathway in metazoans*. Trends Genet, 1999. 15(4): p. 145-9.
42. Schlessinger, J. and A. Ullrich, *Growth factor signaling by receptor tyrosine kinases*. Neuron, 1992. 9(3): p. 383-91.
43. Blume-Jensen, P. and T. Hunter, *Oncogenic kinase signalling*. Nature, 2001. 411(6835): p. 355-65.
44. Wang, H.G., U.R. Rapp, and J.C. Reed, *Bcl-2 targets the protein kinase Raf-1 to mitochondria*. Cell, 1996. 87(4): p. 629-38.
45. del Peso, L., et al., *Interleukin-3-induced phosphorylation of BAD through the protein kinase Akt*. Science, 1997. 278(5338): p. 687-9.
46. Reddy, E.P., et al., *IL-3 signaling and the role of Src kinases, JAKs and STATs: a covert liaison unveiled*. Oncogene, 2000. 19(21): p. 2532-47.
47. Guthridge, M.A., et al., *Mechanism of activation of the GM-CSF, IL-3, and IL-5 family of receptors*. Stem Cells, 1998. 16(5): p. 301-13.

48. Pazdrak, K., et al., *The intracellular signal transduction mechanism of interleukin 5 in eosinophils: the involvement of lyn tyrosine kinase and the Ras-Raf-1- MEK-microtubule-associated protein kinase pathway.* J Exp Med, 1995. 181(5): p. 1827-34.
49. Stephens, L., et al., *Receptor stimulated accumulation of phosphatidylinositol (3,4,5)-trisphosphate by G-protein mediated pathways in human myeloid derived cells.* Embo J, 1993. 12(6): p. 2265-73.
50. Coffey, P.J., J. Jin, and J.R. Woodgett, *Protein kinase B (c-Akt): a multifunctional mediator of phosphatidylinositol 3-kinase activation.* Biochem J, 1998. 335(Pt 1): p. 1-13.
51. Goyal, L., *Cell death inhibition: keeping caspases in check.* Cell, 2001. 104(6): p. 805-8.
52. Clem, R.J., M. Fechheimer, and L.K. Miller, *Prevention of apoptosis by a baculovirus gene during infection of insect cells.* Science, 1991. 254(5036): p. 1388-90.
53. Crook, N.E., R.J. Clem, and L.K. Miller, *An apoptosis-inhibiting baculovirus gene with a zinc finger-like motif.* J Virol, 1993. 67(4): p. 2168-74.
54. Ekert, P.G., J. Silke, and D.L. Vaux, *Caspase inhibitors.* Cell Death Differ, 1999. 6(11): p. 1081-6.
55. Sun, C., et al., *NMR structure and mutagenesis of the third Bir domain of the inhibitor of apoptosis protein XIAP.* J Biol Chem, 2000. 275(43): p. 33777-81.
56. Deveraux, Q.L. and J.C. Reed, *IAP family proteins--suppressors of apoptosis.* Genes Dev, 1999. 13(3): p. 239-52.
57. Chu, Z.L., et al., *Suppression of tumor necrosis factor-induced cell death by inhibitor of apoptosis c-IAP2 is under NF-kappaB control.* Proc Natl Acad Sci U S A, 1997. 94(19): p. 10057-62.
58. Rothe, M., et al., *The TNFR2-TRAF signaling complex contains two novel proteins related to baculoviral inhibitor of apoptosis proteins.* Cell, 1995. 83(7): p. 1243-52.
59. Duckett, C.S., et al., *A conserved family of cellular genes related to the baculovirus iap gene and encoding apoptosis inhibitors.* Embo J, 1996. 15(11): p. 2685-94.
60. Holcik, M. and R.G. Korneluk, *Functional characterization of the X-linked inhibitor of apoptosis (XIAP) internal ribosome entry site element: role of La autoantigen in XIAP translation.* Mol Cell Biol, 2000. 20(13): p. 4648-57.
61. Tamm, I., et al., *Expression and prognostic significance of IAP-family genes in human cancers and myeloid leukemias.* Clin Cancer Res, 2000. 6(5): p. 1796-803.
62. Kato, J., et al., *Expression of survivin in esophageal cancer: correlation with the prognosis and response to chemotherapy.* Int J Cancer, 2001. 95(2): p. 92-5.

63. Liston, P., et al., *Suppression of apoptosis in mammalian cells by NAIP and a related family of IAP genes*. Nature, 1996. 379(6563): p. 349-53.
64. Hofer-Warbinek, R., et al., *Activation of NF-kappa B by XIAP, the X chromosome-linked inhibitor of apoptosis, in endothelial cells involves TAK1*. J Biol Chem, 2000. 275(29): p. 22064-8.
65. Yamaguchi, K., et al., *XIAP, a cellular member of the inhibitor of apoptosis protein family, links the receptors to TAB1-TAK1 in the BMP signaling pathway*. Embo J, 1999. 18(1): p. 179-87.
66. Oeda, E., et al., *Interaction of Drosophila inhibitors of apoptosis with thick veins, a type I serine/threonine kinase receptor for decapentaplegic*. J Biol Chem, 1998. 273(16): p. 9353-6.
67. Sanna, M.G., et al., *Selective activation of JNK1 is necessary for the anti-apoptotic activity of hILP*. Proc Natl Acad Sci U S A, 1998. 95(11): p. 6015-20.
68. Birkey Reffey, S., et al., *X-linked inhibitor of apoptosis protein functions as a cofactor in transforming growth factor- β signaling*. J Biol Chem, 2001. 16: p. 16.
69. Deveraux, Q.L., et al., *X-linked IAP is a direct inhibitor of cell-death proteases*. Nature, 1997. 388(6639): p. 300-4.
70. Roy, N., et al., *The c-IAP-1 and c-IAP-2 proteins are direct inhibitors of specific caspases*. Embo J, 1997. 16(23): p. 6914-25.
71. Huang, Y., et al., *Structural basis of caspase inhibition by XIAP: differential roles of the linker versus the BIR domain*. Cell, 2001. 104(5): p. 781-90.
72. Riedl, S.J., et al., *Structural basis for the inhibition of caspase-3 by XIAP*. Cell, 2001. 104(5): p. 791-800.
73. Bratton, S.B., et al., *Recruitment, activation and retention of caspases-9 and -3 by Apaf-1 apoptosome and associated XIAP complexes*. Embo J, 2001. 20(5): p. 998-1009.
74. Harvey, A.J., A.P. Bidwai, and L.K. Miller, *Doom, a product of the Drosophila mod(mdg4) gene, induces apoptosis and binds to baculovirus inhibitor-of-apoptosis proteins*. Mol Cell Biol, 1997. 17(5): p. 2835-43.
75. Vucic, D., W.J. Kaiser, and L.K. Miller, *Inhibitor of apoptosis proteins physically interact with and block apoptosis induced by Drosophila proteins HID and GRIM*. Mol Cell Biol, 1998. 18(6): p. 3300-9.
76. McCarthy, J.V. and V.M. Dixit, *Apoptosis induced by Drosophila reaper and grim in a human system. Attenuation by inhibitor of apoptosis proteins (cIAPs)*. J Biol Chem, 1998. 273(37): p. 24009-15.

77. Liu, Z., et al., *Structural basis for binding of Smac/DIABLO to the XIAP BIR3 domain*. Nature, 2000. 408(6815): p. 1004-8.
78. Wu, G., et al., *Structural basis of IAP recognition by Smac/DIABLO*. Nature, 2000. 408(6815): p. 1008-12.
79. Srinivasula, S.M., et al., *A conserved XIAP-interaction motif in caspase-9 and Smac/DIABLO regulates caspase activity and apoptosis*. Nature, 2001. 410(6824): p. 112-6.
80. Roberts, D.L., et al., *The inhibitor of apoptosis protein-binding domain of Smac is not essential for its proapoptotic activity*. J Cell Biol, 2001. 153(1): p. 221-8.
81. Joazeiro, C.A. and A.M. Weissman *RING finger proteins: mediators of ubiquitin ligase activity*. Cell, 2000. 102(5): p. 549-52.
82. Yang, Y., et al., *Ubiquitin protein ligase activity of IAPs and their degradation in proteasomes in response to apoptotic stimuli*. Science, 2000. 288(5467): p. 874-7.
83. Huang, H., et al., *The inhibitor of apoptosis, cIAP2, functions as a ubiquitin-protein ligase and promotes in vitro monoubiquitination of caspases 3 and 7*. J Biol Chem, 2000. 275(35): p. 26661-4.
84. Gross, A., J.M. McDonnell, and S.J. Korsmeyer, *BCL-2 family members and the mitochondria in apoptosis*. Genes Dev, 1999. 13(15): p. 1899-911.
85. Adams, J.M. and S. Cory, *Life-or-death decisions by the Bcl-2 protein family*. Trends Biochem Sci, 2001. 26(1): p. 61-6.
86. Yaffe, M.B., et al., *The structural basis for 14-3-3:phosphopeptide binding specificity*. Cell, 1997. 91(7): p. 961-71.
87. Soucie, E.L., et al., *Myc potentiates apoptosis by stimulating bax activity at the mitochondria*. Mol Cell Biol, 2001. 21(14): p. 4725-36.
88. Greenberger, J.S., et al., *Demonstration of permanent factor-dependent multipotential (erythroid/neutrophil/basophil) hematopoietic progenitor cell lines*. Proc Natl Acad Sci U S A, 1983. 80(10): p. 2931-5.
89. von Gise, A., et al., *Apoptosis suppression by Raf-1 and MEK1 requires MEK- and phosphatidylinositol 3-kinase-dependent signals*. Mol Cell Biol, 2001. 21(7): p. 2324-36.
90. Cleveland, J.L., et al., *v-raf suppresses apoptosis and promotes growth of interleukin-3-dependent myeloid cells*. Oncogene, 1994. 9(8): p. 2217-26.
91. Carter, B.D. and G.R. Lewin, *Neurotrophins live or let die: does p75NTR decide?* Neuron, 1997. 18(2): p. 187-90.
92. Barker, P.A., *p75NTR: A study in contrasts*. Cell Death Differ, 1998. 5(5): p. 346-56.

93. Ye, X., et al., *TRAF family proteins interact with the common neurotrophin receptor and modulate apoptosis induction*. J Biol Chem, 1999. 274(42): p. 30202-8.
94. Kaplan, D.R. and F.D. Miller, *Neurotrophin signal transduction in the nervous system*. Curr Opin Neurobiol, 2000. 10(3): p. 381-91.
95. Yamashita, T., K.L. Tucker, and Y.A. Barde, *Neurotrophin binding to the p75 receptor modulates Rho activity and axonal outgrowth*. Neuron, 1999. 24(3): p. 585-93.
96. Frade, J.M., *Unscheduled re-entry into the cell cycle induced by NGF precedes cell death in nascent retinal neurons*. J Cell Sci, 2000. 113(Pt 7): p. 1139-48.
97. Aloyz, R.S., et al., *p53 is essential for developmental neuron death as regulated by the TrkA and p75 neurotrophin receptors*. J Cell Biol, 1998. 143(6): p. 1691-703.
98. Chittka, A. and M.V. Chao, *Identification of a zinc finger protein whose subcellular distribution is regulated by serum and nerve growth factor*. Proc Natl Acad Sci U S A, 1999. 96(19): p. 10705-10.
99. Casademunt, E., et al., *The zinc finger protein NRIF interacts with the neurotrophin receptor p75(NTR) and participates in programmed cell death*. Embo J, 1999. 18(21): p. 6050-61.
100. Salehi, A.H., et al., *NRAGE, a novel MAGE protein, interacts with the p75 neurotrophin receptor and facilitates nerve growth factor-dependent apoptosis*. Neuron, 2000. 27(2): p. 279-88.
101. Digby M, U.R., Rudolf Götz, Geng Pei, Ludmilla Wixler, John Lowenthal, David Bowtell, Jakob Troppmair , Stefan Wiese and Michael Sendtner, *Expression of the IAP Homologue, ITA, Suppresses NGF-induced Differentiation and TNF α -induced Apoptosis in PC12 Cells*. Submitted to JCB, 2001.
102. Liston, P., et al., *Identification of XAF1 as an antagonist of XIAP anti-Caspase activity*. Nat Cell Biol, 2001. 3(2): p. 128-33.
103. Kalmes, A., et al., *Interaction between the protein kinase BRaf and the alpha-subunit of the 11S proteasome regulator*. Cancer Res, 1998. 58(14): p. 2986-90.
104. Ohman Forslund, K. and K. Nordqvist, *The melanoma antigen genes--any clues to their functions in normal tissues?* Exp Cell Res, 2001. 265(2): p. 185-94.
105. Baffy, G., et al., *Apoptosis induced by withdrawal of interleukin-3 (IL-3) from an IL-3-dependent hematopoietic cell line is associated with repartitioning of intracellular calcium and is blocked by enforced Bcl-2 oncoprotein production*. J Biol Chem, 1993. 268(9): p. 6511-9.

106. Vanhaesebroeck, B., et al., *Effect of bcl-2 proto-oncogene expression on cellular sensitivity to tumor necrosis factor-mediated cytotoxicity*. *Oncogene*, 1993. 8(4): p. 1075-81.
107. Tibbles, L.A., et al., *MLK-3 activates the SAPK/JNK and p38/RK pathways via SEK1 and MKK3/6*. *Embo J*, 1996. 15(24): p. 7026-35.
108. Ludwig, S., et al., *3pK, a novel mitogen-activated protein (MAP) kinase-activated protein kinase, is targeted by three MAP kinase pathways*. *Mol Cell Biol*, 1996. 16(12): p. 6687-97.
109. Yoneda, Y., *Nucleocytoplasmic protein traffic and its significance to cell function*. *Genes Cells*, 2000. 5(10): p. 777-87.
110. Vucic, D., et al., *Inhibition of reaper-induced apoptosis by interaction with inhibitor of apoptosis proteins (IAPs)*. *Proc Natl Acad Sci U S A*, 1997. 94(19): p. 10183-8.
111. Hozak, R.R., G.A. Manji, and P.D. Friesen, *The BIR motifs mediate dominant interference and oligomerization of inhibitor of apoptosis Op-IAP*. *Mol Cell Biol*, 2000. 20(5): p. 1877-85.
112. Digby, M.R., et al., *ITA, a vertebrate homologue of IAP that is expressed in T lymphocytes*. *DNA Cell Biol*, 1996. 15(11): p. 981-8.
113. You, M., et al., *ch-IAP1, a member of the inhibitor-of-apoptosis protein family, is a mediator of the antiapoptotic activity of the ν Rel oncoprotein*. *Mol Cell Biol*, 1997. 17(12): p. 7328-41.
114. Wiese, S., et al., *The anti-apoptotic protein ITA is essential for NGF-mediated survival of embryonic chick neurons*. *Nat Neurosci*, 1999. 2(11): p. 978-83.
115. Ambrosini, G., C. Adida, and D.C. Altieri, *A novel anti-apoptosis gene, survivin, expressed in cancer and lymphoma*. *Nat Med*, 1997. 3(8): p. 917-21.
116. Borden, K.L., *RING domains: master builders of molecular scaffolds?* *J Mol Biol*, 2000. 295(5): p. 1103-12.
117. Olsson, P.A., et al., *MIR is a novel ERM-like protein that interacts with myosin regulatory light chain and inhibits neurite outgrowth*. *J Biol Chem*, 1999. 274(51): p. 36288-92.
118. Suzuki, Y., Y. Nakabayashi, and R. Takahashi, *Ubiquitin-protein ligase activity of X-linked inhibitor of apoptosis protein promotes proteasomal degradation of caspase-3 and enhances its anti-apoptotic effect in Fas-induced cell death*. *Proc Natl Acad Sci U S A*, 2001. 10: p. 10.
119. Goyal, L., et al., *Induction of apoptosis by Drosophila reaper, hid and grim through inhibition of IAP function*. *Embo J*, 2000. 19(4): p. 589-97.
120. Wang, H.G., et al., *Apoptosis regulation by interaction of Bcl-2 protein and Raf-1 kinase*. *Oncogene*, 1994. 9(9): p. 2751-6.

121. Scaffidi, C., et al., *Two CD95 (APO-1/Fas) signaling pathways*. *Embo J*, 1998. 17(6): p. 1675-87.
122. Medema, J.P., et al., *Bcl-xL acts downstream of caspase-8 activation by the CD95 death-inducing signaling complex*. *J Biol Chem*, 1998. 273(6): p. 3388-93.
123. Wajant, H., M. Grell, and P. Scheurich, *TNF receptor associated factors in cytokine signaling*. *Cytokine Growth Factor Rev*, 1999. 10(1): p. 15-26.
124. Lucas, S., F. Brasseur, and T. Boon, *A new MAGE gene with ubiquitous expression does not code for known MAGE antigens recognized by T cells*. *Cancer Res*, 1999. 59(16): p. 4100-3.
125. Hennuy, B., et al., *A novel messenger ribonucleic acid homologous to human MAGE-D is strongly expressed in rat Sertoli cells and weakly in Leydig cells and is regulated by follitropin, lutropin, and prolactin*. *Endocrinology*, 2000. 141(10): p. 3821-31.
126. Masuda, Y., et al., *Dlxin-1, a novel protein that binds dlx5 and regulates its transcriptional function*. *J Biol Chem*, 2001. 276(7): p. 5331-8.
127. Suzuki, N., et al., *A cytoplasmic protein, bystin, interacts with trophinin, tastin, and cytokeratin and may be involved in trophinin-mediated cell adhesion between trophoblast and endometrial epithelial cells*. *Proc Natl Acad Sci U S A*, 1998. 95(9): p. 5027-32.
128. Maruyama, K., et al., *A novel brain-specific mRNA encoding nuclear protein (necdin) expressed in neurally differentiated embryonal carcinoma cells*. *Biochem Biophys Res Commun*, 1991. 178(1): p. 291-6.
129. Aizawa, T., et al., *Expression of necdin, an embryonal carcinoma-derived nuclear protein, in developing mouse brain*. *Brain Res Dev Brain Res*, 1992. 68(2): p. 265-74.
130. Taniura, H., et al., *Necdin, a postmitotic neuron-specific growth suppressor, interacts with viral transforming proteins and cellular transcription factor E2F1*. *J Biol Chem*, 1998. 273(2): p. 720-8.
131. Taniura, H., K. Matsumoto, and K. Yoshikawa, *Physical and functional interactions of neuronal growth suppressor necdin with p53*. *J Biol Chem*, 1999. 274(23): p. 16242-8.
132. Sutcliffe, J.S., et al., *Neuronally-expressed necdin gene: an imprinted candidate gene in Prader- Willi syndrome*. *Lancet*, 1997. 350(9090): p. 1520-1.
133. Holcik, M., H. Gibson, and R.G. Komeluk, *XIAP: Apoptotic brake and promising therapeutic target*. *Apoptosis*, 2001. 6(4): p. 253-61.
134. Gomez, N. and P. Cohen, *Dissection of the protein kinase cascade by which nerve growth factor activates MAP kinases*. *Nature*, 1991. 353(6340): p. 170-3.

135. Tanaka, S., T. Ouchi, and H. Hanafusa, *Downstream of Crk adaptor signaling pathway: activation of Jun kinase by v-Crk through the guanine nucleotide exchange protein C3G*. Proc Natl Acad Sci U S A, 1997. 94(6): p. 2356-61.
136. Rana, A., et al., *The mixed lineage kinase SPRK phosphorylates and activates the stress-activated protein kinase activator, SEK-1*. J Biol Chem, 1996. 271(32): p. 19025-8.
137. Yoon, S.O., et al., *Competitive signaling between TrkA and p75 nerve growth factor receptors determines cell survival*. J Neurosci, 1998. 18(9): p. 3273-81.
138. Xu, Z., et al., *The MLK Family Mediates c-Jun N-Terminal Kinase Activation in Neuronal Apoptosis*. Mol Cell Biol, 2001. 21(14): p. 4713-24.
139. Minden, A., et al., *Differential activation of ERK and JNK mitogen-activated protein kinases by Raf-1 and MEKK*. Science, 1994. 266(5191): p. 1719-23.
140. Leppa, S., et al., *Differential regulation of c-Jun by ERK and JNK during PC12 cell differentiation*. Embo J, 1998. 17(15): p. 4404-13.
141. Teramoto, H., et al., *Signaling from the small GTP-binding proteins Rac1 and Cdc42 to the c-Jun N-terminal kinase/stress-activated protein kinase pathway. A role for mixed lineage kinase 3/protein-tyrosine kinase 1, a novel member of the mixed lineage kinase family*. J Biol Chem, 1996. 271(44): p. 27225-8.
142. Hartkamp, J., J. Troppmair, and U.R. Rapp, *The JNK/SAPK activator mixed lineage kinase 3 (MLK3) transforms NIH 3T3 cells in a MEK-dependent fashion*. Cancer Res, 1999. 59(9): p. 2195-202.
143. Gao, Z.H., J. Metherall, and D.M. Virshup, *Identification of casein kinase I substrates by in vitro expression cloning screening*. Biochem Biophys Res Commun, 2000. 268(2): p. 562-6.
144. Beyaert, R., et al., *Casein kinase-1 phosphorylates the p75 tumor necrosis factor receptor and negatively regulates tumor necrosis factor signaling for apoptosis*. J Biol Chem, 1995. 270(40): p. 23293-9.
145. Zhang, H., et al., *Heterodimerization of Msx and Dlx homeoproteins results in functional antagonism*. Mol Cell Biol, 1997. 17(5): p. 2920-32.
146. Acampora, D., et al., *Craniofacial, vestibular and bone defects in mice lacking the Distal-less-related gene Dlx5*. Development, 1999. 126(17): p. 3795-809.
147. Boudreaux, J.M. and D.A. Towler, *Synergistic induction of osteocalcin gene expression: identification of a bipartite element conferring fibroblast growth factor 2 and cyclic AMP responsiveness in the rat osteocalcin promoter*. J Biol Chem, 1996. 271(13): p. 7508-15.

148. Newberry, E.P., et al., *Fibroblast growth factor receptor signaling activates the human interstitial collagenase promoter via the bipartite Ets-AP1 element*. Mol Endocrinol, 1997. 11(8): p. 1129-44.
149. Ben-Levy, R., et al., *Nuclear export of the stress-activated protein kinase p38 mediated by its substrate MAPKAP kinase-2*. Curr Biol, 1998. 8(19): p. 1049-57.
150. Eisenstat, D.D., et al., *DLX-1, DLX-2, and DLX-5 expression define distinct stages of basal forebrain differentiation*. J Comp Neurol, 1999. 414(2): p. 217-37.
151. Dodig, M., et al., *Identification of a TAAT-containing motif required for high level expression of the COL1A1 promoter in differentiated osteoblasts of transgenic mice*. J Biol Chem, 1996. 271(27): p. 16422-9.
152. Sanger, F., S. Nicklen, and A.R. Coulson, *DNA sequencing with chain-terminating inhibitors*. 1977. Biotechnology, 1992. 24: p. 104-8.
153. Rothe, M., et al., *A novel family of putative signal transducers associated with the cytoplasmic domain of the 75 kDa tumor necrosis factor receptor*. Cell, 1994. 78(4): p. 681-92.
154. Bradford, M.M., *A rapid and sensitive method for the quantitation of microgram quantities of protein utilizing the principle of protein-dye binding*. Anal Biochem, 1976. 72: p. 248-54.

APPENDIX

Abbreviations

β -Gal	β -Galactosidase
$\alpha\alpha$	Amino acid
AD	(Gal4) Activation domain
Amp.	Ampicillin
ASK1	Apoptosis signal-regulated kinase
APS	Ammoniumpersulphate
ATP	Adenosine 5'-triphosphate
BIR	Baculovirus IAP repeat
BLAST	basic local alignment tool
BMP	Bone morphogenic protein
bzw	beziehungsweise
Ce	Caenorhabditis elegans
ca.	circa
cAMP	cyclic Adenosine monophosphate
CARD	Caspase recruitment domain
cfu	colony forming unit
CIP	Calf Intestinal Phosphatase
CKI	Casein kinase I
DAG	Diacylglycerin
DART	Domain architecture retrieval tool
DB	(Gal4) DNA-Binding domain
DD	Death domain
DED	Death effector domain
DISC	Death inducing signalling complex
(d)dNTP	(Di)Desoxynucleotide triphosphate
DMEM	Dulbecco's Modified Eagle Medium
DMF	Dimethylformamide
DMSO	Dimethylsulphoxide
DTT	Dithiothreitol
E. coli	Escherichia coli
ECL	Enhanced Chemoluminescence
EDTA	Ethylendiamintetra acetic acid
EGF	Epidermal growth factor
ERK	Extracellular signal regulated kinase
EST	Expressed sequence tag
FADD	Fas-associated protein with death domain
FCS	Foetal calf serum
GST	Guanidine-S-transferase
HA	Haemagglutinin

His	Histidine
I κ B	Inhibitor of κ B
IAP	Inhibitor of apoptosis protein
IKK	I κ B kinase
IL	Interleukin
IP	Immunoprecipitation
IRES	Internal ribosomal entry site
ITA	Inhibitor of T-cell apoptosis
JAK	Janus kinase
JNK	c-Jun N-terminal kinase
JNKK	JNK kinase
bp	basepairs
kbp	Kilobasepairs
kD	Kilo Dalton
Leu	Leucine
LiAc	Lithium acetate
MAGE	Melanoma associated antigen
MAPK	Mitogen activated protein kinase
MAP2K	MAPK kinase
MAP3K	MAP2K kinase
MEK	MAPK/ERK activating kinase
MEKK	MAPK/ERK activating kinase kinase
MKK	MAP kinase kinase
MLK3	Mixed lineage kinase 3
Mod.	Modified
MSZ	Institut für Medizinische Strahlenkunde und Zellforschung
NAIP	Neuronal IAP
NCBI	National Center for Biotechnology Information
NF- κ B	Nuclear factor κ B
NGF	Nerve growth factor
NRAGE	Neurotrophin receptor interacting MAGE homologue
NP40	Nonidet 40
OD	Optical density
ON	Overnight
ORF	Open reading frame
p75NTR	p75 neurotrophin receptor
PAGE	Polyacrylamide-Gel electrophoresis
PBS	Phosphate buffered saline
PC12	Phaeochromocytoma cell 12
PCD	Programmed cell death
PCR	polymerase chain reaction
PDGF	Platelet derived growth factor
PKC	Protein kinase C
PTB	tyrosine binding domain
PTK	Protein tyrosine kinase
rpm	revolutions per minute
RPTK	Receptor protein tyrosine kinase
RT	Room temperature
Sc	Saccharomyces cerevisiae

Sp	Schizosaccharomyces pombe
SAPK	Stress-activated protein kinase
Ser	Serine
SH	Src Homology
Sos	Son of sevenless
STAT	Signal transducers and activators of transcription
TAK-1	TGF- β -activating kinase
TGF	Transforming growth factor
THC	Tentative human consensus sequence
Thr	Threonine
TIGR	The institute of genomic research
TNF	Tumour necrosis factor
TRADD	TNF-R1 associated death domain protein
TRAF	TNFR associated factor
TNFR	TNF receptor
Trp	Tryptophan
Tyr	Tyrosine
Ub	Ubiquitin
v	Volume
w	Weight
XIAP	X-linked IAP

CURRICULUM VITAE

PERSONAL DETAILS

Name: Bruce Jordan
e-mail: bruce.jordan@mail.uni-wuerzburg.de
Date of birth: 01.06.1971
Place of birth: London, England
Nationality: British
Sex: Male
Marital status: Single

EDUCATION

Since Jan. 1997 Graduate student at the Institut für Medizinische Strahlenkunde und Zellforschung (MSZ), Universität Würzburg, leading to the qualification Doktor rer.nat. Thesis "The identification of novel inhibitor of apoptosis protein interacting proteins".

Aug. 1995 Council for Professions Supplementary to Medicine (CPSM) qualification in haematology and transfusion medicine, at Southampton General Hospital

Sept. 1990- University of Portsmouth, Portsmouth U.K., BSc.(Hons)
July 1994 Biomedical Sciences. Graduation with Upper Second (2.i) Honours degree

June 1984- Secondary education at Epsom College, Esher College and
July 1990 Kingston College, 10 'O' Levels, 2 'A' Levels

WORK EXPERIENCE

Oct. 1995- Biomedical Scientist grade I in haematology and transfusion
Dec. 1996 medicine at the Royal Marsden Hospital, London. Diagnostic haematology, transfusion medicine and emergency 'on call' duties.

Aug. 1994- Trainee Biomedical Scientist at Southampton General Hospital,
Sept. 1995 Haematology Department. Rotation through routine haematology, coagulation, haemoglobinopathies and transfusion medicine.

PUBLICATIONS:

NRAGE is an inducible IAP-interacting protein that augments cell death

Jordan, B. W. M., Dinev, D., LeMellay, V., Troppmair, J., Götz, R., Wixler, L., Sendtner M., Ludwig, S., and Ulf R. Rapp, J Biol Chem. 2001 Oct 26;276(43):39985-9.

Extracellular signal regulated kinase 5 (ERK5) is required for the differentiation of muscle cells, Dinev, D., **Jordan, B.W.M.**, Neufeld, B., Lee, J.D., Lindemann, D., Rapp, U.R., Ludwig, S., EMBO Rep. 2001 Sep;2(9):829-34.

Transactivation of naturally occurring HIV-1 long terminal repeats by the JNK signaling pathway. The most frequent naturally occurring length polymorphism sequence introduces a novel binding site for AP-1 factors.

Chen P, Flory E, Avots A, **Jordan B.W.M**, Kirchhoff F, Ludwig S, Rapp UR., J Biol Chem. 2000 Jul 7;275(27):20382-90.

Serine/ Threonine kinase 3pK and MAPK-activated protein kinase 2 interact with the basic Helix-Loop-Helix transcription factor E47 and repress its transcriptional activity, Neufeld, B., Grosse-Wilde, A., Hoffmeyer, A., **Jordan, B.W.M.**, Chen, P., Dinev, D., Ludwig, S., Rapp, U.R., J. Biol. Chem., 2000, 275(27) 20239:20242.